Curriculum Vitae

Drs. Ing. Niels van Boxtel was born on the 11th of December, 1985 in Tilburg, The Netherlands. He completed his secondary school in 2002 at Pauluslyceum in Tilburg and his Bachelor studies in Chemistry at Avans Hogeschool in Breda, The Netherlands. This degree was completed in 2007 after which he started to work in various functions as a chemical analyst. Next to a fulltime job, he completed a master in Chemistry at the Free University of Amsterdam, the Netherlands. During this study, a specialisation was done in analytical chemistry and was completed in 2011. In the same year he started his PhD research at the Pharmaceutical Analysis laboratory of KU Leuven in Belgium under the supervision of promoter Prof. Dr. Erwin Adams and co-promoter Prof. Dr. Ann Van Schepdael. The focus of his research was on alternative approaches around sensitivity issues within GC analysis.

Acknowledgements

When I began my PhD studies at KU Leuven, the idea of completing a thesis seemed overwhelming. As the years passed by, it has come together slowly, step by step and finally came into focus. All of this would not have been accomplished without the help and support of countless people.

First, I would like to express my gratitude to my promoter Prof. Dr. Erwin Adams for giving me the opportunity to start my PhD studies in the Pharmaceutical Analysis lab, Thank you for all the help and support I received from you during my stay in the lab. I am also grateful to my co-promoter Prof. Dr. Ann Van Schepdael as head of laboratory allowing me to start my PhD and for the support during my stay. I also would like to thank Prof. Dr. Deirdre Cabooter as well for being a nice colleague and I wish you all the best with your future research. Thanks to the jury members (Prof. Dr. Guy Bormans, Prof. Dr. Eva Cuypers, Prof. Dr. Kristin Verbeke, Prof. Dr. Christophe Stove and Dr. Eric Deconinck) for reading my thesis manuscript and for their suggestions on how to improve it as well, as for their comments while being a part of my thesis advisory committee.

During the past years as a PhD student, I spend my time with a lot of different people and would like to thank all of them for creating a pleasant environment to work in: Jochen, Bart, Stijn, Pranov, Karina, Huiying, Glenn, Stani, Lynch, Marwa, Shengyun, Matthias, Jasper, Getu, Adissu, Prasanta, Ann, Didi, Mohamed, Peter, Hui, Stephanie and Sonia. From all the colleagues, there is one that deserves special credits: Kris Wolfs for his great support and help during my PhD. Throughout the years he helped me to overcome many problems around my research projects. I really appreciated the ‘straight to the point’ approach you used in your assistance during this work. Moreover, I always enjoyed our chats about all kinds of topics, especially when I needed some distraction from the daily work. During my stay, I have supervised several bachelor and master students in the framework of their final thesis. It was my pleasure to guide you in your work. So thank you Marta, Nand, Maria, Joren, Jasper and Valerie for being very nice colleagues.

Also, I would like to thank my parents for their support during my PhD. I don’t think I could have finished it without that. Not everyone gets a chance to study in a university and I am therefore grateful that my parents offered me this chance. Last but not least, I would like to thank my friends for their support: Jelle, Dave, Frank, Jop, Bob, Floran and many more. Thanks for everything!

Niels

List of publications

1. N. van Boxtel, K. Wolfs, A. Van Schepdael, E. Adams, Evaluation of the full evaporation technique for quantitative analysis of high boiling compounds with high affinity for apolar matrices, J. Chromatogr. A, 1348 (2014) 63.

2. N. van Boxtel, K. Wolfs, A. Van Schepdael, E. Adams, Application of acetone acetals as water scavengers and derivatization agents prior to the gas chromatographic analysis of polar residual solvents in aqueous samples, J. Chromatogr. A., 1425 (2015) 62.

3. N. van Boxtel, K. Wolfs, M. Guillén Palacín, A. Van Schepdael, E. Adams, A headspace gas chromatography based methodology for the analysis of aromatic substituted quaternary ammonium salts, (Submitted to Journal of Chromatography A).

4. N. van Boxtel, K. Wolfs, M. Guillén Palacín, A. Van Schepdael, E. Adams, Comprehensive headspace gas chromatographic analysis of denaturants including denatonium benzoate in denaturated ethanol samples (To be submitted to Talanta).

5. N. van Boxtel, K. Wolfs, W. D'Autry, A. Van Schepdael, E. Adams, Development and characterization of an atmospheric micro cavity hollow cathode discharge based GC-detector (To be submitted to Analytical Chemistry).

Table of contents

Curriculum Vitae ii
Acknowledgements iii
List of publications iv
List of abbreviations and symbols viii
Chapter 1 - General introduction 1
1.1. Gas chromatography as analytical tool 3
1.1.1. Introduction 3
1.1.2. Inlet 3
1.1.3. Column 4
1.1.4. Carrier gas 4
1.2. Headspace sample introduction 4
1.2.1. Overview of sample introduction techniques 4
1.2.2. Basic theory of HS sampling 5
1.2.3. Balanced pressure system 7
1.2.4. Full evaporation technique (FET) 8
1.2.5. Shortcomings of HS sampling 8
1.3. GC detectors 10
1.3.1. Thermal conductivity detector (TCD) 10
1.3.2. Flame ionization detector (FID) 11
1.3.3. Electron capture detector (ECD) 12
1.3.4. Thermoionic ionization detector (TID) 12
1.3.5. Chemiluminescence based sulphur and nitrogen detectors 14
1.3.6. Photoionization detector (PID) 15
1.3.7. Helium ionization detector (HID) 15
1.3.8. Mass spectrometer as detection system 16
1.3.9. Shortcomings of GC detectors 17
1.4. Aim of the study 18
1.5. References 19
Chapter 2 - Evaluation of the full evaporation technique for quantitative analysis of high boiling compounds with high affinity for apolar matrices 24
2.1. Introduction 27
2.2. Theory 28
2.3. Experimental 29
2.3.1. Reagents and samples 29
2.3.2. Chromatographic system and sampling conditions for the sHS-method 30
2.3.3. Chromatographic system and HS sampler conditions for FET 31
2.3.4. Preparation of solutions 32
2.3.5. Sample vials 33
2.3.6. FET evaluation 33
2.3.7. Stability evaluation 34
2.3.8. Matrix-matched vs. solvent-based calibration 34
2.3.9. Recovery experiments 34

2.3.10. Analysis of commercial samples 34
2.4. Results & discussion 35
2.4.1. Evaluation of the sample volume in the vial used for FET 35
2.4.2. Evaluation of matrix effects 35
2.4.3. Stability evaluation 39
2.4.4. Recovery and repeatability 39
2.4.5. Limit of quantification (LOQ) 41
2.4.6. Analysis of commercial samples 41
2.5. Conclusions 43
2.6. References 44
Chapter 3 - Application of acetone acetals as water scavengers and derivatization agents prior to the gas chromatographic analysis of polar residual solvents in aqueous samples 47
3.1. Introduction 50
3.2. Experimental 53
3.2.1. Reagents 53
3.2.2. Chromatographic systems 53
3.2.3. Preparation of solutions 54
3.2.4. Method validation 56
3.3. Results & Discussion 56
3.3.1. Investigation of DMP treatment parameters 56
3.3.2. Influence of sample acidity on the response of analytes and choice of neutralising agent 59
3.3.3. Optimization of the solvent evaporation step (FET-GC) 62
3.3.4. Identification of EG-DMP derivative 63
3.3.5. Further improvement 65
3.3.6. Method validation 65
3.3.7. Analysis of residual NMP in an aqueous solution of a cefotaxime analogue 67
3.3.8. Analysis of EG in contact lens fluids 68
3.4. Conclusions 68
3.5. References 69
Chapter 4 - A headspace gas chromatography based methodology for the analysis of aromatic substituted quaternary ammonium salts 73
4.1. Introduction 76
4.2. Experimental 77
4.2.1. Reagents 77
4.2.2. Chromatographic systems 78
4.2.3. Preparation of solutions and samples 80
4.2.4. Procedures 82
4.3. Results & Discussion 85
4.3.1. Screening of various QAS 85
4.3.2. Equilibration time 88
4.3.3. Method validation HS-GC method 89
4.3.4. Analysis of DB in commercial cooling liquid samples 91
4.3.5. Analysis of BZTCl in a mouth spray 95
4.3.6. Analysis of BZOCl in a mouth spray 95

4.4. Conclusions 95
4.5. References 96
Chapter 5 - Development and characterization of an atmospheric micro cavity hollow cathode discharge based GC-detector 99
5.1. Introduction 102
5.2. Experimental 107
5.2.1. Reagents 107
5.2.2. Chromatographic system and headspace (HS) sampler conditions 107
5.2.3. Preparation of solutions and sample vials 108
5.2.4. µCHCD set-ups investigated 109
5.3. Results & Discussion 114
5.3.1. Initial testing with the co-axial µCHCD detector set-up 114
5.3.2. Serial axial µCHCD detector – version 1 116
5.3.3. Serial axial µCHCD detector – version 2 119
5.3.4. Comparison to other techniques 126
5.4. Conclusions 127
5.5. References 128
Chapter 6 - General discussion **133**
Summary **142**
Samenvatting **144**

List of abbreviations and symbols

A	anode
AD	analog-to-digital
AED	atomic emission detector
Ag	silver
Amp	amplifier
β	phase ratio
BA	benzyl alcohol
Bp	boiling point
BSTFA	N,O-Bis(trimethylsilyl)trifluoroacetamide
BZOCl	benzoxonium chloride
BZTCl	benzethonium chloride
C	camphor
°C	degrees Celsius
C_0	Analyte concentration in a sample
Cap	capture electrode
CCl_4	carbon tetrachloride
CE	capillary electrophoresis
CFD	Computational Fluid Dynamics
C_g	concentration in the gas phase
C_l	concentration in the liquid phase
CPE	cloud point extraction
d	cathode-anode distance
D	internal diameter of a hollow cathode
DB	denatonium benzoate
DBD	dielectric barrier discharge
DC	direct current
2,2-DD	2,2-dimethyl-1,3-dioxolane
df	degrees of freedom
d_f	film thickness
2D-GC	two dimensional gas chromatography
DH	detector housing
dHS	dynamic headspace

DMA	N,N-dimethylacetamide
DMF	N,N-dimethylformamide
DMP	2,2-dimethoxypropane
DMSO	dimethylsulfoxide
ECD	electron capture detector
EG	ethylene glycol
EI	electron ionization
EtS	ethyl salicylate
eV	electron volts
FET	full evaporation technique
FID	flame ionization detector
g	grams
GC	gas chromatography
GD	glow discharge
HC	hollow cathode
HCl	hydrochloric acid
He^+	helium ions
He-PDPID	helium pulsed discharge photo ionization detector
HS	headspace
ICH	International Conference on Harmonisation
ICP	inductively coupled plasma
I.D.	internal diameter
IMS	ion mobility spectrometry
Ir	iridium
K	distribution coefficient
K	Kelvin
kHz	kilohertz
kPa	kilopascal
LC	liquid chromatography
LOQ	limit of quantification
M	DL-menthol
m	metre
µA	micro ampere
MEK	methyl ethyl ketone

MeS	methyl salicylate
mg	milligram
µCHCD	micro cavity hollow cathode discharge
MHE	multiple headspace extraction
mL	milliliter
µg	microgram
µL	microliters
µm	micrometres
mm	millimetres
Mo	molybdenum
MΩ	mega ohm
MS	mass spectrometry
MTBE	methyl t-butyl ether
mV	millivolt
NCD	nitrogen chemiluminescence detector
ng	nanogram
^{63}Ni	nickel 63 isotope
nL	nano litre
NMP	N-methyl-2-pyrrolidone
NO	nitric oxide
NO_2	nitrogen dioxide
NPD	nitrogen-phosphorus detector
O_3	ozone
O.D.	outer diameter
Pb	lead
p*d	product of pressure and electrode distance
PDD	pulsed discharge detector
PDECD	pulsed discharge electron capture detector
PDED	pulsed discharge emission detector
pg	picogram
PID	photo ionization detector
PLOT	porous layer open tubular
$p_{partial}$	partial gas pressure
PTFE/Sil	polytetrafluoroethylene/silicone

p_{total}	total gas pressure
PTV	programmed temperature vaporizer
Q	quartz
QAS	quaternary ammonium salts
R^2	determination coefficient
R_b	ballast resistance
RSD	relative standard deviation
SAM	standard addition method
SBSE	stir bar sorptive extraction
SCD	sulphur chemiluminescence detector
SCOT	support coated open tubular
SDME	single drop micro extraction
SFE	supercritical fluid extraction
sHS-GC	static headspace-gas chromatography
Sn	tin
SO_2	sulphur dioxide
SPME	solid phase micro-extraction
S_{slope}	standard error of the slope
SWE	super critical water extraction
S_{yx}	standard error of estimate
STEL	short term exposure limit
T	temperature in Kelvin
$t_{crit.}$	critical t-value for a number of degrees of freedom
t (min)	time in minutes
TCD	thermal conductivity detector
TCE	trichloroethylene
$t_{experimental}$	experimental t-value
Torr	Torricelli
U	power source
U-I	voltage-current
UV	ultraviolet
V	volt
V_b	breakdown voltage
$V.cm^{-1}$	unit for electric field strength

vs.	versus
% v/v	volume per volume percentage
W	tungsten
WCOT	wall coated open tubular
x_i	mole fraction
γ_i	activity coefficient

Chapter 1 - General introduction

1.1. Gas chromatography as analytical tool

1.1.1. Introduction

Separation techniques such as liquid chromatography (LC) and capillary electrophoresis (CE) are often used to separate non-volatile and often large molecules in various matrices. These techniques are however less suitable for small volatile molecules such a many residual solvents. Therefore, such molecules are usually analysed with gas chromatography (GC). GC is one of the most versatile analytical techniques available for the separation of volatile analytes in various sample matrices for both qualitative and quantitative analysis. In GC, a sample is introduced in the instrument as a vapour by injection into a heated inlet. The vapours are swept through the inlet by an inert carrier gas into an analytical column for separation. Separation of various analytes is occurring by equilibration between the stationary phase and the carrier gas. The separated analytes are detected using various detectors after elution from the column. The response signal of the detector is recorded in function of time (retention time) in which analytes appear as nearly Gaussian shaped peaks. The area under an analyte peak is proportional to its concentration in the original sample matrix. A schematic overview of a GC system is depicted in Figure 1.1.

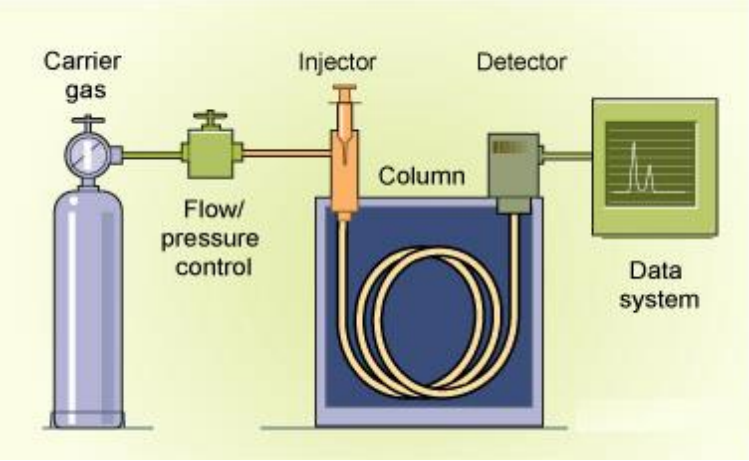

Figure 1.1: Schematic overview of a GC system[1].

1.1.2. Inlet

There are basically three different types of inlets: the split/splitless inlet [1,2], the programmed temperature vaporizer (PTV) [3,4] and the on-column inlet [5]. The most often used inlet is the split/splitless injector where the split mode is used for more concentrated samples to avoid overloading of the analytical column and/or detection signal. On the other hand, splitless injection transfers the complete sample to the column and is used when more sensitivity is required. An on-column inlet also introduces the sample entirely on the column, but without prior evaporation. The PTV inlet is usually used to perform large volume injections for

more sensitivity. During the sample introduction, solvent is vented at a low inlet temperature to prevent backflash of solvent causing contamination of the GC system.

1.1.3. Column

The column is where the separation takes place after introduction of the sample. Within GC analysis, two different types of columns exist: packed columns and capillary columns. A packed column is typically made from a glass or stainless steel coil with lengths ranging from 1 – 5 m. The column is filled with particles that act as stationary phase. Nowadays, packed columns are merely used for preparative work and have been replaced by capillary columns due to superior separation efficiencies. Capillary columns consist of fused silica with a polyimide coating on the exterior and can have lengths from 15 m up to 100 m with internal diameters from 0.10 to 0.53 mm. Three different types of capillary columns can be distinguished, which are the Wall Coated Open Tubular (WCOT), the Support Coated Open Tubular (SCOT) and the Porous Layer Open Tubular (PLOT) columns. A WCOT column uses a thin film coated on the inner surface of the fused silica as stationary phase. SCOT columns use particles that are modified with a stationary phase and are deposited on the column wall. With the PLOT columns particles act as the stationary phase itself.

1.1.4. Carrier gas

As mentioned above, the carrier gas is responsible for the transport of analytes through the column. The carrier gas is inert towards the analytes and separation mainly depends on the characteristics of the stationary phase. Typical carrier gasses include helium, nitrogen, hydrogen, carbon dioxide and argon. Helium is used most often for its safety in comparison with hydrogen and the higher separation efficiency compared to the other gasses [6].

1.2. Headspace sample introduction

1.2.1. Overview of sample introduction techniques

For the introduction of a sample into a GC system, direct injection is the most widely used approach. The sample is usually dissolved in an appropriate solvent and injected in a heated injection port to evaporate the volatile sample constituents using a syringe. Since the development of GC, several alternative sample introduction and isolation techniques have been developed and implemented. These include techniques such as thermal desorption using solid phase micro extraction (SPME), stir bar sorptive extraction (SBSE), single drop micro extraction (SDME). Other techniques include headspace (HS) sampling methods, pyrolysis and purge and trap. SPME and SBSE rely on the adsorption of analytes on an adsorbent for sample enrichment and analytes are released into a GC by heating of the adsorbent. SDME uses a solvent drop to

extract analytes from samples. This can be performed in two ways: the extraction is performed by direct immersion in the sample solution in which the solvent drop is immiscible. Another approach is to suspend the droplet above the headspace for extraction.

In this thesis, three research chapters are devoted to the alternative use of HS equipment. Therefore, the following paragraphs will cover some items related to HS sampling.

1.2.2. Basic theory of HS sampling

The theory of HS sampling has been extensively explained in literature [7] and only relevant aspects of this technique will be described here. When HS sampling is used, a sample is heated and an aliquot of the vapour phase (headspace) containing the volatile analytes is introduced on the column for analysis. HS analysis can be performed both statically (sHS) and dynamically (dHS). dHS is performed by purging with an inert gas whilst heating in an open vial in contrast to sHS sampling that occurs in a closed vial. sHS sampling can be done by using a gas tight syringe, a sample loop system or a balanced pressure system. With sHS analysis, a particular sample is usually dissolved in a suitable high boiling solvent after which a part of the sample is transferred to a HS vial and closed with a cap having a septum. Afterwards, the sample vial is heated for a certain time causing the volatile analytes to move towards the vapour phase until a thermodynamic equilibrium is reached (Figure 1.2).

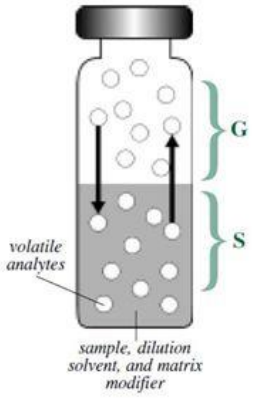

Figure 1.2: Schematic overview of a HS vial in sHS conditions[8].

The HS vial containing the sample is characterised by the so-called phase ratio β according to (1):

$$\beta = \frac{V_g}{V_l} \qquad (1)$$

In which V_g and V_l are the volume of the gas phase and liquid phase, respectively.

The partition of a given analyte between the two phases under a certain situation can be expressed by the partition coefficient K:

$$K = \frac{C_l}{C_g} \qquad (2)$$

C_l is the concentration of the analyte in the liquid phase and C_g is the concentration in the gas phase. Under sHS conditions both β and K are constant. The analyte concentration in the gas phase is then given by:

$$C_g = \frac{C_0}{K+\beta} \qquad (3)$$

Which relates the initial sample concentration (C_0) with the gas phase concentration after thermodynamic equilibrium is established. A certain analyte having a concentration C_0 will generate a concentration C_g giving rise to a peak with a proportional area depending on K and β. In practice, the partition coefficient K is very difficult to predict and is influenced by many different factors. In the text below, various relevant factors will be briefly explained.

Dalton's law

Dalton's law describes that the total pressure (p_{total}) of a given gas mixture can be considered as the sum of the partial pressures ($p_{partial}$) of all the separate constituents present in the gas mixture. This means that the gas phase concentration of an analyte is depending on its partial pressure:

$$p_{partial} \propto C_g \qquad (4)$$

The partial pressure of a certain analyte is depending on the temperature. Increasing the temperature will increase the partial pressure and also C_g so that K will change as well.

Raoult's law

The partial pressure of an analyte is directly proportional to its mole fraction (x_i) in a sample solution:

$$p_{partial} = p_i^0 \times x_i \qquad (5)$$

In which p_i^0 is the vapour pressure of a certain analyte which is influenced by the temperature as well according to Antoine's equation:

$$\log p_i^0 = A - \frac{B}{T+C} \qquad (6)$$

A,B and C are so-called Antoine coefficients and are specific for an analyte. T is the temperature in Kelvin. Raoult's law is only valid in situations where analytes are completely inert towards each other. However, most sample solutions deviate from this as there are interactions and usually an adapted form of Raoult's law is used:

$$p_{partial} = p_i^0 \times \gamma_i \times x_i \quad (7)$$

This adapted form of Raoult's law uses the activity coefficient γ_i to correct for any possible interaction of a certain analyte with components from its environment.

1.2.3. Balanced pressure system

The balanced pressure system is depicted in Figure 1.3. Sampling with this system proceeds in 3 phases. Firstly, the vial is thermostatted and the sampling needle (SN) will be in its standby position (stage A). Carrier gas flowing through valve 1 (V_1) is split up between the transferline connecting the HS sampler with the inlet of the GC and the hollow needle that contains two holes. Valve 2 (V_2) is open enabling the carrier gas to leave the system. After heating of the sample vial and establishing thermodynamic equilibrium, the needle punctures the septum of the vial which is pressurized (stage B). By closing both valves 1 and 2, a part of the headspace is injected to the GC column (COL) (stage C).

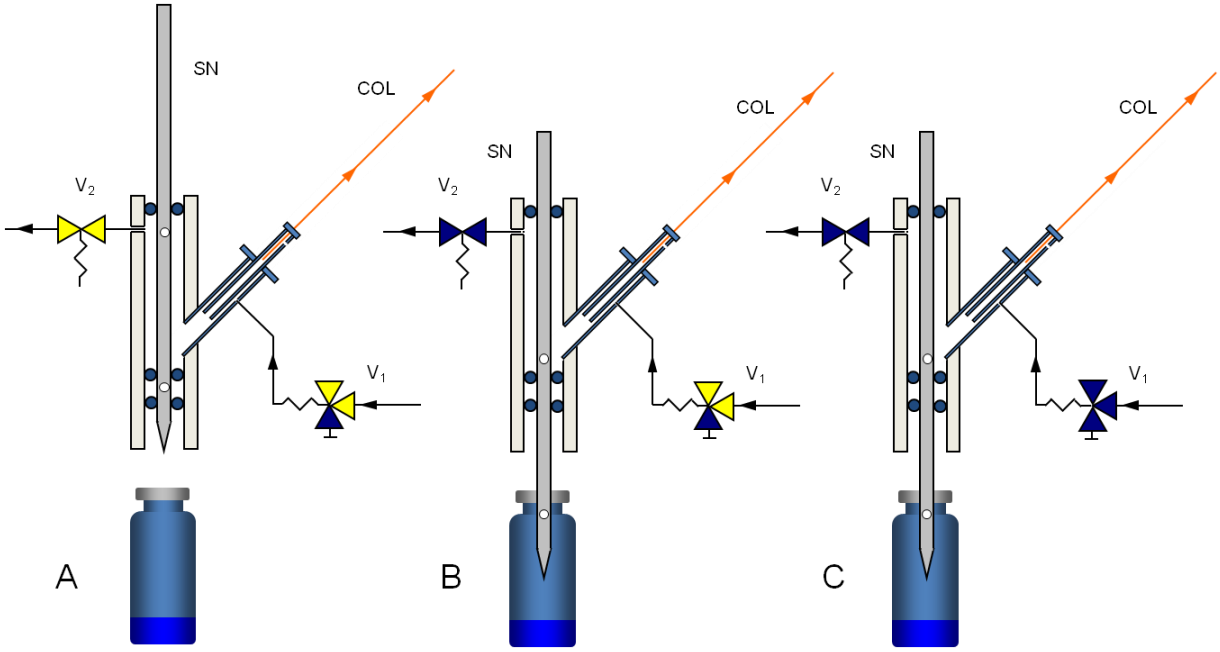

Figure 1.3: Schematic drawing of the balanced pressure system and stages of operation. A = thermostatting, B = pressurisation, C = injection. Reproduced from [7].

1.2.4. Full evaporation technique (FET)

FET is a form of HS sampling in which the compounds of interest are completely evaporated in the vial, to ensure that a given analyte has no sample phase to have interaction with (no equilibrium). This feature eliminates possible matrix effects and allows quantification without the need for a matching matrix. It has been applied to solid and liquid samples [9-14]. Furthermore, FET was found to be particularly useful for analytes that have a higher boiling point than the sample matrix [15]. More background information about this technique will be given in chapter 2.

1.2.5. Shortcomings of HS-GC

In various fields of chemical analysis GC is the tool of choice for the screening and determination of volatile substances. sHS-GC in combination with various detectors is an established technique that is often used for the analysis of various volatiles in many different matrices due to its aforementioned advantages. Despite these advantages, several shortcomings can be summed up for this technique. First of all, sHS sampling is often suffering from matrix effects as predicted by Raoult's law. Matrix effects influence the resulting partial pressure of an analyte and thus the response factor can differ from a calibration standard which is made without matrix components. This issue can be circumvented by matching the calibration solution with that of the sample. However, blank matrix or information about the exact composition is often not available. Besides, the sHS approach does generally not provide adequate sensitivity for analytes with a high affinity

for a particular matrix. Increasing the HS temperature does generally promote more analyte to the gas phase. However, at some point, the sample solvent starts to boil which results in a pressure that is too high for a HS instrument to handle. Therefore, the determination of high boiling analytes in a low boiling matrix is problematic. Besides, thermally labile compounds could start to degrade when the used temperature is too high. To address the problem of possible matrix effects and to overcome sensitivity issues often encountered with sHS sampling, FET has been used to fully evaporate typical polar high boiling residual solvents such as N,N-dimethylformamide (DMF) or dimethylsulfoxide (DMSO) in aqueous samples. These solvents are high boiling compared to water and have a large affinity for water (miscible). In contrast to the sHS methodology, FET does provide adequate sensitivity for such analytes. Possible matrix effects are circumvented as the complete volatile part of the sample is evaporated so that no equilibrium between analytes and matrix can be formed. The sensitivity that can be obtained by FET is still rather limited as the sample volume should not exceed a certain volume. A sample volume that is too large could lead to incomplete evaporation thereby creating sHS conditions again. Also, the pressure in the vial can exceed the maximum tolerable pressure at a certain sample volume. The pressure in a vial is especially governed by both the vapour pressure of the solvent and the air that is already present in the vial and expands upon heating. As predicted by the ideal gas law, smaller molecular masses lead to lower maximum tolerable sample volumes. Due to this, the sample volume for aqueous samples is limited to approximately 10 µL in a HS vial of 22 mL. The analysis of analytes as aforementioned remains problematic when higher sensitivity is required. When large amounts of aqueous samples are introduced in the GC system to increase the sensitivity, there is a serious risk to damage the GC column. Moreover, aqueous samples do generally not allow derivatization of analytes to improve their volatility, chromatographic properties or sensitivity. Some analytes such as certain polymers or quaternary ammonium salts (QAS) are not volatile at all and require pyrolysis to generate representative volatile products for GC analysis. When these types of analytes have to be determined in aqueous samples, the water will create the aforementioned issues, especially when pyrolysis is carried out with direct injection.

1.3. GC detectors

Apart from various sampling techniques, various detectors have been developed. Detectors can be either universal or selective. In the following paragraphs an overview is given of detectors that are commercially available.

1.3.1. Thermal conductivity detector (TCD)

The TCD or 'hot wire' was the first detector used for GC and is a universal detector that can detect every possible analyte. When gas flows over a hot filament, the electric resistance will be stable as long as the thermal conductivity remains constant. Since every gas has a different thermal conductivity, the TCD will produce a different signal when an analyte passes through. The TCD works with two filaments: one acts as reference in which the pure carrier gas is monitored, the second one is exposed to the carrier gas with the separated analytes (Figure 1.4). Both filaments are connected by a 'Wheatstone bridge' that measures the difference in their resistance. When no sample constituents pass through the detector, no difference in thermal conductivity is detected. When an analyte passes by, a small change in resistance is established which is a measure for the concentration of a certain analyte. The TCD is usually used for the detection of permanent gasses such as carbon dioxide and carbon monoxide and is considered to be a very simple low cost detector that is non-destructive to the sample. An example of a TCD application is the determination of carbonate in black liquor samples using HS-GC [16]. Samples were acidified with sulphuric acid in a HS vial and the released carbon dioxide was detected using TCD allowing the indirect determination of carbonate.

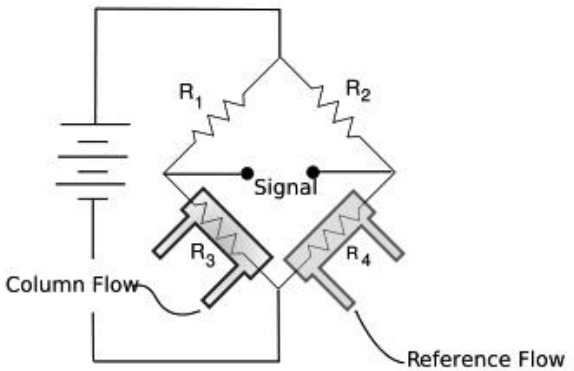

Figure 1.4: Schematic overview of a TCD[1].

1.3.2. Flame ionization detector (FID)

Since its introduction as a detector for GC by McWilliam and Dewar [17] and Harley and his co-workers [18], the FID has become the most popular GC detector due to its excellent sensitivity for organic analytes, robustness and exceptional linear range. The FID is a near universal detector, providing an almost equal molar response for hydrocarbons which is based on the number of carbon atoms present in the analyte molecule. A schematic overview of an FID is given in Figure 1.5.

Analytes that elute from the column are directed towards a hydrogen-air diffusion flame and are subsequently combusted to produce carbon dioxide, water and CH-radicals which can react further to form charged species:

$CH^{\cdot} + O^{\cdot} \rightarrow CHO^{+} + e^{-}$

These charged species react with water molecules present in the flame to produce hydronium ions and carbon monoxide:

$CHO^{+} + H_2O \rightarrow H_3O^{+} + CO$

The positively charged species are captured by a negatively biased collector electrode which is positioned above the flame to produce a measurable current proportional to the number of carbon atoms present in the flame at a certain time. Collection of ions is facilitated by the use of an extraction potential or a make-up gas flow to accelerate the formed ions towards the collector.

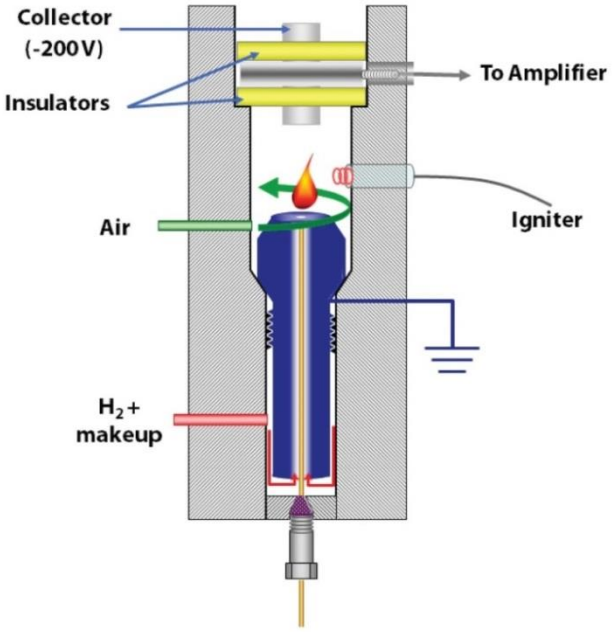

Figure 1.5: Schematic overview of a FID[19].

1.3.3. Electron capture detector (ECD)

The ECD [20-22] is a detector that provides a selective response towards analytes possessing electronegative functional groups such as halogen atoms and nitro groups. A response is provided by the fact that these analytes capture low energy thermal electrons which are usually generated by high energy beta-electrons coming from a foil containing ^{63}Ni through interaction with the carrier gas.

The electrons are collected at an anode and a change in the existing current occurs when an electron capturing analyte passes through the detector. Due to its excellent sensitivity for such analytes, it is a popular detector for the determination of pesticides and other electronegative atom containing analytes in the environment [23-25] and food [26-28]. An example of such application is the determination of organochlorine pesticides in water samples [29]. Typical persistent organochlorine pesticides such as Endosulfan I and II were first extracted using a special designed molecular imprinted SPME prior to GC-ECD detection. The SPME was imprinted with Endosulfan to serve as selective binding site for Endosulfan in aqueous samples. Detection limits for this approach were found to be in the lower ng L^{-1} range.

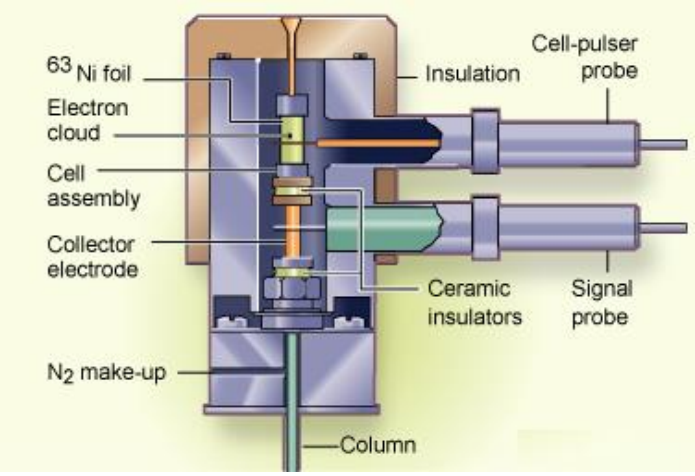

Figure 1.6: Schematic overview of the ECD[1].

1.3.4. Thermoionic ionization detector (TID)

The TID, sometimes also called alkali flame detector or nitrogen-phosphorus detector (NPD), is basically an adapted FID [30-31]. When an alkali metal salt is introduced in the hydrogen-air diffusion flame of an FID during analysis, it improves the sensitivity for compounds that contain hetero-atoms such as nitrogen, phosphorus, sulphur and bromine. In early versions of the TID, an alkali salt was introduced by means of a constant supply of an aqueous solution containing an alkali salt such as sodium hydroxide. Nowadays, a TID makes use of a ceramic or glass bead that is doped with Rubidium or Cesium. During operation of the detector, this bead is heated by an electrical wire to temperatures between 400 and 800 °C.

In contrast to FID, the detector gas flows are significantly lower and insufficient to form a flame. Instead, a low temperature plasma is formed in which hydrogen, oxygen and hydroxyl radicals are formed from the detector gasses. The collector electrode is positioned right above the bead and is positively biased for negative ion collection. Although the detection mechanism of this detector is not fully understood, negative ions are thought to originate from decomposition products such as CN^- from $CN^\cdot$ in case of nitrogen species and PO^-, PO_2^-, PO_3^- out of $PO_2^\cdot$ when analytes containing phosphorus atoms are measured. The TID can be set to detect both phosphorus and nitrogen species by using a hydrogen rich plasma (NP-mode) or a hydrogen poor oxidative plasma for higher selectivity towards phosphorus analytes (P-mode), respectively. The TID is especially important for the analysis of drugs, pesticides and herbicides as these analytes often contain nitrogen or phosphorus heteroatoms [32-35]. A typical example for the application is the determination of organophosphorus pesticides such as diazinon in animal matrices [36]. These types of pesticides can accumulate in animals due to the consumption of contaminated feed and water. Animal derived products can therefore be an indirect source and can be a risk for human health. A method was developed for the determination of several organophosphorus pesticides in cow milk and liver tissue from wild boar. After extraction and clean-up of the samples, they were subjected to GC-NPD analysis for quantification. Detection limits were found to be in the lower ppb range for each analyte. A schematic overview of a NPD detector is given in Figure 1.7.

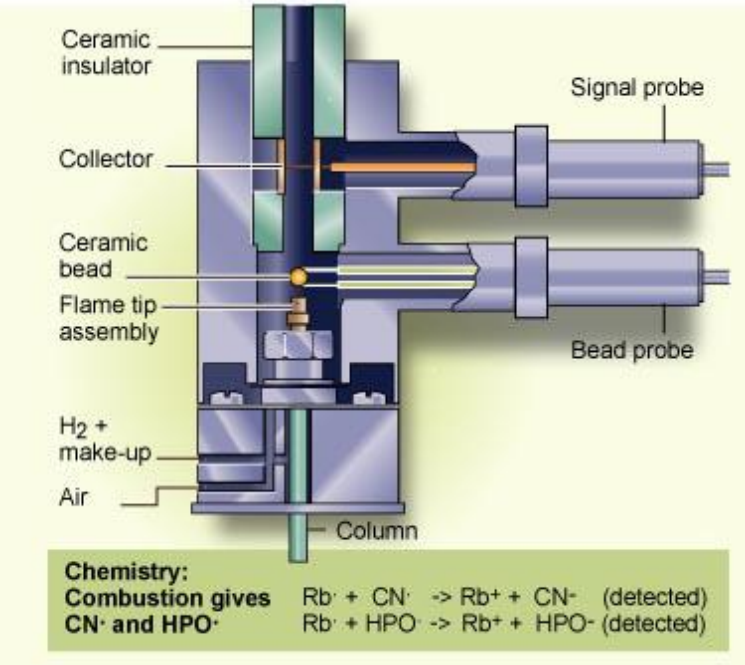

Figure 1.7: Schematic overview of the TID[1].

1.3.5. Chemiluminescence based sulphur and nitrogen detectors

One of the most well-known chemiluminescence based detectors are the sulphur luminescence detector (SCD) and the nitrogen chemiluminescence detector (NCD). These detectors (Figure 1.8) are often used for the 2D-GC analysis of crude oil samples for sulphur [37-41] and nitrogen atom [42] containing species such as thiols, sulphides, polysulfides and thiophenes.

Crude oil is an extremely complex mixture consisting of alkanes, naphthenes, olefins, monoaromatics, polyaromatics and many others. Such samples are even challenging for 2D-GC and selective sulphur and nitrogen detection is therefore needed. The SCD is superior among various types of sulphur selective detectors. It has many advantages including a linear ($>10^5$) and equimolar response to all sulphur compounds, modest quenching effects of hydrocarbons, excellent sensitivity (<0.5 pg S/s), and by far the best selectivity (S/C $>10^7$). Both the NCD and the SCD operate according to a similar mechanism. The first step is the universal conversion of nitrogen or sulphur containing analytes to either sulphur dioxide (SO_2) or nitric oxide (NO) (1). The second step for the detection of sulphur species is the reaction of SO_2 with hydrogen gas (2) to form chemiluminescent species. Then these sulphur species react with ozone (O_3) to form excited state SO_2 that emits light upon relaxation (3). In case of nitrogen analytes, the resulting NO from the first step reacts with O_3 to form excited state nitrogen dioxide (NO_2) that also emits light (4).

$$\text{R-S (N)} + O_2 \rightarrow CO_2 + H_2O + SO_2 \quad (NO) \qquad (1)$$

$$SO_2\,(NO) + H_2 \rightarrow \text{chemiluminescent sulphur species} \qquad (2)$$

$$\text{chemiluminescent sulphur species} + O_3 \rightarrow SO_2^{*} \rightarrow SO_2 + h\nu \qquad (3)$$

$$NO + O_3 \rightarrow NO_2^{*} \rightarrow NO_2 + h\nu \qquad (4)$$

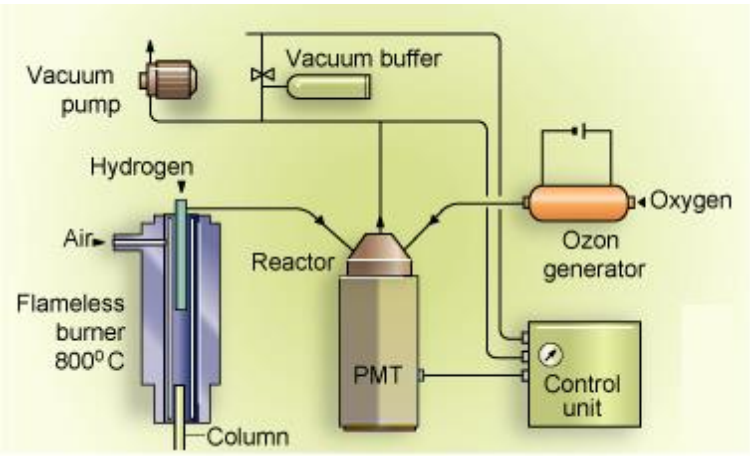

Figure 1.8: Schematic overview of SCD/NCD detection system[1].

1.3.6. Photoionization detector (PID)

By irradiating molecules with photons that exceed the ionization energy, ionization can take place. This is the basic working principle of the PID and typically requires photon energies between 5 and 20 eV. A schematic overview of a PID is given in Figure 1.9 and employs a low-pressure gas discharge lamp, which depending on the filling gas emits typical spectral lines. Examples of filling gases are Xenon, Krypton or Argon to produce photon energies up to 11.7 eV. By carefully selecting the type of lamp, selectivity can be obtained that is based on the difference in ionization potential of various analytes. During operation, analytes eluting from a GC column are ionised in an ionization chamber and directed towards a biased electrode to produce a current. In contrast to FID, ECD and TID, no additional make-up or fuel gas is needed and PID is therefore often used in portable applications where for instance no flame can be used for hazard reasons. For example in [43], a mobile robot was equipped with a PID for the detection and quantification of volatiles. The PID was calibrated for the detection of acetone vapour to demonstrate the applicability of the robot.

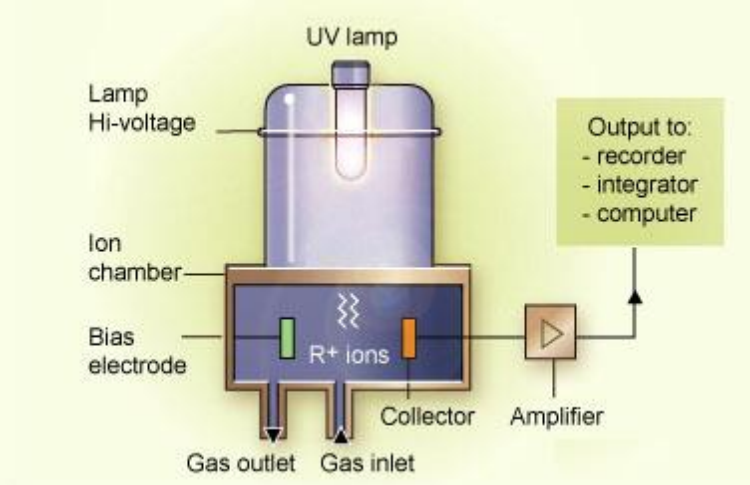

Figure 1.9: Schematic overview of the PID[1].

1.3.7. Helium ionization detector (HID)

HIDs are detectors that are often used to detect permanent gases such as hydrogen, oxygen or nitrogen in cases where more sensitivity than with the TCD is needed. Also, organic compounds such as carbon tetrachloride can be measured with this type of detector. There are basically two different types of HIDs: one uses a radioactive material, while the other uses a pulsed discharge source. In case of HIDs that utilise a radioactive material, helium molecules collide with high energy beta electrons that are emitted from usually a Scandium tritide foil with high activity. This creates a plasma that contains metastable species responsible for analyte ionization. More modern HIDs make use of a high voltage pulsed discharge (PDHID) [44-51] and consist of a discharge chamber and a region where incoming analytes are ionized mainly by photoionization

as the gas discharge emits high energy photons (Figure 1.10). These high energy photons come from the dissociation of diatomic helium with energies ranging from 11.3 to 20.7 eV. Actual analyte detection is usually performed by electrons released from analytes due to ionization that migrate towards a biased collector electrode. The PDHID can be operated in an electron capture mode as well (PDECD) [52] which is done by generation of thermal ions from a dopant gas such as methane or Xenon. These thermal electrons (as with the ECD) can be captured by for instance halogenated analytes.

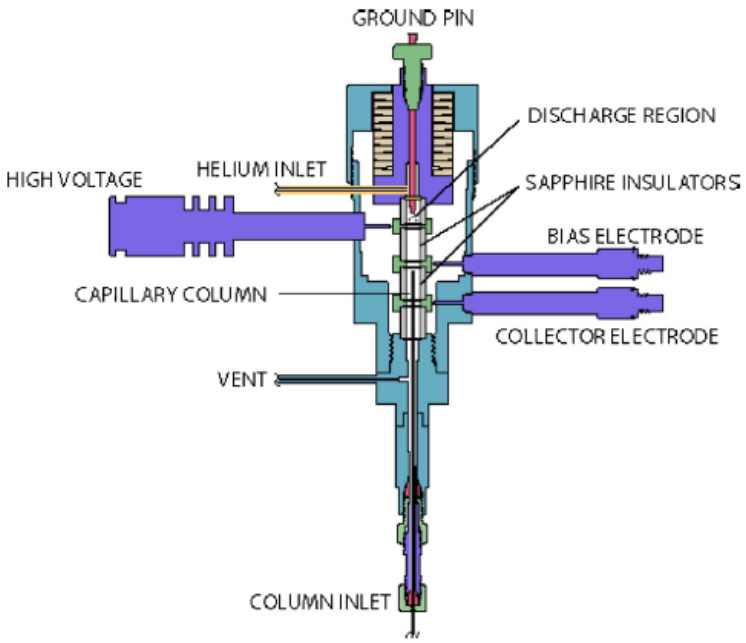

Figure 1.10: Schematic overview of a PDHID[53].

1.3.8. Mass spectrometer as detection system

A mass spectrometer (MS) is in fact a second separation dimension that separates ions according to their mass-to-charge (*m/z*) ratios after ionization. An MS consists of three parts: the ion source, mass analyser and ion detector. The most common form of mass spectrometry in combination with GC is electron impact (EI) with a quadrupole mass analyser. Analytes that elute from the column are bombarded with high energy electrons (70 eV) and mostly positive molecular ions will be formed. These molecular ions will break into fragment ions that can be used to identify unknown analytes. A quadrupole MS (used in this work) is often operated in full scan mode for confirmation in which a certain *m/z* range is continuously scanned over time to produce mass spectra. This results in a total ion current (TIC) chromatogram and at each time point (scan number), the mass spectrum can be consulted. In case of EI mass spectrometry, analytes produce a unique mass spectrum which can be compared with library spectra. Although an MS is not a true detector for quantification, it is often used as such by operation in single ion monitoring mode (SIM).

With SIM, only ions with particular *m/z* values are allowed to be detected and target analytes will be selectively detected for quantification.

1.3.9. Shortcomings of GC detectors

Since its development, the FID became the workhorse for quantitative GC analysis of various carbon atom containing compounds. The FID is known for its simple construction, ease of operation, robustness and unsurpassed sensitivity for alkanes. However, compounds containing heteroatoms such as oxygen, nitrogen, sulphur, phosphorus, chlorine, bromine and iodine are detected with less sensitivity because carbon atoms are only partly oxidised in such substances. This makes the FID detector unsuitable for the detection of analytes such as carbon tetrachloride which contains only one fully substituted carbon atom that cannot be oxidised. Moreover, the FID does not provide the possibility to identify or provide structural information for unknown compounds that could be detected during screening. Identification is only possible with suitable reference standards of which retention times are compared with these of unknowns. For this reason, analytes such as polychlorobiphenyls (PCBs), nitrogen or phosphorus containing pesticides and herbicides are usually detected with the aforementioned selective detectors such as the ECD or TID. However, the radio-active element that is used in the ECD gives rise to legislation issues and as with all selective detectors universality is lost. Mass spectrometry (MS) can both serve to identify and quantify analytes. However, MS needs an expensive vacuum system to operate and the ionization efficiency of the used filament with EI is rather low like the hydrogen diffusion flame of the FID. Where the TCD is generally not sensitive enough, the PDHID is often employed as detector for trace analysis. However, this detector uses a fairly high helium make-up flow (30 mL/min) to counteract the column flow containing the analytes to avoid direct interaction with the discharge. The necessity for high helium flows is not desired as helium becomes increasingly more expensive and possible ionization pathways are limited due to the detector set-up. It is true that many of the described GC detectors need additional gases and vacuum (in case of the SCD, NCD and MS) for operation which limits the portability. PID on the other hand is not sensitive for halogenated aliphatics and has no response at all for methane.

1.4. Aim of the study

Seen the drawbacks of sHS, in chapter 2 the use of FET is explored for the analysis of different high boiling apolar analytes in apolar matrices. To avoid the problems related to GC analysis of aqueous samples, removal of water prior to GC analysis of aqueous samples is necessary. This can be performed with techniques such as HS trap which uses an adsorbent to selectively retain analytes and allows sample enrichment. However, this approach could still result in problems with analytes such as ethylene glycol (EG) that are prone to interact with parts of the system. An easier approach would be to remove the water before GC analysis is performed. So, Chapter 3 is devoted to the application of water scavenging using acetone acetals in an attempt to enrich aqueous samples prior to FET analysis. Chapter 4 deals with the problems related to the analysis of QAS in aqueous samples by investigating whether the use of HS sampling can generate volatile products for the indirect quantification of various QAS. Such approach would be beneficial as non-volatile degradation products are not introduced in the GC system leading to a more robust method.

Where chapters 2-4 mainly cover aspects of improved sample introduction and sample preparation, chapter 5 is focusing on GC detectors. Many issues around the existing GC detectors are related to their ion source and a detection system that can circumvent the issues discussed in 1.3.9. would be very beneficial. A prototype GC detector using a microhollow cathode discharge (MHCD) as ion source is presented as alternative to the described detectors. A detector using an ion source with higher ionization efficiency and possibility to obtain structural information could possibly replace many of the aforementioned GC detectors. In this chapter, the theory around MHCD's is covered and experimental results around the development are presented.

1.5. References

[1] D.C. Harris, 2005, Quantitative chemical analysis, W.H. Freeman and Company, USA 7th Ed., 538-540

[2] Snow, N. H. In Modern Practice of Gas Chromatography, 4th ed.; Grob, R. L., Barry, E. F., Eds.; John Wiley & Sons: Hoboken, NJ, 2004.

[3] K. Grob, T. Laubli, High oven temperature on-column injection in capillary gas chromatography II. Avoidance of peak distortion, J. Chromatogr. A, 357 (1986) 345-355

[4] W. Vogt, K. Jacob, H.W. Obwexer, Sampling method in capillary column gas—liquid chromatography allowing injections of up to 250 µL, J. Chromatogr. A, 174 (1979) 437-439

[5] W. Vogt, K. Jacob, A. Ohnesorge, H.W. Obwexer, Capillary gas chromatographic injection system for large sample volumes, J. Chromatogr. A, 186 (1979) 197-205

[6] J.J. van Deemter, F.J. Zuiderweg, A. Klinkenberg, Longitudinal diffusion and resistance to mass transfer as causes of nonideality in chromatography, Chem. Eng. Sci. 5 (1956) 271-289

[7] B. Kolb, L. Ettre, Static Headspace – Gas chromatography: Theory and Practice, 2nd ed.; Wiley-VCH: Weinheim, 1997.

[8] A Technical Guide for Static Headspace Analysis Using GC, Restek Corp. (2000).

[9] A. Brault, V. Agasse, P. Cardinael, J.C. Combret, The full evaporation technique: A promising alternative for residual solvent analysis in solid samples, J. Sep. Science, 28 (2005) 380-386

[10] X.S. Chai, Q.X. Hou, F.J. Schork, Determination of residual monomer in polymer latex by full evaporation headspace gas chromatography, J. Chromatogr. A, 1040 (2004) 163-167

[11] H. Li, H. Zhan, S. Fu, M. Lui, X.S. Chai, Rapid determination of methanol in black liquors by full evaporation headspace gas chromatography, J. Chromatogr. A, 1175 (2007) 133-136

[12] M. Markelov, J.P. Guzowski Jr, Matrix independent headspace gas chromatographic analysis. The full evaporation technique, Anal. Chim. Acta, 276 (1993) 235-245

[13] J. Schuberth, Volatile organic compounds determined in pharmaceutical products by full evaporation technique and capillary gas chromatography/ion-trap detection, Anal. Chem., 68 (1996) 1317-1320

[14] J. Schuberth, A full evaporation headspace technique with capillary GC and ITD: A means for quantitating volatile organic compounds in biological samples, J. Sep. Science, 34 (1996) 314-319

[15] D.M. Kialengila, K. Wolfs, J. Bugulama, A. Van Schepdael, E. Adams, Full evaporation headspace gas chromatography for sensitive determination of high boiling point volatile organic compounds in low boiling matrices, J. Chromatogr. A, 1315 (2013) 167-175

[16] X.S. Chai, Q. Luo, J.Y. Zhu, Analysis of non-volatile species in a complex matrix by headspace gas chromatography, J. Chromatogr. A, 909 (2001) 249-257

[17] I.G. McWilliam, R. A. Dewar, Flame ionization detector for gas chromatography, Nature, 181 (1958) 760-760

[18] J. Harley, W. Nel, V. Pretorius, Flame ionization detector for gas chromatography, Nature, 181 (1958) 177-178

[19] www.sepscience.com. Accessed on 1-7-2016.

[20] J.E. Lovelock, The electron capture detector, J. Chromatogr., 99 (1974) 3-12

[21] E.D. Pellizari, Electron capture detection in gas chromatography, J. Chromatogr., 98 (1974) 323-361

[22] J.E. Lovelock, A.J. Watson, Electron capture detector. Theory and practice, J. Chromatogr., 158 (1978) 123-138

[23] Y.S. Su, J.F. Jen, Determination of organophosporous pesticides in water using in-syringe ultrasound-assisted emulsification and gas chromatography with electron-capture detection, J. Chromatogr. A, 1217 (2010) 5043-5049

[24] N. Fattahi, Y. Assadi, M.R.M. Hosseini, E.Z. Jahromi, Determination of chlorophenols in water samples using simultaneous dispersive liquid-liquid microextraction and derivatization followed by gas chromatography-electron-capture detection, J. Chromatogr. A, 1157 (2007) 23-29

[25] M.Y. Tsai, P.V. Kumar, H.P. Li, J.F. Jen, Analysis of hexachlorocyclohexanes in aquatic samples by one-step microwave-assisted headspace controlled-temperature liquid-phase microextraction and gas chromatography with electron capture detection, J. Chromatogr. A, 1217 (2010) 1891-1897

[26] C.K. Zacharis, I. Rotsias, P.G. Zachariadis, A. Zotos, Dispersive liquid-liquid microextraction for the determination of organochlorine pesticides residues in honey by gas chromatography-electron capture and ion trap mass spectrometric detection, Food Chemistry, 134 (2012) 1665-1672

[27] P.C. Abhilash, V. Singh, N. Singh, Simplified determination of combined residues of lindane and other HCH isomers in vegetables, fruits, wheat, pulses and medicinal plants by matrix solid-phase dispersion (MSPD) followed by GC-ECD, Food Chemistry, 113 (2009) 267-271

[28] G.P. de Pinho, A.A. Neves, M.E.L.R. de Querioz, F.O. Silvério, Optimization of the liquid-liquid extraction method and low temperature purification (LLE-LTP) for pesticide residue analysis in honey samples by gas chromatography, Food Control, 21 (2010) 1307-1311

[29] H. Shaikh, N. Memon, M.I. Bhanger, S.M. Nizamani, A. Denizli, Core shell molecularly imprinted polymer-based solid-phase microextraction fiber for ultra trace analysis of endosulfan I and II in real aqueous matrix through gas chromatography-micro electron capture detector, J. Chromatogr. A, 1337 (2014) 179-187

[29] E. D. Conte, E. F. Barry, Alkali flame ionization detector for gas chromatography using an alkali salt aerosol as the enhancement source, J. Chromatogr., 644 (1993) 349-355

[30] H. Snijders, H. Janssen, C. Cramers, Design and optimization of a novel type nitrogen-phosphorus detector for capillary gas chromatography, J. Chromatogr. A, 732 (1996) 51-61

[31] V.V. Brazhnikov, E.B. Shmidel, Thermoionic ionization detector for the analysis of phosphorus and nitrogen containing organic compounds, J. Chrom., 122 (1976) 527-534

[32] A. Salemi, R. Rasoolzadeh, M.M. Nejad, M. Vosough, Ultrasonic assisted headspace single drop micro-extraction and gas chromatography with nitrogen-phosphorus detector for determination of organophosphoros pesticides in soil, Anal. Chim. Acta, 769 (2013) 121-126

[33] J.J. Jiménez, J.L. Bernal, M.J. del Nozal, L. Toribio, E. Arias, Analysis of pesticide residues in wine by solid-phase extraction and gas chromatography with electron capture and nitrogen-phosphorus detection, J. Chromatogr. A, 919 (2001) 147-156

[34] G. Pagliuca, T. Gazotti, E. Zironi, P. Sticca, Residue analysis of organophosphorus pesticides in animal matrices by dual column capillary gas chromatography with nitrogen-phosphorus detection, J. Chromatogr. A, 1071 (2005) 67-70

[35] J. Fenoll, P. Hellín, C.M. Martínez, M. Miguel, P. Flores, Multiresidue method for analysis of pesticides in pepper and tomato by gas chromatography with nitrogen-phosphorous detection, Food Chemistry, 105 (2007) 711-719

[36] G. Pagliuca, T. Gazotti, E. Zironi, P. Sticca, Residue analysis of organophosphorus pesticides in animal matrices by dual column capillary gas chromatography with nitrogen-phosphorus detection, J. Chromatogr. A, 1071 (2005) 67-70

[37] X. Yan, Sulfur and nitrogen chemiluminescence detection in gas chromatographic analysis, J. Chromatogr. A, 976 (2002) 3-10

[38] R. Hua, J. Wang, H. Kong, J. Lui, X. Lu, G. Xu, Analysis of sulfur-containing compounds in crude oils by comprehensive two-dimensional gas chromatography with sulphur chemiluminescence detection, J. Sep. Sci., 27 (2004) 691–698

[39] B. Chawla, F. Di Sanzo, Determination of sulfur components in light petroleum streams by high-resolution gas chromatography with chemiluminescence detection, J. Chromatogr. A, 589 (1992) 271-279

[40] R. Hua, Y. Li, W. Liu, J. Zheng, H. Wei, J. Wang, X. Lu, H. Kong, G. Xu, Determination of sulfur-containing compounds in diesel oils by comprehensive two-dimensional gas chromatography with a sulfur chemiluminescence detector, J. Chromatogr. A, 1019 (2003) 101-109

[41] C. L. Garcia, M. Becchi, M.F. Grenier-Loustalot, O. Païsse, R. Szymanski, Analysis of aromatic sulfur compounds in gas oils using GC with sulfur chemiluminescence detection and high-resolution MS, Anal. Chem., 74 (2002) 3849-3857

[42] H.E. Toraman, T. Dijkmans, M.R. Djokic, K.M. Van der Geem, G.B. Marin, Detailed compositional characterization of plastic waste pyrolysis oil by comprehensive two-dimensional gas-chromatography coupled to multiple detectors, J. Chromatogr. A, 1359 (2014) 237-246

[43] D. Martínez, J. Moreno, M. Tresanchez, M. Teixidó, D. Font, A. Pardo, S. Marco, J. Palacín, Experimental application of an autonomous mobile robot for gas leak detection in indoor environments, Fusion 2014, 17th International Conference on Information Fusion

[44] D.S. Forsyth, Pulsed discharge detector: theory and applications, J. Chrom. A, 1050 (2004) 63-68

[45] W.E. Wentworth, H. Cai, S. Stearns, Pulsed discharge helium ionization detector. Universal detector for inorganic and organic compounds at the low picogram level, J. Chromatogr. A, 688 (1994) 135-152

[46] S. Mendoca, W.E. Wentworth, E.C.M. Chen, S.D. Stearns, Relative responses of various classes of compounds using a pulsed discharge helium photoionization detector: Experimental determination and theoretical calculations, J. Chromatogr. A, 749 (1996) 131-148

[47] M.T. Roberge, J.W. Finley, H.C. Lukaski, A.J. Borgerding, Evaluation of the pulsed discharge helium ionization detector for the analysis of hydrogen and methane in breath, J. Chromatogr. A, 1027 (2004) 19-23

[48] J.G. Dojahn, W.E. Wentworth, S.N. Deming, S.D. Stearns, Determination of percent composition of a mixture analysed by gas chromatography. Comparison of a helium pulsed-discharge photoionization detector with a flame ionization detector, J. Chromatogr. A, 917 (2001) 187-204

[49] H. Cai, S.D. Stearns, Pulsed discharge helium ionization detector with multiple combined bias/collecting electrodes for gas chromatography, J. Chromatogr. A, 1284 (2013) 163-173

[50] S.H. Kim, S.M. Nam, K.O. Koh, Y.W. Choi, Analysis of natural gas using single capillary column and a pulsed discharge helium ionization detector, Bull. Korean. Chem. Soc., 20 (1999) 843-845

[51] M.C. Hunter, K.D. Bartle, P.W. Seakins, A.C. Lewis, Direct measurement of atmospheric formaldehyde using gas chromatography-pulsed discharge ionisation detection, Anal. Commun., 36 (1999) 101-104

[52] W.E. Wentworth, K. Sun, D. Zhang, J. Madabushi, S.D. Stearns, Pulsed discharge emission detector: an element-selective detector for gas chromatography, J. Chromatogr. A, 872 (2000) 119-140

[53] www.vici.com. Accessed on 1-7-2016.

Chapter 2 - Evaluation of the full evaporation technique for quantitative analysis of high boiling compounds with high affinity for apolar matrices

Niels van Boxtel, Kris Wolfs, Ann Van Schepdael, Erwin Adams

Pharmaceutical Analysis, Department of Pharmaceutical and Pharmacological Sciences

KU Leuven, Leuven, Belgium

J. Chromatogr. A 2014, 1348, 63–70

Abstract

In order to reduce inaccuracies due to possible matrix effects in conventional static headspace-gas chromatography (sHS-GC), it is standard practice to match the composition of calibration standards towards the composition of the sample to be analysed by adding blank matrix. However, the latter is not always available and in that case the full evaporation technique (FET) could be a solution. With FET a small sample volume is introduced in a HS vial and compounds of interest are completely evaporated. Hence no equilibrium between the condensed phase and vapour phase exists. Without the existence of an equilibrium, matrix effects are less likely to occur. Another issue often encountered with sHS-sampling is that low vapour pressure compounds with a high affinity for the dilution medium show a limited sensitivity. FET has proven to be an appropriate solution to address this problem too.

In this work, the applicability of FET for the quantitative analysis of high boiling compounds in different complex apolar matrices is examined. Data show that FET is an excellent tool to overcome matrix effects often encountered with conventional sHS analysis. The tested method shows excellent recovery with recovery values around 100% as well as repeatability with RSD values around 1% for the quantification of high boiling compounds (bp. > 200 °C) such as camphor, menthol, methyl salicylate and ethyl salicylate in various matrices. LOQ values were found to be around 0.3 µg per vial. Following validation of the technique, several topical pharmaceutical formulations like ThermoCream®, Reflexspray®, Vicks Vaporub® and Radosalil® were examined. For the latter, a comparison has been made with a sHS-method described in literature.

Keywords

Matrix effect, Full Evaporation Technique, Static headspace

2.1. Introduction

Static headspace (sHS) sampling is widely used for the quantitative analysis of volatile compounds in a variety of matrices due to its simplicity and cleanliness of introducing volatiles of interest into a gas chromatograph. A disadvantage of this technique is the possibility of matrix effects causing signal differences between the sample and calibration standards [1]. Matrix effects are any form of interaction in the condensed phase that influences the equilibrium between the condensed and vapour phase in a HS vial. A way to solve this problem is to add blank matrix to calibration standards in order to compensate for the matrix. However, this is not always possible as blank matrix is not always available. So, quantification of volatiles can be inaccurate because matrix effects can influence the established equilibrium between the condensed and vapour phase in a HS vial and thus can give rise to different response factors for a certain compound in different matrices. Possible methods to address this problem are multiple headspace extraction (MHE), standard addition method (SAM) and full evaporation technique (FET). However, MHE can be very time consuming and SAM can only be performed when enough sample is available. In contrast to these techniques, FET only uses very small amounts of sample and this procedure does not take more time to perform than conventional sHS. With FET, all volatile compounds of interest are transferred completely to the vapour phase and the matrix no longer influences the equilibrium between vapour and condensed phase. FET has proven to be a useful technique to avoid matrix effects during analysis of both solid and liquid samples [2-7]. FET has also proven to be useful for the analysis of high boiling solvents (low vapour pressure) with high affinity for water (high K value) in an aqueous matrix. Using conventional sHS-sampling, this determination is difficult since the sensitivity for these high boiling compounds is limited [8]. The same issue regarding sensitivity could arise when high boiling compounds have high affinity for apolar matrices and/or dilution media.

The aim of this work was to investigate the applicability of FET on the quantification of high boiling compounds (bp > 200 °C) with high affinity for different apolar matrices. The quantitative analysis of camphor (C), DL-menthol (M), methyl salicylate (MeS) and ethyl salicylate (EtS) in different pharmaceutical products was taken as an example. These compounds are usually analysed with either sHS-sampling or direct injection [9-11]. The drawbacks of sHS are mentioned above while direct injection suffers from clogging and sample adsorption in the injector. Aspects like linearity, repeatability and recovery were evaluated. Calibration curves obtained with matrix-matched standards were compared with those obtained with solvent-based standards to check for the absence of matrix effects. In order to evaluate the advantage of FET over

sHS for the analysis of apolar high boiling compounds in an apolar matrix, a typical sample containing the aforementioned compounds was analysed with both techniques.

2.2. Theory

With conventional sHS-GC, an equilibrium exists in a sealed HS vial containing a condensed and a vapour phase, both with a particular volume:

$$V_v = V_g + V_l \ (1)$$

Where V_g is the volume of the vapour phase, V_l the volume of the liquid phase (condensed phase) and V_v the total volume (volume of the vial). If a sample with volume V_0 containing a concentration C_0 is transferred in a vial, the sum of the absolute amounts in the vapour and condensed phase after equilibration equals the total amount of sample before equilibration:

$$C_0 * V_0 = C_l * V_l + C_g * V_g \ (2)$$

Where C_l is the concentration of the analyte in the liquid phase and C_g the concentration in the gas phase. With FET, only a very small amount of sample is transferred into the vial and sufficiently heated. As a result, V_l will approach zero due to near complete evaporation. Consequently eq. 2 becomes:

$$C_0 * V_0 = C_g * V_g \ (3)$$

so that the amount of the compound of interest in the gas phase is directly determined by the sample amount in the HS vial. The approximate maximum volume of solvent and absolute amount of compounds that can be introduced in a HS vial in order to meet the criterion for FET can be calculated by combining Antoine's equation and the Ideal Gas law [8]. When the maximum amount of a certain compound is exceeded, condensation will occur and the requirements for FET will not be met as the system is in sHS-mode, and hence, possible matrix effects can occur. When performing FET-analysis, the compound that has the highest abundance in the vial is the solvent. It has to be ensured that the pressure at equilibrium in the vial does not exceed the pressure applied on the vial during injection. The latter pressure is determined by the chromatographic conditions. During heating of the vial, the air that is present in the vial will also exert a certain pressure depending on the temperature (thermal expansion). When the applied injection pressure is not high enough to counteract the equilibration pressure, an amount of gas phase will flow into the injection system when the needle punctures the vial. This will result in loss of sample with pressure loop systems or

pre-injection with balanced pressure systems. Therefore, in practice the maximum amount of solvent that can be introduced in a vial will be lower than the calculated maximum amount that can be evaporated.

2.3. Experimental

2.3.1. Reagents and samples

C, M, MeS, EtS, (structure, boiling points and Antoine's constants are given in Table 2.1) and Radosalil® stick were kindly donated by Will Pharma (Wavre, Belgium). Salicylic acid, paraffin, petroleum jelly, cetiol, capsaicin oleoresin (containing 8% of capsaicin) and Lanette SX for the preparation of blank Radosalil® matrix were obtained from Will Pharma as well. ThermoCream® and its blank matrix were obtained from Sterop (Brussels, Belgium). Reflexspray® and Vicks Vaporub® were obtained from a local pharmacy. 1-Octanol (98%) was obtained from Janssen Chimica (Geel, Belgium), o-xylene (99%) from VWR International (Heverlee, Belgium), DMF from Fischer Chemical (Loughborough, United Kingdom). The boiling points and Antoine's coefficients of o-xylene and DMF are given in Table 2.1. n-Dodecane was purchased from Sigma-Aldrich (Diegem, Belgium). The composition of each matrix is given in Table 2.2.

Table 2.1: Chemical structure, boiling points and Antoine's constants of the investigated compounds and used solvents.

Compounds	**C**	**M**	**MeS**	**EtS**
Chemical structure	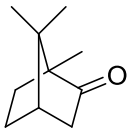	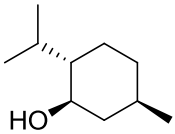	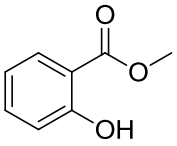	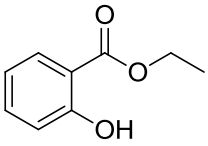
Boiling point (°C)	204	212	220-224	231-233
****Antoine's constant A**	3.30967	5.383470	4.02455	*
****Antoine's constant B**	1096.291	2405.946	1585.874	*
****Antoine's constant C**	-148.579	-37.853	-99.173	*

Solvent	**o-xylene**	**DMF**
Boiling point (°C)	144.4	153
****Antoine's constant A**	4.12928	3.93068
****Antoine's constant B**	1478.244	1337.716
****Antoine's constant C**	-59.076	-83.648

*Antoine's constants unknown ** From NIST data

Table 2.2: Composition of the analysed samples. For the volatile components that are determined (C, M, MeS and EtS), the label claim is added.

	ThermoCream®	**Radosalil®**	**Reflexspray®**	**Vicks Vaporub®**
Volatile active ingredients determined by GC	M (57.5 mg/g) MeS (57.5 mg/g)	C (4.41 mg/g) M (55.14 mg/g) MeS (26.47 mg/g) EtS (17.64 mg/g)	C (40 mg/mL) M (40 mg/mL) MeS (27 mg/mL)	C (50 mg/g) M (27.5 mg/g)
Other ingredients (including excipients)	Capsicum oleoresin Lanette SX Water	Salicylic acid Mono-glycol salicylate Capsicum oleoresin Paraffin Petroleum jelly Cetiol Lanette SX	Turpentine oil Benzyl alcohol DMSO Isopropyl alcohol Lilac oil	Thymol Turpentine oil Eucalyptus oil Petroleum jelly Cedarwood oil

2.3.2. Chromatographic system and sampling conditions for the sHS-method

FET was compared with a sHS-method described in literature [9] used for the quantification of C, M, MeS and EtS in Radosalil®, a typical petroleum jelly/paraffin based matrix for which these compounds have a high affinity. The method was slightly adapted by using n-dodecane as solvent as the prescribed liquid paraffin does not allow to work with volumetric flasks.

2.3.3. Chromatographic system and HS sampler conditions for FET

FET-GC analysis was performed with a Varian 3500 GC equipped with a Perkin Elmer (Waltham, MA, USA) Turbomatrix 40 HS autosampler (balanced pressure system). HS vials and PTFE/Sil-caps were purchased from Perkin Elmer as well. Separations were carried out on an AT^{TM}-Aquawax column (30 m x 0.53 mm, d_f = 0.50 µm) from Grace (Lokeren, Belgium) in case of Radosalil®, Reflexspray® and Vicks Vaporub® or a ZB-624 column (30 m x 0.53 mm, d_f = 3.00 µm) from Phenomenex (Utrecht, The Netherlands) in case of ThermoCream® using the oven program from Table 2.3. It was necessary to use a longer GC oven program following FET compared to this following sHS since the increased sensitivity with FET gave rise to more peaks so that a better separation was needed. The low volatility of the analytes demands the highest possible equilibration temperature (limited by the apparatus used) in order to get the maximum dynamic range and to transfer the analytes completely into the gas phase. The optimized settings of the FET method are given in Table 2.4. Preliminary experiments on Radosalil® have shown that an incubation temperature of 180 °C is a good compromise between operating limits, signal intensity and maximum sample amount to operate in FET-mode when analysing C, M, MeS and EtS. Increasing the temperature could not be done for the sHS-method as RSD values went up. These settings were used for all experiments during this work. Chromeleon software (Dionex, Germering, Germany) was used to process all data.

Table 2.3: GC-oven program for FET-GC.

t (min)	T (°C)
0	100
10	100
22	160
23.5	220
28.5	220

Table 2.4: Used HS-parameters.

HS-parameters	Settings
Equilibration temperature	180 °C
Equilibration time	10 min
Needle temperature	190 °C
Transfer line temperature	195 °C
Pressurization time	1.0 min
Injection time	0.04 min
Needle withdrawal time	0.4 min
Injection port temperature	200 °C
Split ratio	1:5
Carrier gas pressure	180 kPa
Detector type	Flame Ionization Detector
Detector temperature	250 °C
Analysed volume	o-xylene: 40 µL DMF: 25 µL

2.3.4. Preparation of solutions

Internal standard solution for FET: 1-octanol was selected as internal standard and approximately 40 µL was dissolved in 25 mL of solvent (o-xylene or DMF) using a volumetric flask. The internal standard was used to correct for variations on the small volumes that are introduced in vials for FET-analysis.

Sample solution for FET: a sample solution was prepared by dissolving the appropriate amount of sample in either o-xylene or DMF using a volumetric flask of 25 mL to which 1 mL of internal standard solution was added. o-Xylene was used as solvent for the matrices containing paraffin or petroleum jelly (Radosalil® and Vicks Vaporub®) and DMF for the others (ThermoCream® and Reflexspray®). The following amounts were dissolved for each type of sample: 250 mg of Radosalil®, 100 mg of ThermoCream®, 1 mL of Reflexspray® and 150 mg of Vicks Vaporub®.

Sample solution for sHS: approximately 1 g of Radosalil® was dissolved in 50 mL of n-dodecane using a volumetric flask. As described in the original method, sample solutions needed to be heated to dissolve the sample in the n-dodecane before adding up to volume [9].

*Blank ThermoCream® matrix: a*ppropriate amounts of water, Lanette SX and capsicum oleoresin (8% capsaicin) were heated at 50 °C and mixed until a homogeneous cream was obtained. The cream was allowed to cool down to room temperature before use.

Blank Radosalil® matrix: appropriate amounts of salicylic acid, paraffin, petroleum jelly, cetiol, capsicum oleoresin (8% capsaicin), Lanette SX and a magnetic stir bar were put in a conical flask and sealed with a glass stopper. The conical flask was heated and stirred until the solution was homogeneous. The solution was allowed to cool down to room temperature to obtain solid Radosalil® blank matrix.

Calibration solutions for FET: appropriate amounts of C, M, MeS and EtS were dissolved in either DMF or o-xylene. Dilutions were made by diluting appropriate volumes in volumetric flasks of 25 mL and adding 1 mL of internal standard solution.

Calibration solutions for FET to check the influence of the matrix: to each of the above calibration solutions for FET, 100 mg of blank ThermoCream® or 250 mg of blank Radosalil® was added.

Calibration solutions for sHS: appropriate amounts of C, M, MeS and EtS were dissolved in n-dodecane, followed by diluting appropriate volumes in volumetric flasks of 50 mL. Each calibration solution contained 1 g of blank Radosalil® for matrix compensation.

2.3.5. Sample vials

In case of FET, 40 µL of sample or calibration solution was transferred to a HS vial when o-xylene was used; 25 µL when DMF was used as solvent. With the sHS-method, a sample volume of 5 mL was brought into the vial. Each vial was sealed with a PTFE-Sil-cap before analysis.

2.3.6. FET evaluation

Before recovery experiments were performed, it was first evaluated whether the conditions for FET-mode were met in this particular case by analysing a range of sample volumes transferred into the vial.

So, Radosalil® sample solution in o-xylene was analysed using sample volumes ranging from 10 to 50 µL with increments of 10 µL. In contradistinction with water [8], o-xylene will have almost no influence on the viscosity of the gas phase. If FET conditions are fulfilled, a linear curve should be obtained when peak areas of C, M, MeS and EtS are plotted vs. the introduced volume. Measurements were performed in triplicate.

2.3.7. Stability evaluation

Another important aspect of the method is to check whether thermal degradation occurs during incubation of a sample. Experiments were performed by heating HS vials containing Radosalil® sample for different periods of time.

2.3.8. Matrix-matched vs. solvent-based calibration

Calibration series prepared in o-xylene containing 100 mg of blank ThermoCream® (matrix) were compared with neat standard solutions containing appropriate amounts of M and MeS. 1 mL of internal standard solution was added to each solution. The same was done with Radosalil® by comparing calibration series in which 250 mg of blank Radosalil® was added. Every calibration point was injected twice for both calibration series. This experiment could not be performed for the other samples as blank matrix was not available.

2.3.9. Recovery experiments

Recovery experiments for ThermoCream® were carried out by dissolving 100 mg of blank ThermoCream® in DMF and spiking with M and MeS. Spiked concentration levels were 80%, 100% and 120% with 100% referring to the label content of ThermoCream®.

Recovery experiments for Radosalil® were carried out by dissolving 250 mg of blank Radosalil® in 25 mL of o-xylene and spiking with C, M, MeS and EtS. Spiked concentration levels were 80%, 100% and 120% with 100% referring to the label content of a Radosalil® stick.

Since no blank matrix was available for Reflexspray® and Vicks Vaporub®, recovery experiments were carried out by spiking the samples dissolved in DMF or o-xylene with C, M and MeS to confirm that no headspace related matrix effects were occurring.

2.3.10. Analysis of commercial samples

Commercial samples of all four formulations were analysed using FET. Two Radosalil® samples were analysed with FET as well as sHS, so that the results of both methods could be compared.

2.4. Results & discussion

2.4.1. Evaluation of the sample volume in the vial used for FET

The calculated (using Antoine's equation and the Ideal Gas law) amount of solvent which can be evaporated with the chosen conditions is ~94 µL for DMF and ~170 µL for o-xylene. However, due to injection pressure requirements (<180 kPa) the volumes should be kept below ~55 µL for DMF and ~85 µL for o-xylene. To include some margin, sample volumes of 25 µL in case of DMF as solvent and 40 µL in case of o-xylene were used. Although the same approach could be used for the analytes if all the Antoine coefficients are known, there would be no verification on the absence of intermolecular effects. Increasing sample volumes were analysed in triplicate taking Radosalil® dissolved in o-xylene as example. A graph was constructed (Figure 2.1) in which the obtained peak areas vs. sample volume were plotted for all compounds studied. It can be seen clearly that for all 4 compounds a linear relationship was obtained, which indicates that the method was operating in FET-mode. Above the maximum introducible volume, sHS-conditions would be met due to condensation of the solvent resulting in a change of the slope of the curves depicted in Figure 2.1 and hence possible matrix effects could occur.

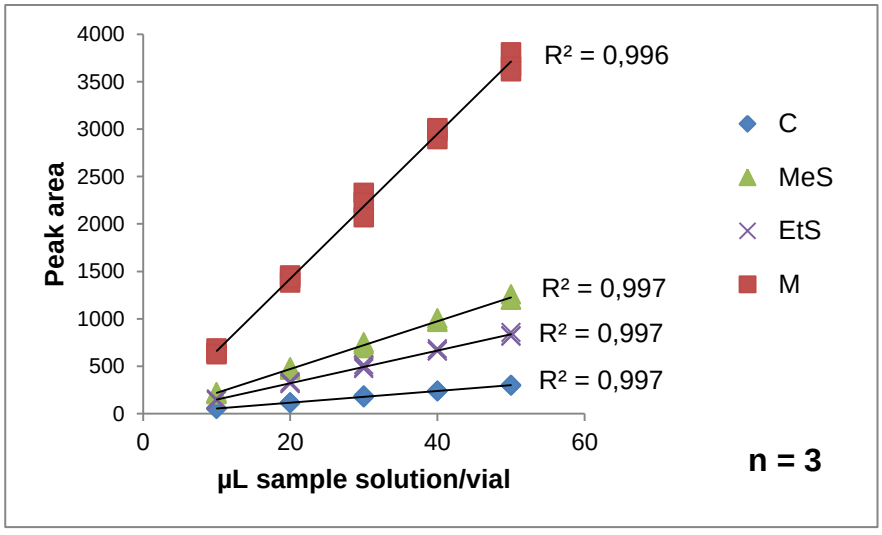

Figure 2.1: Evaluation of the FET requirements concerning sample volume (Radosalil® sample in o-xylene).

2.4.2. Evaluation of matrix effects

Matrix effects can be considered in two ways: (1) chromatographic ones in the sense that compounds from the matrix can interfere with analyte peaks in the chromatogram and (2) sampling ones in the sense that analytes can interact (mainly physically) with matrix components and/or solvent in the HS vial, leading to inaccurate results when no matrix-matched calibration is used. Although FET cannot help to solve chromatographic problems (interfering analyte and matrix peaks), it should bring a solution for the second

issue. First, chromatographic effects from the matrix were studied for the two samples for which blank matrix was available: ThermoCream® and Radosalil®. The chromatogram obtained by injecting the blank for ThermoCream® on an AT™-Aquawax is shown in Figure 2.2. As can be seen, a peak at 15.3 min interfering with the determination of M appeared in the chromatogram together with a peak at 13.6 min. Further investigation revealed that these were due to impurities originating from DMF. Analysis on a ZB-624 column provided separation with no interference (Figure 2.3).

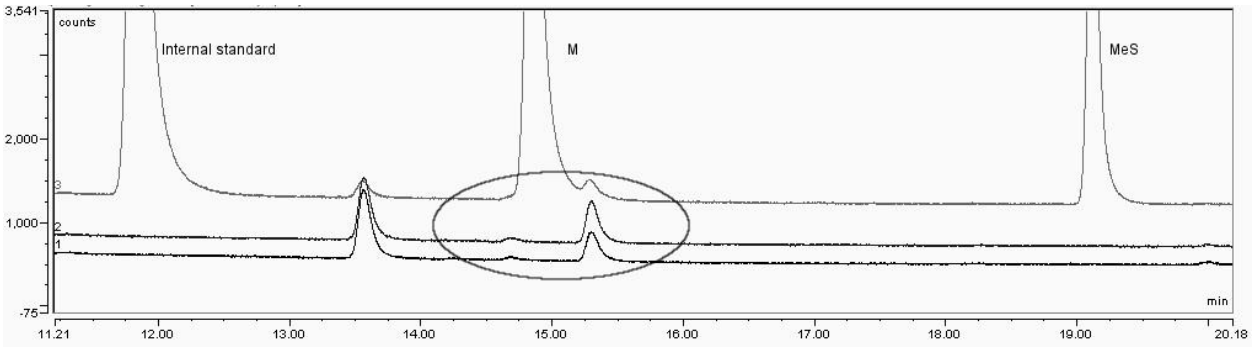

Figure 2.2: Overlay of chromatograms obtained by injecting (1) DMF, (2) matrix blank of ThermoCream® and (3) calibration standard (column used: AT™-Aquawax). Chromatograms were recorded using the instrumental parameters described in 2.3.3.

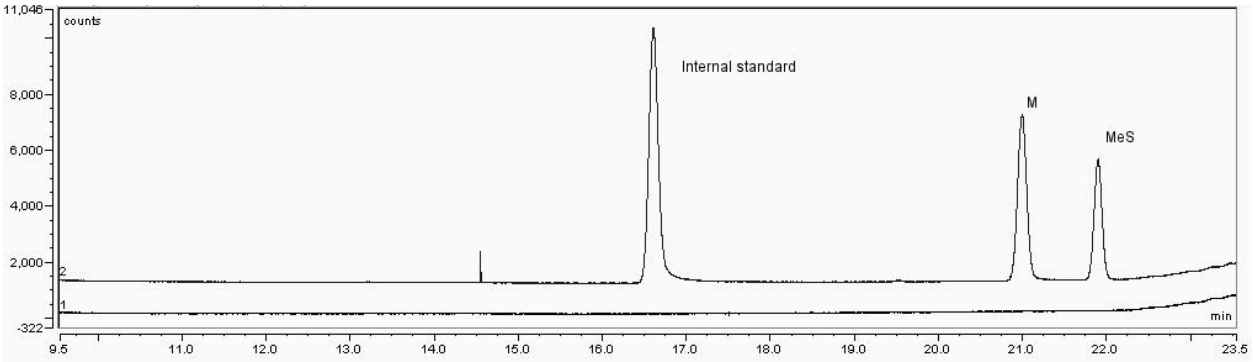

Figure 2.3: Overlay of chromatograms obtained by injecting (1) matrix blank of ThermoCream® and (2) calibration standard (column used: ZB-624). Chromatograms were recorded using the instrumental parameters described in 2.3.3.

The same procedure was followed to evaluate the method for Radosalil®. Here a compound from the matrix was eluted at the same retention time as MeS (Figure 2.4). Changing the chromatographic conditions could not solve the problem. So, in this case a correction had to be carried out by subtracting this blank peak from the analyte peak.

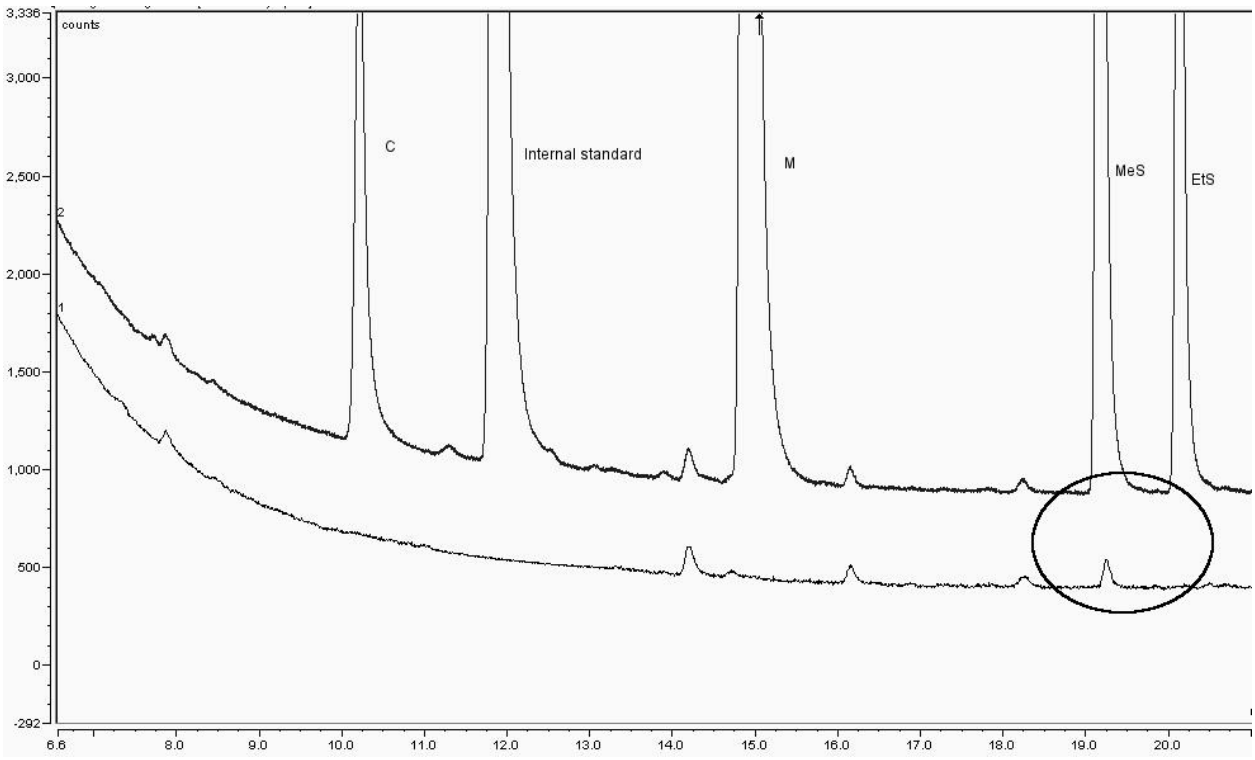

Figure 2.4: Overlay of (1) a blank chromatogram and (2) a chromatogram of a calibration standard for Radosalil® (column used: AT™-Aquawax). Chromatograms were recorded using the instrumental parameters described in 2.3.3.

Next, matrix effects on the sampling were evaluated by comparing matrix-matched and solvent-based calibration curves. Those curves were constructed by plotting the concentration of the compound in question vs. the ratio of the peak $area_{compound}$/peak $area_{internal\ standard}$. Results are shown in Table 2.5 for ThermoCream® and Table 2.6 for Radosalil®. In order to evaluate whether there are significant differences between matrix-matched and solvent-based calibration, a *t*-test on the obtained slopes was performed. It was found that there is no significant difference between both calibration methods for the analysis of ThermoCream® and Radosalil® indicating that no significant matrix-effects during FET sampling occurred. This implies that for routine analyses just solvent based calibration curves can be used without the need to add each time blank matrix to the calibration solutions as necessary in sHS. This considerably simplifies the calibration procedure.

Table 2.5: Regression data for M and MeS in ThermoCream®.

	Matrix-matched M	Solvent-based M	Matrix-matched MeS	Solvent-based MeS
R^2	0.9996	0.9998	0.9992	0.9991
Slope	0.00215	0.00214	0.00144	0.00141
S_{slope} [a]	$1.55 * 10^{-5}$	$1.30 * 10^{-5}$	$1.14 * 10^{-4}$	$1.62 * 10^{-5}$
S_{yx} [b]	$1.94 * 10^{-3}$	$1.56 * 10^{-3}$	$1.74 * 10^{-3}$	$1.95 * 10^{-3}$
$t_{crit.\ (df = 9)}$	2.262		2.262	
$t_{experimental}$	0.719		1.020	

S_{slope} = standard deviation of the slope S_{yx} = standard error of estimate

Table 2.6: Regression data for C, M, MeS and EtS in Radosalil®.

	Matrix-matched C	Solvent-based C	Matrix-matched M	Solvent-based M
R^2	0.9996	0.9997	0.9999	0.9998
Slope	0.001911	0.001953	0.002106	0.002136
S_{slope} [a]	$1.91 * 10^{-5}$	$1.10 * 10^{-5}$	$8.60 * 10^{-6}$	$1.14 * 10^{-5}$
S_{yx} [b]	$1.56 * 10^{-3}$	$8.9 * 10^{-4}$	$8.52 * 10^{-3}$	$1.13 * 10^{-2}$
$t_{crit.\ (df = 9)}$	2.262		2.262	
$t_{experimental}$	1.89		2.10	

	Matrix-matched MeS	Solvent-based MeS	Matrix-matched EtS	Solvent-based EtS
R^2	0.9999	0.9997	0.9998	0.9995
Slope	0.001387	0.001395	0.001412	0.001435
S_{slope} [a]	$4.29 * 10^{-6}$	$8.86 * 10^{-6}$	$6.94 * 10^{-6}$	$1.47 * 10^{-5}$
S_{yx} [b]	$2.03 * 10^{-3}$	$4.18 * 10^{-3}$	$2.27 * 10^{-3}$	$3.76 * 10^{-3}$
$t_{crit.\ (df = 9)}$	2.262		2.262	
$t_{experimental}$	0.797		1.72	

S_{slope} = standard deviation of the slope S_{yx} = standard error of estimate

2.4.3. Stability evaluation

Radosalil® samples were heated at 180 °C from 5 to 30 minutes with increments of 5 minutes. The acquired data were evaluated by plotting the heating time vs. the ratio of the peak $area_{compound}$/peak $area_{internal\ standard}$ as shown in Figure 2.5. It is clear that there are no considerable differences in responses for the different analytes, suggesting that no thermal degradation occurs using the described FET-method.

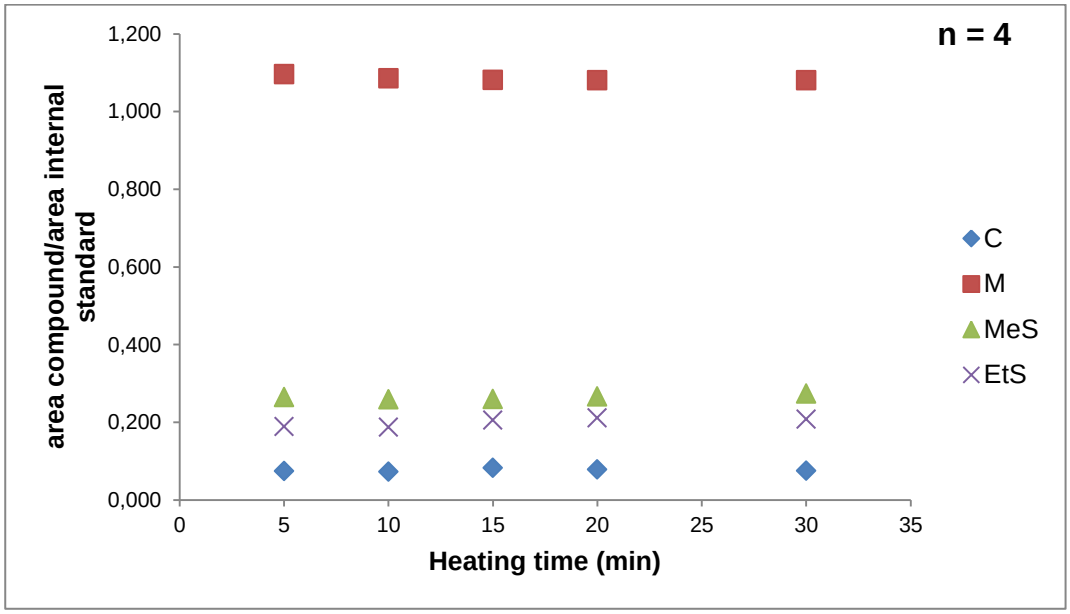

Figure 2.5: Evaluation of thermal degradation by using different heating periods.

2.4.4. Recovery and repeatability

Quantification results using FET for recovery experiments on ThermoCream®, Radosalil®, Reflexspray® and Vicks Vaporub® are given in Tables 2.7 and 2.8. Solvent based calibration standards were used for all samples. Recovery values found were between 98% and 102% and RSD values (as a measure of the repeatability) did not exceed 1.6 %. The spiking experiments also indicated that there were no headspace related matrix effects.

Table 2.7: Recovery and repeatability data on the quantification of high boiling compounds in ThermoCream® and Radosalil® on different concentration levels.

level		80%		100%		120%	
		Recovery (%)	RSD (%) n = 4	Recovery (%)	RSD (%) n = 4	Recovery (%)	RSD (%) n = 4
ThermoCream®	**M**	99.0	0.5	100.8	0.3	100.7	0.3
	MeS	100.4	0.7	99.6	0.9	99.4	1.4
Radosalil®	**C**	100.3	0.7	99.3	1.3	99.5	0.8
	M	99.0	0.2	99.0	0.7	99.1	0.4
	MeS	99.4	0.3	99.8	0.6	99.1	0.7
	EtS	98.1	1.6	99.8	1.4	98.8	0.8

Table 2.8: Recovery and repeatability data on the quantification of high boiling compounds in Vicks Vaporub® and Reflexspray®.

Compound	Vicks Vaporub®		Reflexspray®	
	Recovery (%)	RSD (%) n = 4	Recovery (%)	RSD (%) n = 4
C	99.3	0.5	101.2	0.4
M	98.8	0.4	100.6	0.8
MeS	-	-	101.6	0.7

2.4.5. Limit of quantification (LOQ)

LOQ values (S/N = 10) for the FET-method were derived from the calibration curves. Values are expressed as amount per vial and sample concentration (Table 2.9).

Table 2.9: LOQ values of the used FET method.

Compound	LOQ (µg/vial)	LOQ Radosalil® (ppm)	LOQ Vicks Vaporub® (ppm)	LOQ Thermocream® (ppm)	LOQ Reflexspray® (µg/mL)
C	0.3	680	1130	2700	0.27
M	0.3	730	1210	2900	0.29
MeS	0.3	720	1200	2880	0.29
EtS	0.3	680	1140	2730	0.27

2.4.6. Analysis of commercial samples

Results obtained for commercial samples are given in Tables 2.10 and 2.11. The latter table shows results obtained for two Radosalil® samples applying FET and sHS. It has to be remarked that compounds C, M, MeS and EtS are overdosed during the production of the Radosalil® stick so that it is not abnormal that assay values above 100 % are found. From the comparison, it is clear that FET and sHS provide very similar results for all compounds. However, those obtained with FET show less variation on repetitive injections and peaks in the chromatogram are larger (Figure 2.6). This is remarkable since the amount of sample solution introduced into the vial is much smaller for FET than for sHS. Moreover, sample preparation is far more straightforward and requires no heating of the sample solution as with the original sHS method which also required heating of the sample before the actual analysis [9] with risk of losing volatiles. This clearly demonstrates the advantage of FET over sHS-sampling in terms of sensitivity when the compounds of interest have a high affinity for the dilution medium and/or matrix.

Table 2.10: Assay results for commercial samples of ThermoCream®, Reflexspray® and Vicks Vaporub®.

	ThermoCream®		Reflexspray®		Vicks Vaporub®	
Compound	**Assay (%)**	**RSD (%) n = 4**	**Assay (%)**	**RSD (%) n = 4**	**Assay (%)**	**RSD (%) n = 4**
C	-	-	98.0	0.8	94.9	0.6
M	108.0	0.7	100.0	0.9	96.2	0.2
MeS	109.8	0.9	100.1	0.5	-	-

Table 2.11: Assay results obtained after analysis of commercial Radosalil® samples with FET and sHS.

Radosalil®	**Sample A FET**		**Sample A sHS**	
Compound	**Assay (%)**	**RSD (%) n = 4**	**Assay (%)**	**RSD (%) n = 4**
C	106.6	1.0	107.6	1.4
M	108.7	0.3	109.4	1.1
MeS	108.7	0.5	106.9	1.3
EtS	109.6	0.4	110.0	0.8
	Sample B FET		**Sample B sHS**	
	Assay (%)	**RSD (%) n = 4**	**Assay (%)**	**RSD (%) n = 4**
C	106.6	0.9	108.8	1.4
M	108.4	0.2	109.0	2.5
MeS	113.5	0.3	112.0	2.5
EtS	113.2	0.7	109.8	2.1

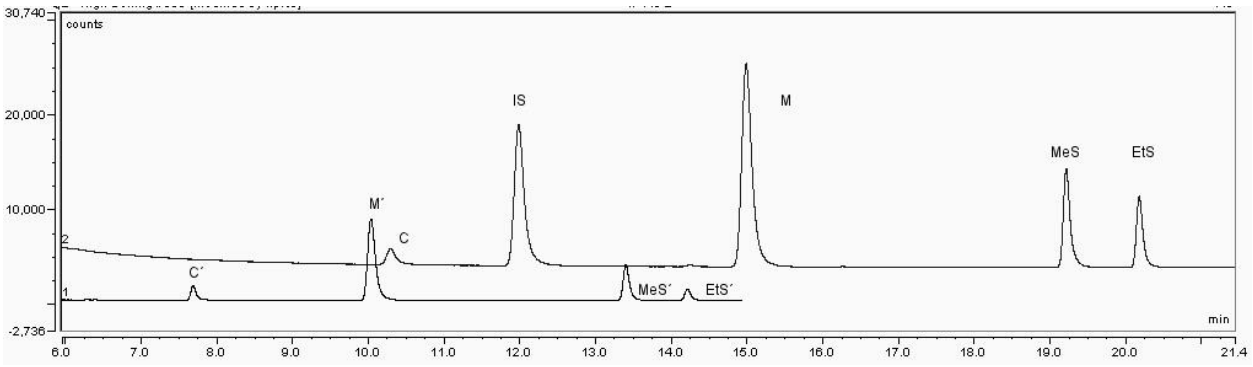

Figure 2.6: Overlay of Radosalil® sample chromatograms obtained with (2) FET (compounds indicated by C, M, MeS, EtS and IS = internal standard) and (1) sHS (compounds indicated by C', M', MeS' and EtS'). The difference in retention time between FET and sHS for the analytes is due to a different oven program and pressure.

2.5. Conclusions

FET is a very interesting sampling technique to be coupled to GC since it can avoid certain sHS related matrix effects. However, FET will not deal with chromatographic shortcomings, so that proper method validation (as always) is needed, preferably using a representative blank.

In this paper, some high boiling compounds like C, M, MeS and EtS with high affinity to their apolar matrices were analysed using FET prior to GC. From the results shown, it can be concluded that FET (1) makes complex matrix-matched calibration superfluous, (2) yields larger analyte peaks leading to improved sensitivity and (3) shows excellent repeatability.

2.6. References

[1] S. Yarramraju, V. Akurathi, K. Wolfs, A. Van Schepdael, J.Hoogmartens, E. Adams, Investigation of sorbic acid volatile degradation products in pharmaceutical formulations using static headspace gas chromatography, J. Pharm. Biomed. Anal., 44 (2007) 456-463

[2] A. Brault, V. Agasse, P. Cardinael, J. C. Combret, The full Evaporation technique: A promising alternative for residual solvent analysis in solid samples, J. Sep. Science, 28 (2005) 380-386

[3] X.S. Chai, Q.X. Hou, F.J. Schork, Determination of residual monomer in polymer latex by full evaporation headspace gas chromatography, J. Chromatogr. A, 1040 (2004) 163-167

[4] H. Li, H. Zhan, S. Fu, M. Lui, X.S. Chai, Rapid determination of methanol in black liquors by full evaporation headspace gas chromatography, J. Chromatogr. A, 1175 (2007) 133-136

[5] M. Markelov, J.P. Guzowski Jr, Matrix independent headspace gas chromatographic analysis. The full evaporation technique, Analytica Chimica Acta, 276 (1993) 235-245

[6] J. Schuberth, Volatile organic compounds determined in pharmaceutical products by full evaporation technique and capillary gas chromatography/ion-trap detection, Anal. Chem., 68, (1996) 1317-1320

[7] J. Schuberth, A full evaporation headspace technique with capillary GC and ITD: A means for quantitating volatile organic compounds in biological samples, J. Sep. Science, 34, (1996) 314-319

[8] D.M. Kialengila, K. Wolfs, J. Bugulama, A. Van Schepdael, E. Adams, Full evaporation headspace gas chromatography for sensitive determination of high boiling point volatile organic compounds in low boiling matrices, J. Chromatogr. A, 1315 (2013) 167-175

[9] J. Pauwels, W. D'Autry, L. Van den Bosche, C. Dewever, M. Forier, S. Vandenwaeyenberg, K. Wolfs, J. Hoogmartens, A. Van Schepdael, E. Adams, Optimization and validation of liquid chromatography and headspace-gas chromatography based methods for the quantitative determination of capsaicinoids, salicylic acid, glycol monosalicylate, methyl salicylate, ethyl salicylate, camphor and l-menthol in a topical formulation, J. Pharm. Biomed. Anal., 60 (2012) 51-58

[10] E. Gonzalez-Penas, M. Lopez-Alvarez, F. Martinez de Narvajas, A Ursua, Simultaneous GC determination of turpentine, camphor, menthol and methyl salicylate in a topical analgesic formulation (Dologex®), Chromatographia, 52 (2000) 245-248

[11] J.S. Valdez, D.K. Martin, M. Maversohn, Sensitive and selective gas chromatographic methods for the quantitation of camphor, menthol and methyl salicylate from human plasma, J. Chromatogr. B Biomed. Sci. Appl., 729 (1999) 163-171

Chapter 3 - Application of acetone acetals as water scavengers and derivatization agents prior to the gas chromatographic analysis of polar residual solvents in aqueous samples

Niels van Boxtel, Kris Wolfs, Ann Van Schepdael, Erwin Adams

Pharmaceutical Analysis, Department of Pharmaceutical and Pharmacological Sciences

KU Leuven, Leuven, Belgium

J. Chromatogr. A 2015, 1425, 62–72

Abstract

The sensitivity of gas chromatography (GC) combined with the full evaporation technique (FET) for the analysis of aqueous samples is limited due to the maximum tolerable sample volume in a headspace vial. Using an acetone acetal as water scavenger prior to FET-GC analysis proved to be a useful and versatile tool for the analysis of high boiling analytes in aqueous samples. 2,2-Dimethoxypropane (DMP) was used in this case resulting in methanol and acetone as reaction products with water. These solvents are relatively volatile and were easily removed by evaporation enabling sample enrichment leading to 10-fold improvement in sensitivity compared to the standard 10 µL FET sample volumes for a selection of typical high boiling polar residual solvents in water. This could be improved even further if more sample is used. The method was applied for the determination of residual NMP in an aqueous solution of a cefotaxime analogue and proved to be considerably better than conventional static headspace (sHS) and the standard FET approach, which do not allow proper analysis in this case. The methodology was also applied to determine trace amounts of ethylene glycol (EG) in aqueous samples like contact lens fluids, where scavenging of the water would avoid laborious extraction prior to derivatization. During this experiment it was revealed that DMP reacts quantitatively with EG to form 2,2-dimethyl-1,3-dioxolane (2,2-DD) under the proposed reaction conditions. The relatively high volatility (bp 93 °C) of 2,2-DD makes it possible to perform analysis of EG using the static headspace (sHS) methodology making additional derivatization reactions superfluous.

Keywords

Full Evaporation Technique, Static Headspace, Dehydration, 2,2-Dimethoxypropane.

3.1. Introduction

Analysis of aqueous samples with gas chromatography (GC) has always been a challenge mainly due to water intolerance of most stationary phases towards repetitive injections of high amounts of water and injection liners that are incompatible towards the introduction of large amounts of water. Standard GC-columns often degrade and injection liners are not able to deal with the gas expansion of water because of the heated injection port. Developed methods for the analysis of aqueous samples are either based on the isolation and enrichment of analytes prior to GC separation or on direct aqueous injections using special retention gaps and/or columns. Isolation of analytes can be done by using techniques such as supercritical fluid extraction (SFE), subcritical water extraction (SWE), cloud point extraction (CPE), solid phase extraction (SPE), solid phase microextraction (SPME), stir-bar sorptive extraction (SBSE) and single drop microextraction (SDME). However, all these techniques are biased towards more volatile compounds or apolar compounds that have a rather low affinity for water. Recently, a method was developed that uses a split injector packed with an adsorbent containing LiCl to enable injections up to 100 µL for the analysis of several high boiling analytes in water [1]. For the analysis of residual solvents in aqueous or water soluble pharmaceutical products, static headspace (sHS) GC and dynamic headspace (dHS) GC are traditionally used [2]. HS analysis is, in contrast to direct injection, a very clean method of introducing analytes on a GC column. When performing HS techniques with aqueous samples, incubation temperatures should be kept relatively low to ensure that the HS pressure does not exceed the limitations of the instrument. This limitation restricts the sensitivity for analytes with a high affinity for water and high boiling points such as N,N-dimethylformamide (DMF), N,N-dimethylacetamide (DMA), dimethylsulfoxide (DMSO), N-methyl-2-pyrrolidone (NMP) and 1,3-dimethyl-2-imidazole (DMI) when sHS is used. Their determination as residual solvents in aqueous samples is really problematic. A work around for DMSO is its reduction to the more volatile dimethylsulfide (DMS) enabling the indirect quantitative analysis of this high boiling polar solvent [3]. An additional possible disadvantage is that HS sampling is known to suffer from matrix effects. The so-called Full Evaporation Technique (FET) in combination with a more water resistant column has proven to be useful to improve the sensitivity for these typical polar residual solvents in aqueous samples [4] and provides elimination of matrix effects [5]. However, as with sHS sampling, pressure limits have to be respected as well, meaning that the introduced sample volume and therefore the sensitivity is still limited for aqueous samples. An approach to avoid this problem is to use desiccants such as $CaCl_2$ or K_2CO_3 to trap water inside a HS vial forming hydrates. A method described in literature uses 6.0 g of $CaCl_2$ to remove water for the analysis of phenol [6]. However, $CaCl_2$ is known to adsorb phenol [7] and might introduce unwanted matrix

effects for other analytes too. Furthermore, introducing 6.0 g of a desiccant in a vial has serious consequences for the partial pressures of the analytes present in the vial. Moreover, water can be released when higher HS temperatures are used for the evaporation of higher boiling analytes. When performing this described method in our lab, most sample vials (~75%) actually ruptured for unclear reasons. Rupturing of the sample vials occurred in the incubation oven of the HS sampler, but when the heating process was repeated in an ordinary oven, vials stayed intact. Recently, FET has been combined with dHS to increase the tolerable sample volume by transferring the whole sample over a Tenax® filled trap thereby eliminating the water [8-10]. Transferring occurs by purging the sample vial until analytes are (nearly) completely transferred to the trap. However, problems could still exist with analytes such as ethylene glycol (EG) which is prone to interact with many parts of the instrument (injector, column, etc.) resulting in erroneous results. Often, EG or other diols are analysed as phenyl boronate (PBA) [11] or trimethylsilyl (TMS) derivatives [12-14]. Unfortunately, most GC derivatization reagents tend to react with water as well and are therefore not easily applicable to aqueous samples. Furthermore, the derivatization of EG with PBA leads to a product with an even higher boiling point than EG itself (2-phenyl-1,3,2-dioxaborolane, 218 – 220 °C) and is susceptible to hydrolysis in an aqueous environment [15].

An approach to circumvent the abovementioned problems could be a selective chemical reaction to remove enough or all water in order to be able to introduce a larger sample volume in a HS vial and enable derivatization and analysis of compounds such as EG; thereby increasing the sensitivity significantly when FET is applied. In fact, such chemical reactions are known including drying reactions with several agents or certain hydrolysis reactions such as the reaction of water with acetone acetals to give acetone and an alcohol as final products. This reaction has proven to be useful in the past for the analysis of DMSO in urine samples using direct injection in which 2,2-dimethoxypropane (DMP) was used as water scavenger [16]. DMP is also known as acetone dimethyl acetal and reacts endothermically with equimolar amounts of water producing methanol and acetone in a molar ratio of 2:1 with the help of an acid as catalyst (Figure 3.1).

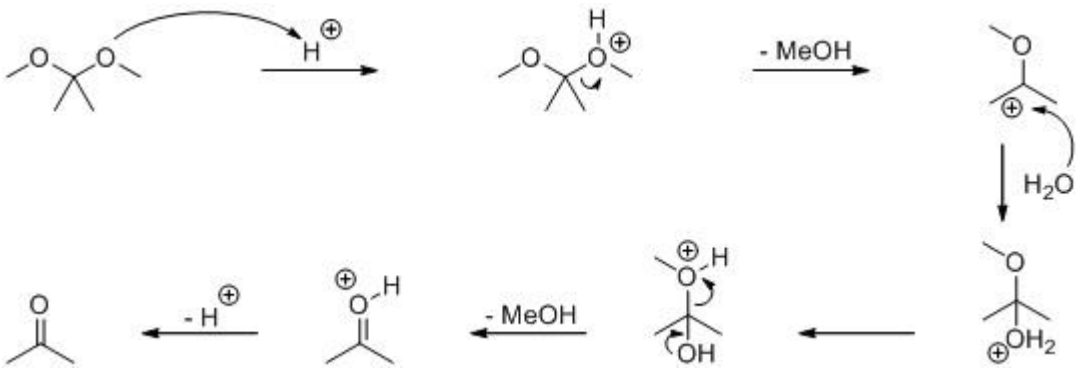

Figure 3.1: Acid catalysed hydrolysis of DMP to produce methanol and acetone.

The reaction consists of several equilibria with their own rate constants and starts by protonation of DMP resulting in methanol that splits off from the molecule. The resulting intermediate will react with a water molecule and lose a second methanol to form a protonated acetone molecule which yields a proton to catalyse further the reaction. This specific reaction has already been used before for the quantitative analysis of water when the well-known Karl-Fischer titration is not applicable [17-19]. Furthermore, samples have been dried using DMP prior to infrared (IR) spectroscopy [20], electron microscopy [21-23] and other histological applications [24,25]. It has been proposed in the past that a volumetric ratio of 1:10 for water:DMP is sufficient for complete water removal.

This work describes the optimization and application of this DMP reaction on the analysis of a selection of typical high boiling residual solvents in aqueous samples. Firstly, the reaction was used for sample enrichment to extend the applicability of FET for aqueous samples and was tested for the analysis of DMF, DMA, DMSO, NMP and DMI. The final method was used for the detection and quantification of NMP in an aqueous solution of an analogue of cefotaxime (cephalosporin antibiotic) which is typically used for intravenous injections. Furthermore, the reaction was used for the analysis of EG in water and contact lens solutions after DMP treatment in which EG forms a cyclic ether named 2,2-dimethyl-1,3-dioxolane (2,2-DD). Contact lens solutions of several suppliers were collected and analysed for EG using the described protocol. Contact lenses can be made sterile by using ethylene oxide which may form EG when it comes into contact with water. Residual EG that is exposed to a person's eyes can cause irritation. The short term exposure limit (STEL) of EG is reported to be 40 ppm according to European guidelines [26]. STEL is the maximum concentration of a chemical to which workers may be exposed continuously for a short period of time without any danger to health, safety or work efficiency.

3.2. Experimental

3.2.1. Reagents

Methanol (99.99%), n-propanol (99+%), EG (99.75%), DMP (98+%) and NMP (>99.5%) were obtained from Acros Organics (Geel, Belgium). DMP was further purified by distillation under a nitrogen atmosphere. Benzyl alcohol (BA, >99%), DMI (>99.99%) and LC-MS grade water were purchased from Sigma Aldrich (St. Louis, MO, USA); DMF (>99.99%), acetone (>99.99%) and triethylamine (99.5%) from Fisher Scientific (Loughborough, United Kingdom) and DMSO from Merck (Darmstadt, Germany). Hydrochloric acid (37.5%) (HCl) was bought from VWR International S.A.S. (Fontenay-sous-Bois, France). Formic acid (65%) and sodium carbonate were from Chem-Lab NV (Zedelgem, Belgium). 2,2-DD (>98%) was purchased from TCI Europe (Zwijndrecht, Belgium).

3.2.2. Chromatographic systems

GC analyses were performed with a Perkin Elmer Autosystem XL (Waltham, MA, USA) equipped with a Perkin Elmer Turbomatrix 40 HS autosampler (balanced pressure system). All FET and sHS-parameters are given in Table 3.1.

Table 3.1: Used HS parameters.

Parameter	FET	sHS
Equilibration temperature (ET)	≥ 170 °C	80 °C
Equilibration time	20 min	20 min
Needle temperature	≥ 5 °C above ET	120 °C
Transfer line temperature	≥ 10 °C above ET	140 °C
Pressurization time	1.0 min	1.0 min
Injection time	0.04 min	0.04 min
Needle withdrawal time	0.4 min	0.4 min
Injection port temperature	≥ 15 °C above ET	200 °C
Carrier gas pressure	160 kPa	160 kPa
Split ratio	1:5	1:5
Detector type	FID /MS	FID /MS
Split ratio FID/MS	3:1	3:1
Detector temperature FID	220°C	220 °C

A minimum FET temperature of 170 °C was selected to ensure the complete evaporation of all analytes. HS-vials and PTFE/Sil-caps were purchased from Perkin Elmer as well. Separations regarding FET-GC of polar residual solvents were carried out on an AT^{TM}-Aquawax column (30 m x 0.53 mm, d_f = 0.50 µm) from Grace (Columbia, MD, USA). Separations for EG analysis and the evaluation of reaction parameters were carried out on a ZB-624 column (30 m x 0.53 mm, d_f = 3.00 µm). The oven program given in Table 3.2 was used for all experiments. The effluent from the column was splitted towards the FID and a Perkin Elmer Turbomass mass spectrometer (MS) operated in full scan mode.

Table 3.2: GC oven program.

t (min)	T (°C)
0	40
10	40
15 (40 °C/min)	240
25	240
40	40

3.2.3. Preparation of solutions

3.2.3.1. Checking of DMP-water reaction parameters

Water scavenging reactions were performed with different volume ratios of water/DMP (1:2.5 to 1:27.5) catalysed by varying volumes of HCl (1 to 10 µL) to determine the optimum reaction conditions. The use of formic acid as a catalyst and the influence of the reaction time were tested as well. Reactions were performed in open HS vials (not capped). After the reaction, 10 mL of DMF was added to create a suitable matrix for the sHS determination of acetone.

3.2.3.2. DMP-water reaction procedure

Reactions with aqueous samples were performed by transferring 4 mL of sample in a volumetric flask of 50 mL and adding 40 mL of DMP to react with water. Reactions were catalysed by adding 10 µL of hydrochloric acid (37.5 w/w %) to the solution. The solution cools down significantly during the hydrolysis reaction which was considered to be completed when the flask was again at room temperature. 1 mL of the appropriate internal standard solution (see 3.2.3.3.) was added before completing to volume with methanol. Samples

were neutralised afterwards by addition of a spoonful (~ 5 g) of sodium carbonate to obtain a saturated solution. Since sodium carbonate does nearly not dissolve in the mixture, solutions were stirred for 10 minutes with a magnetic stir bar to improve contact. Supernatant was decanted in a centrifuge tube and centrifuged at 4500 g for 10 minutes. The same procedure was used to prepare blank solution. As an alternative to sodium carbonate, neutralisation was also performed with 20 µL of triethylamine before adding up to volume. Since triethylamine mixes well with the reaction mixture, neutralisation occurs instantaneously and centrifugation is not necessary anymore.

3.2.3.3. Solutions for FET analysis of polar residual solvents

A stock solution was prepared by dissolving the following high boiling polar residual solvents in methanol: DMF, DMA, DMSO, NMP and DMI (14 mg/mL). For the internal standard solution used for calibration, BA was dissolved in methanol to obtain concentrations of 14 mg/mL. Calibration solutions were prepared by diluting appropriate volumes of the stock solution in methanol. Each time 3 mL of internal standard solution was added before adding up to the volume of 25 mL. 10 µL of calibration solution was transferred to a HS vial and sealed with a PTFE/Sil-cap for FET-GC analysis.

A sample stock solution of the same high boiling polar solvents (1.4 mg/mL each) was also prepared in LC-MS-grade water. Due to the dilution factor of 50 for the internal standard (cfr. 1 mL to 50 mL, section 3.2.3.2.) another internal standard solution was prepared by dissolving BA in methanol to obtain a concentration of 0.84 mg/mL. One mL of neutralised solution obtained by treating a sample with the procedure described in 3.2.3.2. was transferred to a HS vial which was not closed. The vials were placed in a vacuum oven at room temperature set at ≤0.1 kPa for 5.5 min to remove the excess of methanol, acetone and DMP. After evaporation, the vials were capped with a PTFE/Sil-cap to be analysed with FET-GC.

3.2.3.4. Residual NMP determination in cefotaxime analogue solution

The 0.4 % solution of the cefotaxime analogue in water for injection was analysed as such by sHS-GC at 80 °C and standard FET-GC (sample volume of 10 µL) as well as by FET-GC after treatment using the procedure described in 3.2.3.2.

3.2.3.5. Solutions for sHS analysis of EG

A stock solution of EG (2 mg/mL) was prepared in LC-MS grade water. DMSO was used as solvent to prepare a 0.2 mg/mL stock solution of 2,2-DD. Calibration solutions were prepared by diluting appropriate volumes of this 2,2-DD stock solution in DMSO.

Next, 1.0 mL of calibration solution was mixed with 1.0 mL of blank prepared by the procedure described in 3.2.3.2. Samples were treated according to 3.2.3.2 and 1.0 mL of the resulting solution was transferred to a headspace vial followed by addition of 1.0 mL of DMSO. Finally, the vial was closed with a PTFE/Sil-cap to be analysed with sHS-GC.

3.2.4. Method validation

The linearity of the calibration curve was determined by analysing calibration solutions with the described HS methods. In case of FET-GC analysis, peak areas were corrected by normalisation towards the internal standard and plotted vs. the analyte concentrations. The recovery of the polar residual solvents method was determined by preparing aqueous sample dilutions with known concentrations of analytes. Resulting concentrations were in the range of 50-250 ppm. Consequently, an aliquot was treated according to the aforementioned protocol and analysed with the appropriate FET-GC method.

The recovery of the EG method was determined by preparing aqueous samples with known concentrations of EG. Resulting concentrations were in the range of 175-350 ppm and samples were treated according to the aforementioned protocol and analysed with the appropriate sHS-GC method.

3.3. Results & Discussion

3.3.1. Investigation of DMP treatment parameters

3.3.1.1. Amount of acid and reaction time

Important parameters were the amount of acid necessary to catalyse the reaction to completion and the time needed. In order to test the influence of different amounts of HCl and reaction times, reactions were performed with 100 µL of water and 2.5 mL of DMP to which 1, 5, 10 or 20 µL of HCl was added. Adding 2.5 mL of DMP meant that a larger ratio than 1:10 was used. This was done to have an excess of DMP. To evaluate the influence of both parameters the obtained peak area of acetone was plotted against the reaction time. As can be seen from Figure 3.2, the acetone yield stays rather constant for all tested amounts of added HCl. The tendency of the acetone yield curve to decrease over time might be due to the fact that acetone is rather volatile and that therefore acetone might evaporate partially over time. Since a volume of 10 µL was also used for FET analysis, for practical reasons addition of 10 µL of acid was selected.

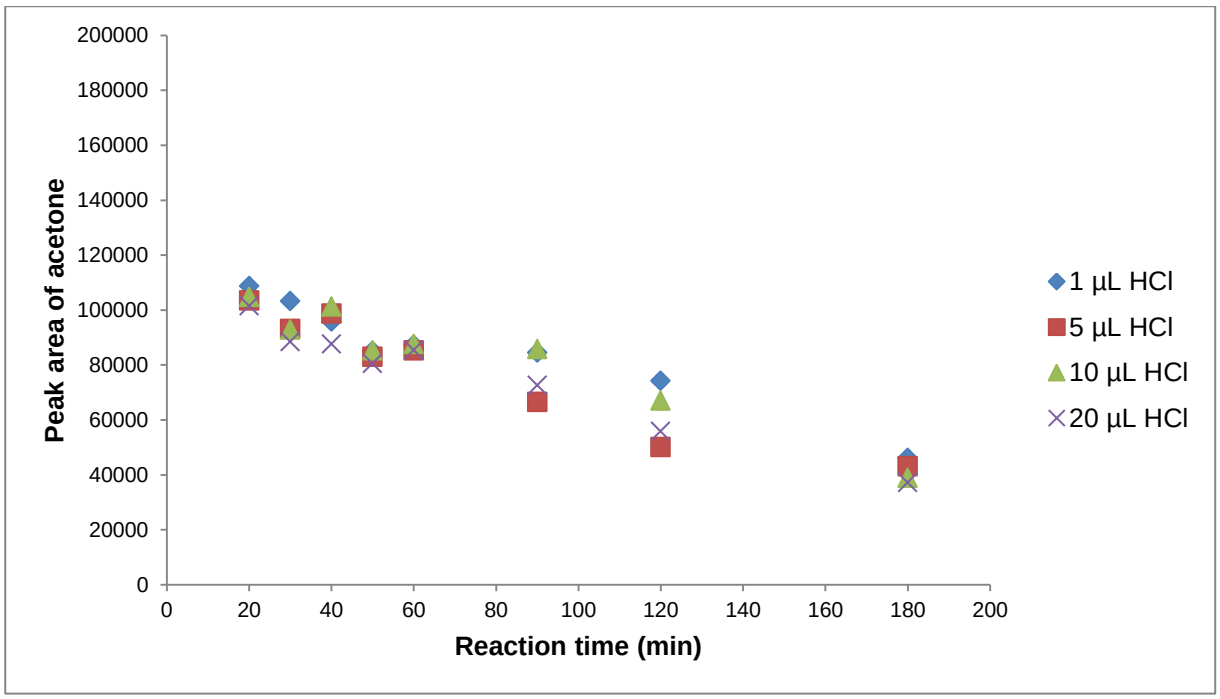

Figure 3.2: Acetone yield vs. reaction time and amount of added HCl.

3.3.1.2. Amount of DMP

As mentioned earlier, a ratio of 1 mL of water to 10 mL of DMP was proposed for complete elimination of water from aqueous samples. In order to check this, different ratios of water:DMP were tested. Each time 10 µL of HCl was added. This experiment was performed for 3 different volumes of water (50; 100 and 150 µL) with increasing volumes of added DMP. By plotting the obtained peak area for acetone *versus* the amount of DMP (Figure 3.3), it was noticed that all three curves flatten from a water DMP ratio of 1:10. MS data of a sample that was treated using a 1:10 ratio were evaluated to check if all water from the sample was removed. However, the air in a HS vial also contains some water so that always a small amount of water is injected on the column. Therefore a comparison was made with an empty vial (just filled with air). Extracting an *m/z* value of 18, it was found that the obtained water peak for the treated sample was even smaller than for the empty vial (Figure 3.4). This could be explained by the fact that residual DMP reacts with the moisture in the air.

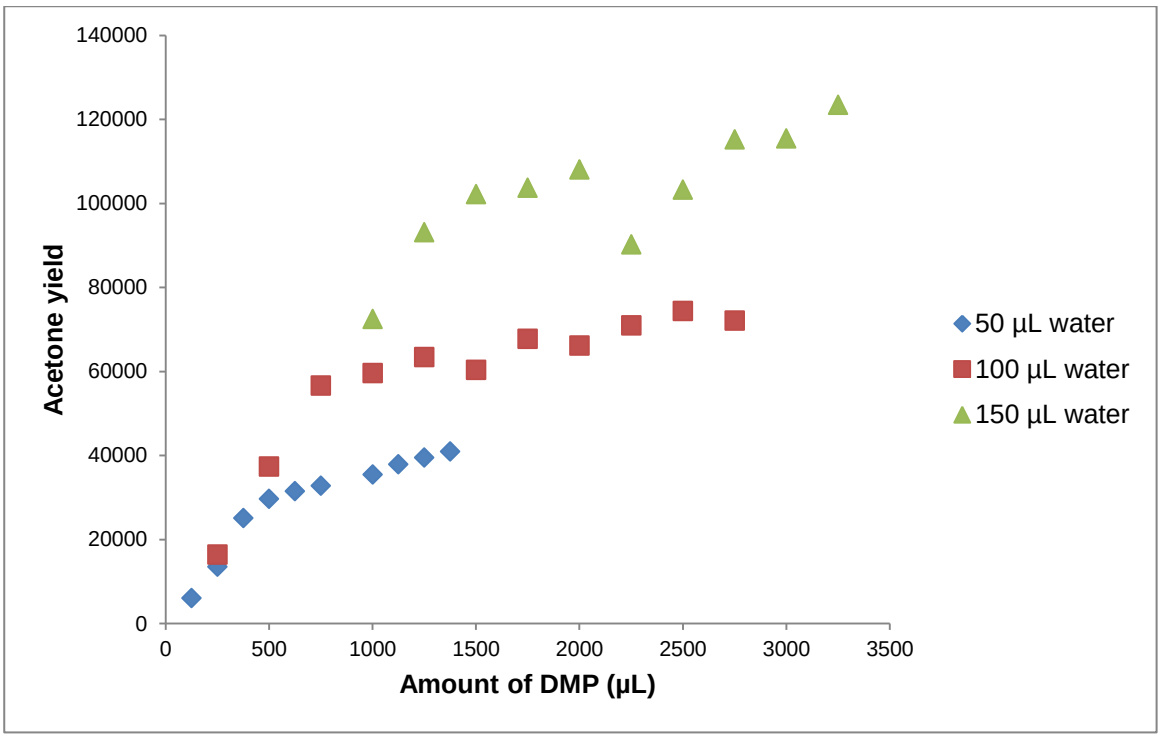

Figure 3.3: Acetone yield vs. different volumes of DMP.

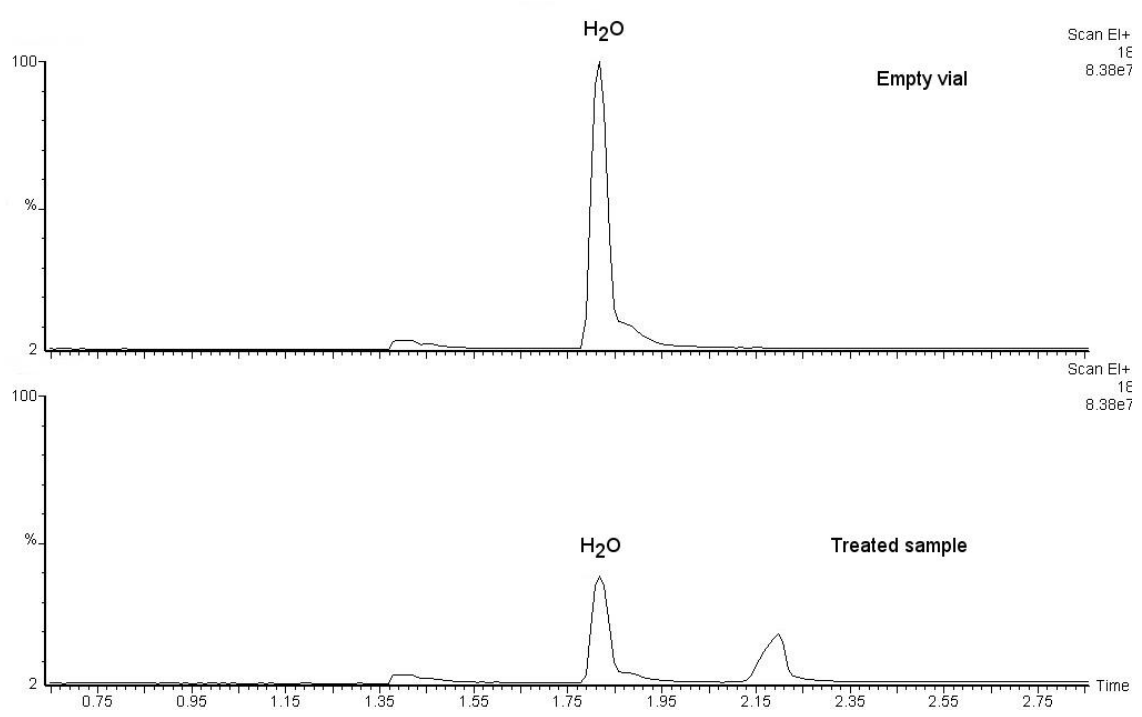

Figure 3.4: Comparison between the water content of an empty vial and a vial containing 10 µL of treated water sample using extracted ion chromatograms of 18 *m/z* from MS data. Chromatograms were recorded using the instrumental parameters described in 3.2.2.

3.3.1.3. Type of acid

Using a weak acid such as formic acid instead of HCl can be an advantage as it is less harmful for the column and volatile too. In order to test the suitability of formic acid, reactions of 100 µL of water with different amounts of DMP were catalysed by using 10 µL of formic acid. The acetone yield was compared with samples catalysed with 10 µL of HCl. As can be seen from the acetone yield depicted in Figure 3.5, a strong acid such as HCl is necessary to catalyse the reaction.

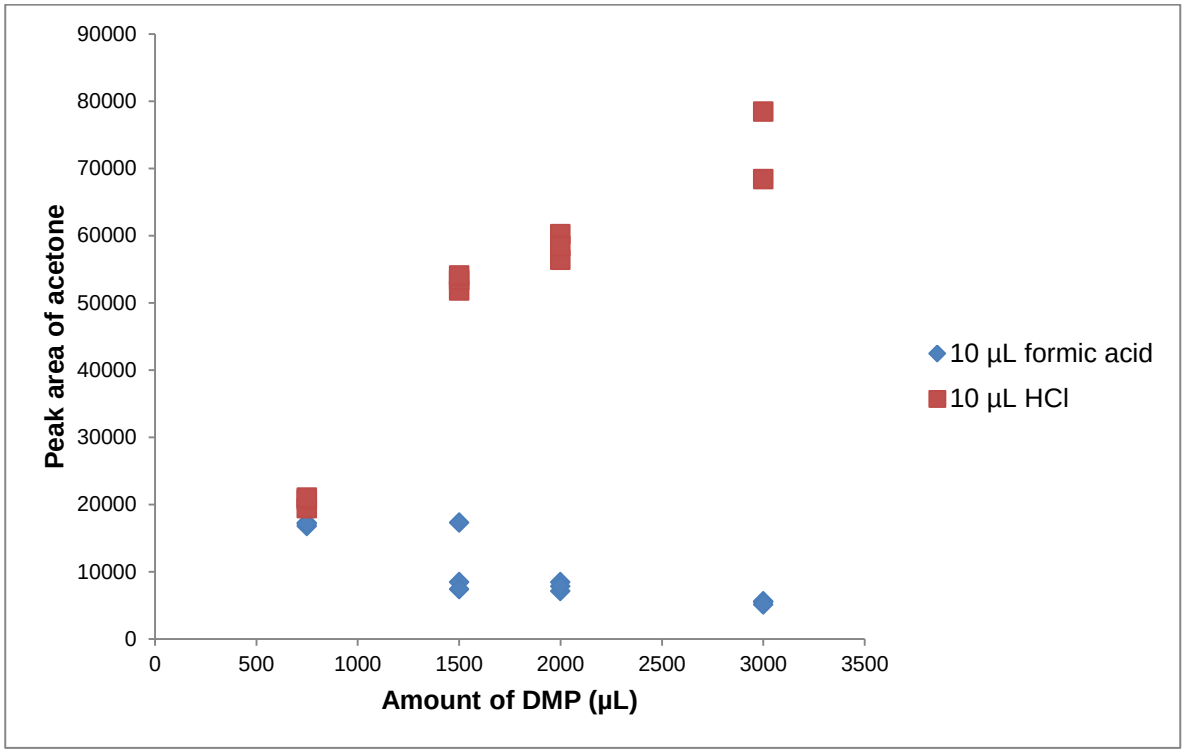

Figure 3.5: Comparison of the acetone yield between HCl and formic acid as catalyst.

3.3.2. Influence of sample acidity on the response of analytes and choice of neutralising agent

After completion of the DMP hydrolysis reaction, there is still hydrochloric acid present in the final solution which can result in degradation of the GC column as well as of the analytes when the sample is not neutralised prior to analysis. For instance, DMSO is known to degrade to dimethylsulfide (DMS) and/or dimethylsulfone ($DMSO_2$) under strong acidic or basic conditions and elevated temperatures. In order to check the influence of the sample acidity, a measurement was performed on an acidified calibration solution and compared with a non-acidified calibration standard. Results depicted in Figure 3.6 clearly show the influence of acid that remains in the sample after treatment.

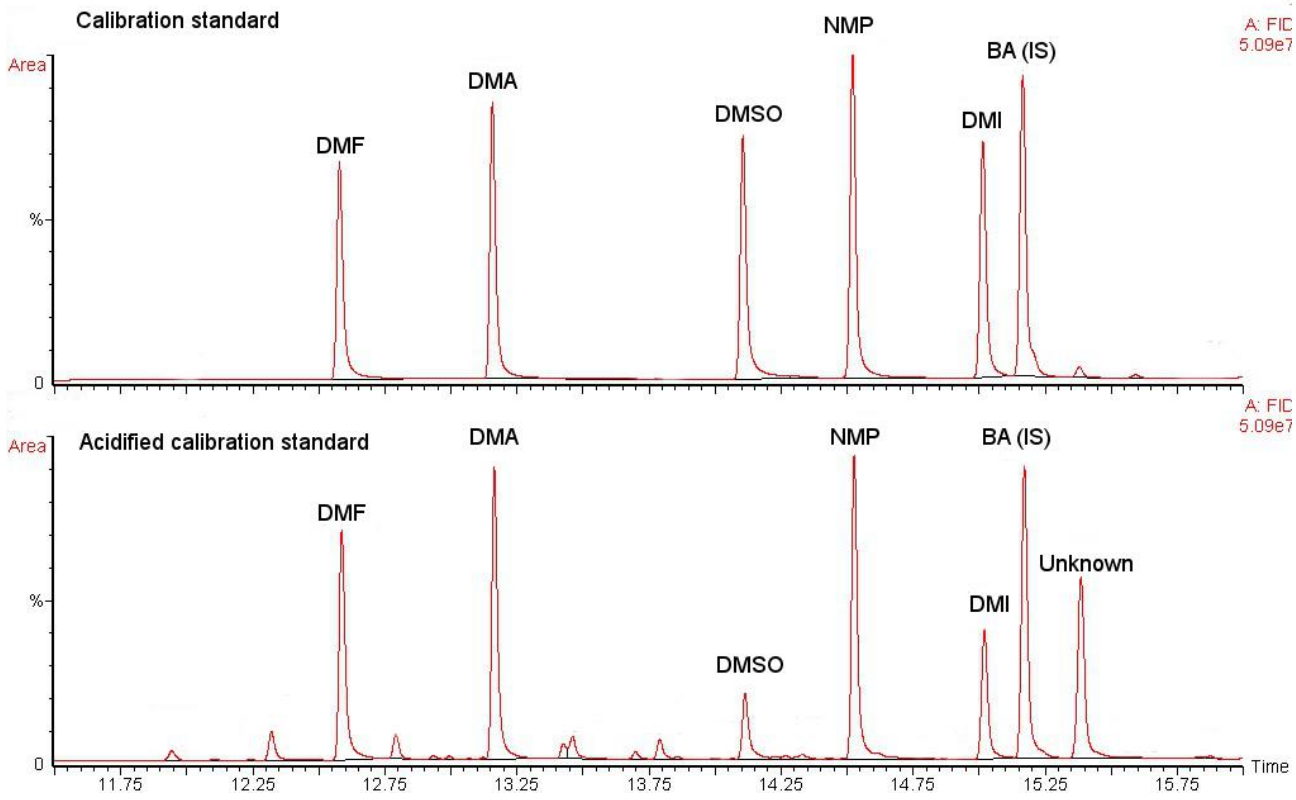

Figure 3.6: GC-FID chromatogram of acidified calibration standard (lower chromatogram) compared with this of a normal calibration standard (upper chromatogram). Ratios of peak areas of an acidified calibration standard vs. a normal calibration standard: DMF = 0.9969, DMA = 1.0093, DMSO = 0.2740, NMP = 0.9536, DMI = 0.5371 and BA = 0.9545. Chromatogram was recorded using the instrumental parameters described in 3.2.2.

In the lower chromatogram of Figure 3.6 several additional little peaks can be noticed while the peaks for DMSO and DMI are clearly smaller. In the ideal case (without degradation) the only difference in peak areas should arise from variations of the small sample volume introduced in the HS vial. So, the area ratio of corresponding peaks in the two chromatograms should be the same. The ratios obtained are given in the legend of Figure 3.6. The ratios for DMF and DMA are both close to 1 meaning that the variation on injection was very small between the two samples and that there is no acid induced degradation occurring. The ratios for NMP and BA are 5% below the optimum which is an indication of degradation and makes BA unsuitable as internal standard under acidic conditions. The most obvious difference is the ratio change for DMSO and DMI and the large extra peak eluting after the internal standard. After evaluation and comparison of the mass spectrum with the NIST library, it was revealed that this peak had a similar fragmentation pattern as $DMSO_2$.

Figure 3.7 depicts the comparison of the obtained mass spectrum (after background subtraction) of the unknown compound with this of the NIST library. From these results it became clear that sample neutralisation is necessary. Addition of sodium carbonate followed by stirring for at least 10 minutes to improve contact with the solution (not optimized) ensured complete neutralisation.

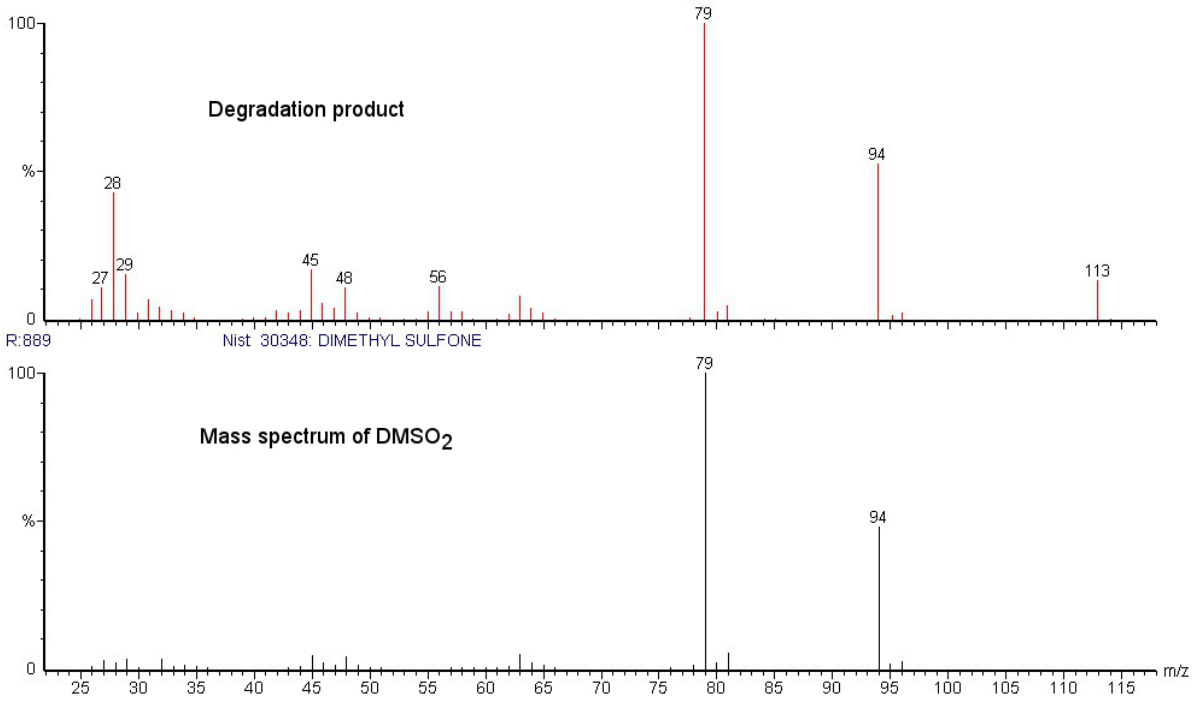

Figure 3.7: Comparison of the mass spectrum of the unknown peak (degradation product) in Figure 3.6 with the mass spectrum of $DMSO_2$.

Triethylamine also ensures complete neutralisation due to its good solubility in the reaction mixture and makes centrifugation unnecessary. However, neutralisation of hydrochloric acid with triethylamine results in the formation of triethylammonium chloride that could compromise the HS analysis. Indeed, triethylammonium chloride does have a rather good solubility in for instance acetone and methanol in contrast to sodium carbonate. Therefore, it is not possible to remove this salt by a simple centrifugation or filtration step. After analysis, deposition of triethylammonium chloride to the vial wall was clearly visible and could possibly result in adsorption effects and a large interference which is eluted in the time frame where also DMA eluted (Figure 3.8). Also, triethylamine caused the response to vary during a sequence, most likely due to adsorption effects of excess of triethylamine in the HS system.

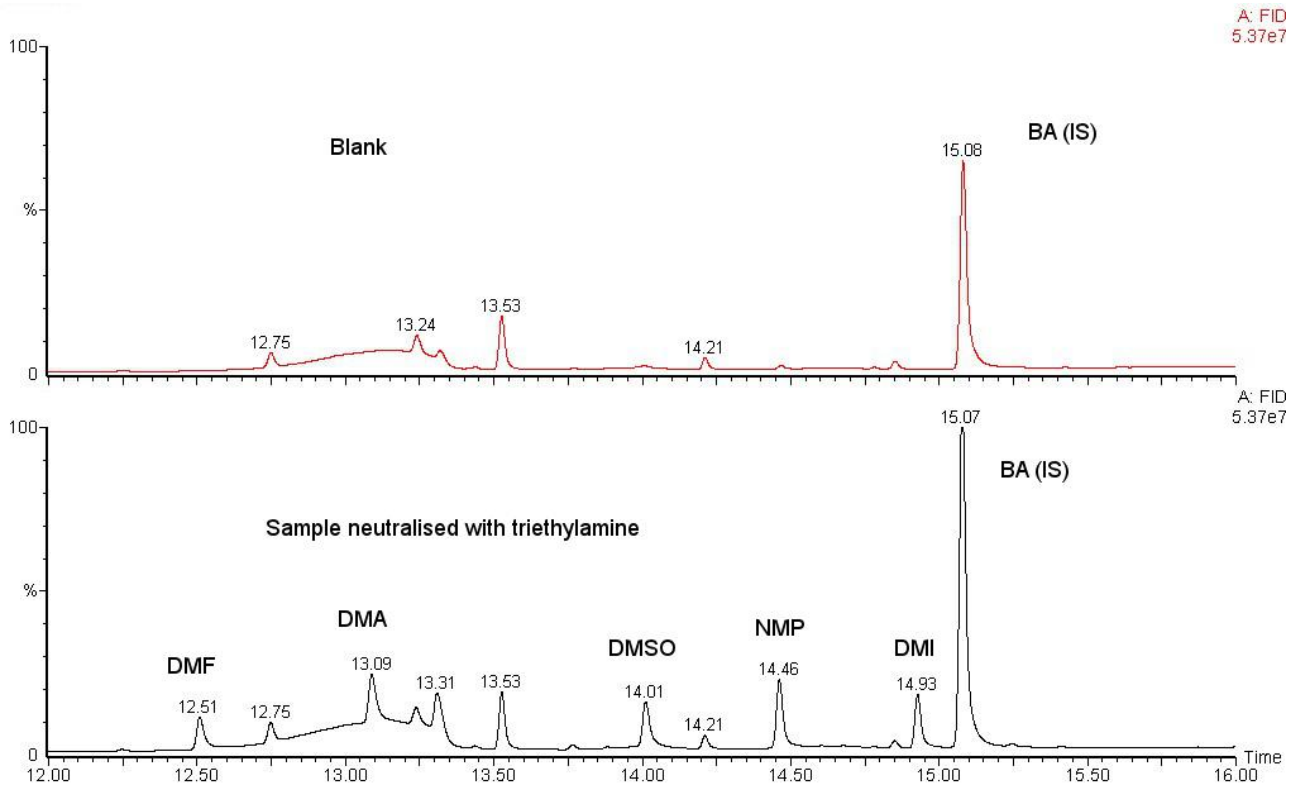

Figure 3.8: Chromatogram of the acid catalysed reaction mixture after neutralisation with triethylamine and blank. Chromatogram was recorded using the instrumental parameters described in 3.2.2.

3.3.3. Optimization of the solvent evaporation step (FET-GC)

The vacuum evaporation of the solvents, formed by the reaction of DMP with water (methanol and acetone) in the sample vials turned out to be a very crucial step to ensure a good recovery of the analytes. If the excess solvents are removed insufficiently, the amount of solvent remaining in the vials would be too large, resulting in a vial pressure that is too high to perform FET analysis. On the other hand, evaporation to complete dryness could result in the loss of analyte. However, since the included analytes have a higher boiling and lower vapour pressure compared to methanol and acetone, this step should be controllable. So, different evaporation times were tested after DMP treatment and as shown in Figure 3.9 it is clearly visible that after 6 minutes the loss of analyte starts to occur under the used vacuum conditions. It was decided to carefully time the evaporation step to ensure an adequate recovery of all analytes. 5.5 minutes provided adequate recoveries for all analytes without crossing the limits of the maximum sample volume. In this case a significant gain in sensitivity is obtained as compared to standard FET where 10 µL is used [4]. After sample treatment, samples are diluted 12.5 times (4 mL to 50 mL, see 3.2.3.2.) but are enriched about a factor 100 when the amount of solvent is reduced to 10 µL. This results in a net gain of about 10 and could even be improved further when a larger volume is treated with the vacuum drying step.

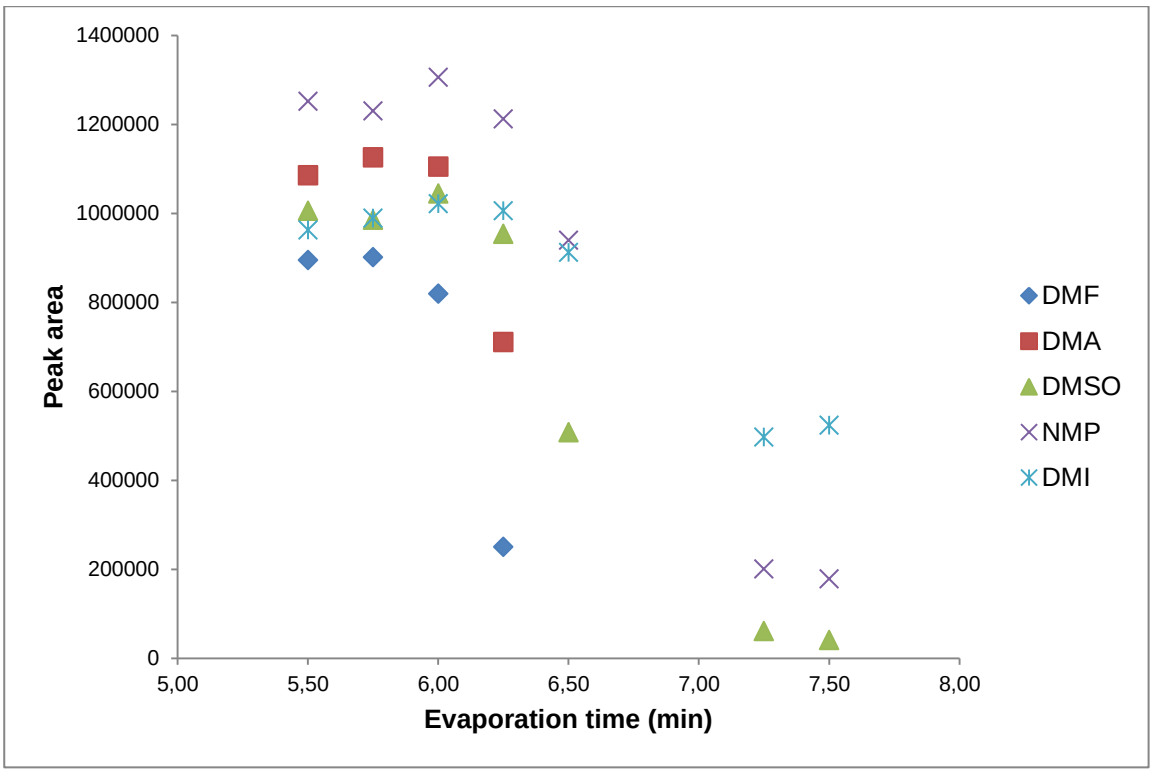

Figure 3.9: Comparison of different evaporation times under the used vacuum conditions.

3.3.4. Identification of EG-DMP derivative

Attempts were done initially to derivatize EG (after water removal by DMP) with phenyl boronic acid (PBA) or N,O-bis(trimethylsilyl)trifluoroacetamide (BSTFA). However, EG derivatives of PBA or BSTFA could not be identified in the samples. This can be explained because a reaction already took place between EG and DMP leading to the quantitative formation of 2,2-DD under the removal of water which is also scavenged by DMP (Figure 3.10). This reaction is well known in organic synthesis where it is used as protecting agent for diols like EG [27]. To the best knowledge of the authors, the application of DMP as a derivatization agent for GC-analysis of EG has never been described before. The obtained mass spectrum of the product is shown in Figure 3.11 and was confirmed by the NIST library. In the chromatogram obtained using an AT^{TM}-Aquawax column, 2,2-DD eluted on the shoulder of methanol that is originating from the DMP treatment. To have more retention for 2,2-DD it was decided to change to a column with a less polar stationary phase like a ZB-624 column. 2,2-DD was analysed with sHS since 2,2-DD has a relatively low boiling point (93 °C) so that it was not possible to apply the solvent evaporation step as with the other polar residual solvents.

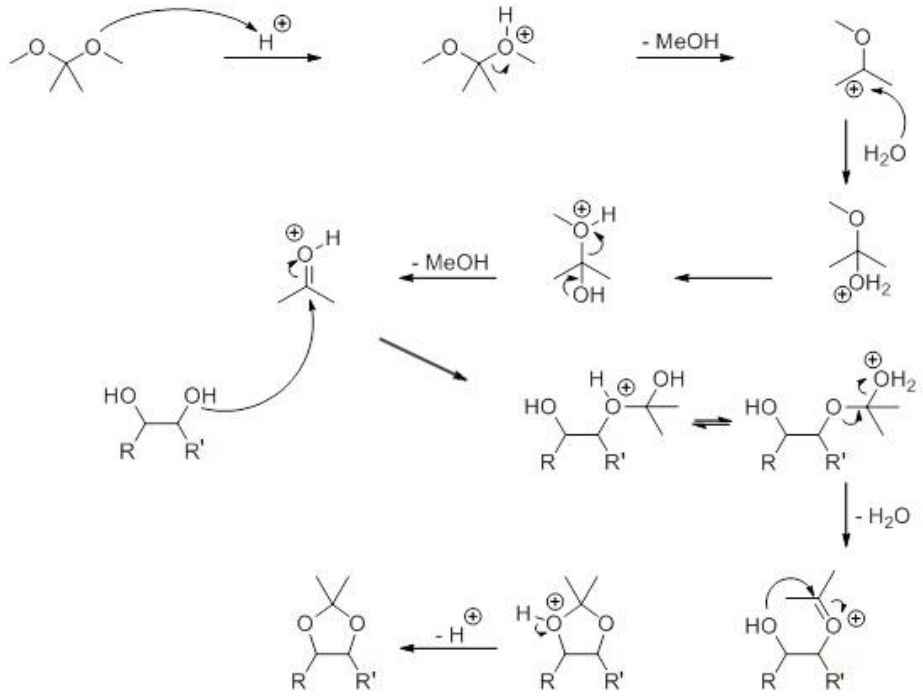

Figure 3.10: Reaction mechanism of the acid catalysed protection of diols with DMP.

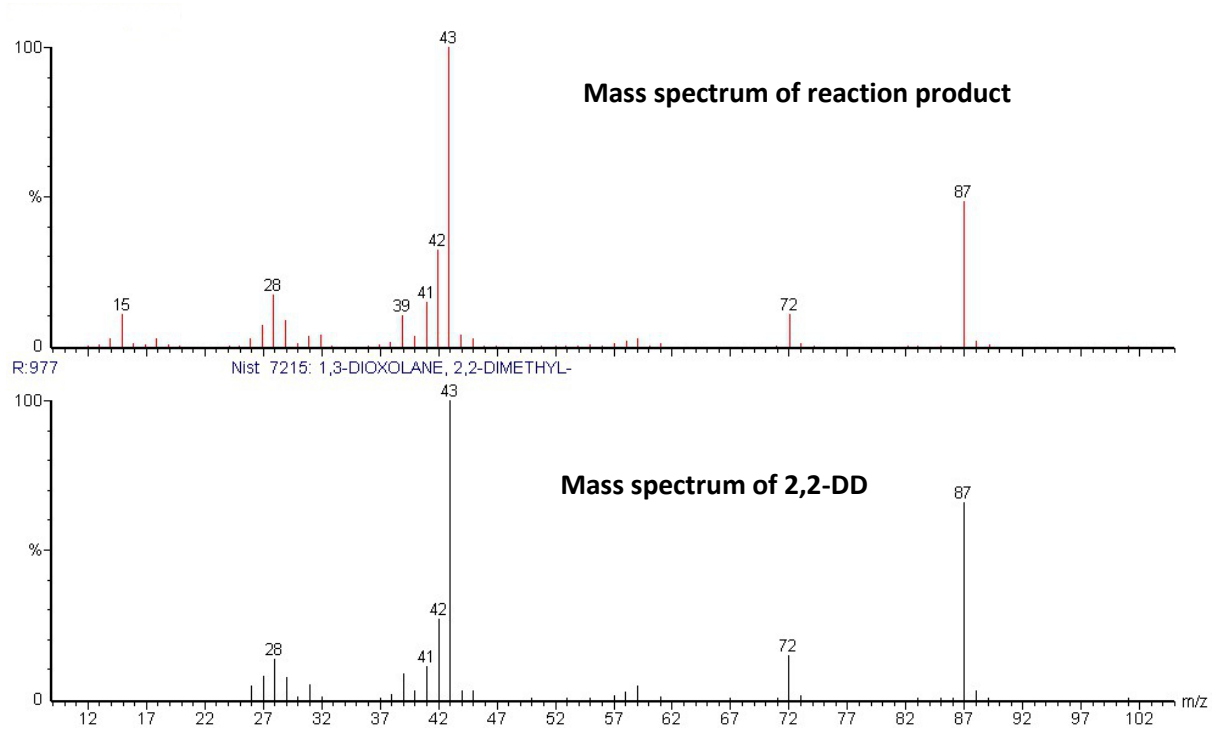

Figure 3.11: Comparison of the mass spectrum of the reaction product of EG after treatment of the aqueous sample by DMP with the mass spectrum of 2,2-DD.

3.3.5. Further improvement

After treatment and derivatization with DMP of aqueous samples containing EG, it is possible to further improve sHS analysis by adding a sHS compatible high boiling diluent such as DMSO. By adding DMSO to the resulting sample solution, partial pressures of methanol and acetone are lowered so that a higher HS temperature can be applied without exceeding the pressure limits that have to be taken into account when performing HS experiments. A potential approach to further extend the applicability is to use an acetal that produces a higher boiling alcohol such as propanol, so that HS temperatures can be increased leading to an increased sensitivity of the method. An example of such an acetal is 2,2-dipropoxypropane to produce acetone and n-propanol. However, this product is not easily commercially available. A mixture of propanol and acetone (in a molar ratio of 1:2) containing 2,2-DD was prepared to which DMSO was added for sHS analysis. It was found that the HS temperature could be increased to 100 °C compared to the maximum temperature of 80 °C when DMP is used as water scavenger. This resulted in a sensitivity gain of a factor 2.4 for 2,2-DD.

3.3.6. Method validation

3.3.6.1. Linearity of calibration curves

Calibration curves using 5 concentration levels for the mixture of polar residual solvents were constructed in the range of 500 – 3000 mg/L by repetitive injections of each calibration point. R^2 values were found to be equal to or higher than 0.999, indicating that a good linear relationship was obtained between concentration and peak areas for all analytes. For EG, a calibration curve with 5 different concentration levels of 2,2-DD was constructed in the range from 2.1 – 24.6 mg/L and an R^2 of 0.999 was obtained. The lowest calibration point of 2.1 mg/L is equal to the limit of quantification (LOQ), determined at a signal-to-noise ratio of 10. Taking into account the dilution and difference in molecular weight between 2,2-DD and EG, this corresponds to 32 ppm of EG, which is lower than the STEL limit of 40 ppm. For all analytes, a lack of fit test was performed (Table 3.3) and the residuals were checked. These results were satisfactory as all obtained F-values were lower than the critical F values.

Table 3.3: Lack of fit results for all analytes.

	DMF	DMA	DMSO	NMP	DMI	EG
MS residuals	0,000068	0.000074	0.000068	0.000062	0.000022	38631
df residuals	10	10	10	10	10	8
MS pure error	0.000085	0.00010	0.000051	0.000048	0.000017	24963
df pure error	7	7	7	7	7	5
MS lack of fit	0,000029	0.000015	0.00011	0.000094	0.000033	61411
df lack of fit	3	3	3	3	3	3
F value	0.34	0.15	2.08	1.94	1.97	2.46
F critical	4.35	4.35	4.35	4.35	4.35	5.41

3.3.6.2. Recovery and repeatability

Results for all analytes are given in Table 3.4. The recovery values found were between 97.5 and 103.9% and RSD-values did not exceed 3.8%, which is acceptable for such small amounts determined by GC.

Table 3.4: Recovery results for the studied polar residual solvents.

	50 ppm		**100 ppm**		**250 ppm**	
Compound	Recovery (%)	RSD (%) n = 8	Recovery (%)	RSD (%) n = 8	Recovery (%)	RSD (%) n = 8
DMF	98.0	3.2	97.6	1.5	100.9	2.6
DMA	97.5	1.1	100.1	1.4	99.7	3.8
DMSO	103.9	1.2	100.7	3.6	101.7	2.5
NMP	101.8	2.3	103.4	1.1	100.3	2.2
DMI	97.9	1.0	97.8	2.5	98.3	2.3
	175 ppm		**250 ppm**		**350 ppm**	
	Recovery (%)	RSD (%) n = 6	Recovery (%)	RSD (%) n = 6	Recovery (%)	RSD (%) n = 6
EG	100.5	2.3	101.8	1.2	101.6	1.2

3.3.7. Analysis of residual NMP in an aqueous solution of a cefotaxime analogue

To demonstrate the applicability of the scavenging method, aqueous solutions of a cefotaxime analogue (0.4%) were analysed. NMP was used during the preparation of this analogue and it was therefore necessary to screen for residual solvents. Using sHS-GC (which is typically used to screen and quantify residual solvents) did not result in detection of NMP in the sample (Figure 3.12). Standard FET-GC did result in a very small peak, but this was too small for reliable quantification. After analysis of the aqueous cefotaxime solution using the described water scavenging method, NMP could be properly detected and quantified. The cefotaxime analogue was found to contain 0.63% (m/m) of NMP.

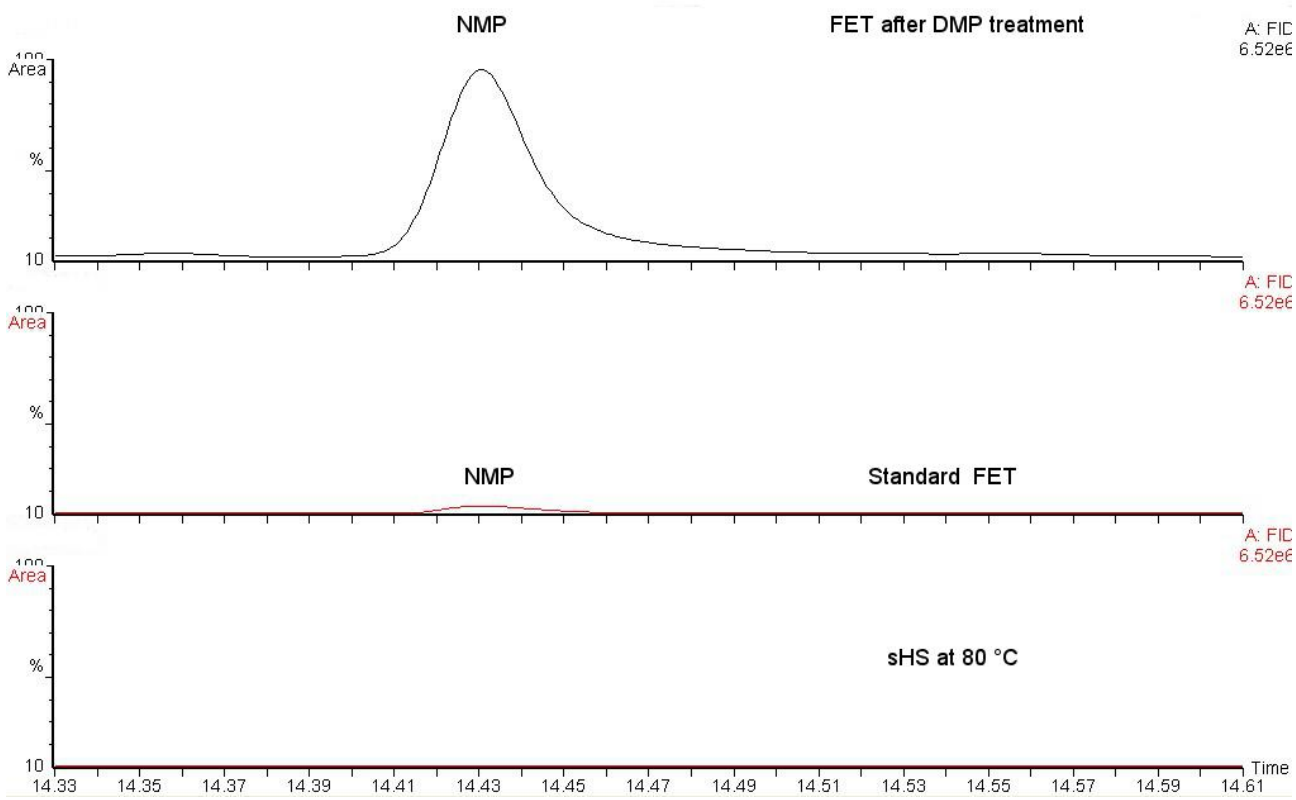

Figure 3.12: Analysis of NMP in an aqueous sample containing 0.4% of a cefotaxime analogue using three approaches: Upper trace: FET after water scavenging and enrichment procedure, Middle trace: standard FET analysis of 10 µL sample, Lower trace: sHS analysis at 80 °C.

3.3.8. Analysis of EG in contact lens fluids

Five different contact lens fluids were examined. In four of them, no traces of EG were detected, but one of the samples did contain 2,2-DD which was formed from EG originally present in the sample. The 2,2-DD concentration was found to be 4.8 mg/L, which was recalculated to 73 ppm of EG in the original sample. This is above the threshold concentration at which harmful effects start to manifest.

3.4. Conclusions

Results have shown that the DMP hydrolysis reaction with water is an excellent method to circumvent several GC related problems. Firstly, the DMP hydrolysis reaction enabled sample enrichment of aqueous samples prior to FET-GC analysis to address the problems related to the maximum tolerable sample volume. In this case a 10-fold increase of sensitivity was obtained compared to standard FET of aqueous samples where 10 µL is used and this can be further improved if a larger sample volume is enriched during the vacuum drying step. The proposed method provides adequate recovery for a set of typical high boiling polar residual solvents after successfully removing water from aqueous samples. The developed method was applied for the determination of residual NMP in an aqueous solution containing a cefotaxime analogue. NMP was successfully detected and quantified using the water scavenging method while standard FET and sHS approaches showed insufficient sensitivity. Furthermore, it was discovered that under the used reaction conditions EG converts quantitatively to 2,2-DD whilst water is eliminated as well. This makes further derivatization with reagents such as PBA or BSTFA superfluous. Adding DMSO to the sample enabled sHS analysis of EG making it possible to quantify 40 ppm of EG in aqueous samples which is the level where EG starts to have an effect on human health according to its STEL limit. As with the high boiling residual solvents, good recoveries were obtained with an acceptable limit of quantification. By selecting another acetone acetal (such as 2,2-dipropoxypropane) higher boiling alcohols could be produced. This has the advantage that higher HS temperatures could be selected leading to a higher sensitivity. Finally, the proposed method could also be used with direct injection as the resulting reaction mixture is not harmful to non-water resistant GC columns and flooding of injection liners would be avoided. This will enable large volume injection with for instance a programmed temperature injector to increase further the sensitivity.

3.5. References

[1] B. Yu, Y. Song, L. Han, H. Yu, Y. Liu, H. Liu, Optimizations of packed sorbent and inlet temperature for large volume-direct aqueous injection-gas chromatography to determine high boiling volatile organic compounds in water, J. Chromatogr. A, 1356 (2014) 221-229

[2] European Pharmacopoeia, 8th ed., Identification and Control of Residual Solvents. (Section 2.4.24), European Department for the Quality of Medicines, Council of Europe, Strasbourg, 2014.

[3] K. Ui, M. Abo, A. Okubo, S. Yamazaki, An improved method for the analysis of mimethyl sulfoxide in water samples, Analytical Sciences 20 (2004) 223-225

[4] D.M. Kialengila, K. Wolfs, J. Bugalama, A. Van Schepdael, E. Adams, Full evaporation headspace gas chromatography for sensitive determination of high boiling point volatile organic compounds in low boiling matrices, J. Chromatogr. A, 1315 (2013) 167-175

[5] N. van Boxtel, K. Wolfs, A. Van Schepdael, E. Adams, Evaluation of the full evaporation technique for quantitative analysis of high boiling compounds with high affinity for apolar matrices, J. Chromatogr. A, 1348 (2014) 63-70

[6] H.C. Hu, X.S. Chai, C.H. Wei, D. Barnes, Increasing the sensitivity of headspace analysis of low volatility solutes through water removal by hydrate formation, J. Chromatogr. A, 1343 (2014) 42-46

[7] www.merck-millipore.com/dryingagents. Accessed on 17-7-2015.

[8] C. Devos, N. Ochiai, K. Sasamoto, P. Sandra, F. David, Full evaporation dynamic headspace in combination with selectable one-dimensional/two-dimensional gas chromatography-mass spectrometry for the determination of suspected fragrance allergens in cosmetic products, J. Chromatogr. A, 1255 (2012) 207-215

[9] N. Ochai, K. Sasamoto, A. Hoffmann, K. Okanoya, Full evaporation dynamic headspace and gas chromatography-mass spectrometry for uniform enrichment of odor compounds in aqueous samples, J. Chromatogr. A, 1240 (2012) 59-68

[10] N. Ochai, K. Sasamoto, K. MacNamara, Characterization of sulfur compounds in whisky by full evaporation dynamic headspace and selectable one-dimensional/two-dimensional retention time locked gas chromatography-mass spectrometry with simultaneous element specific detection, J. Chromatogr. A, 1270 (2012) 296-304

[11] N.B. Smith, Determination of serum ethylene glycol by capillary gas chromatography, Clin. Chim. Acta, 144 (1984) 269-272

[12] W.H. Porter, P.H. Rutter, H. H. Yao, Simultaneous determination of ethylene glycol and glycolic acid in serum by gas chromatography-mass spectrometry, J. Anal.Toxicol., 23 (1999) 591-597

[13] V. Gembus, J.P. Goullé, C. Lacroix, Determination of glycols in biological specimens by gas chromatography-mass spectrometry, J. Anal.Toxicol., 26 (2002) 280-285

[14] M.R. Meyer, A.A. Weber, H.H. Maurer, A validated GC-MS procedure for fast, simple, and cost-effective quantification of glycols and GHB in human plasma and their identification in urine and plasma developed for emergency toxicology, Anal. Bioanal. Chem., 400 (2011) 411-414

[15] C. Achili, A. Ciana, M. Fagnoni, C. Balduini, G. Minetti, Susceptibility to hydrolysis of phenylboronic pinacol esters at physiological pH, Cent. Eur. J. Chem., 11 (2013) 137-139

[16] A. Takeuchi, S. Yamamoto, R. Narai, M. Nishida, M. Yashiki, N. Sakui, A. Namera, Determination of dimethyl sulfoxide and dimethyl sulfone in urine by gas chromatography-mass spectrometry after preparation using 2,2-dimethoxypropane, Biomed. Chromatogr., 24 (2010) 465-471

[17] K.D. Dix, P.A. Sakkinen, J.S. Fritz, Gas chromatographic determination of water using 2,2-dimethoxypropane and a solid acid catalyst, Anal. Chem., 61 (1989) 1325-1327

[18] F.E. Critchfield, E.T. Bishop, Water determination by reaction with 2,2-dimethoxypropane, Anal. Chem., 33 (1961) 1034-1035

[19] N.Y. Mary, Gas chromatographic determination of water in natural products by reaction with 2,2-dimethoxypropane, J. Pharm. Sci., 58 (1969) 1089-1092

[20] D. Erley, 2,2-dimethoxypropane as a drying agent for preparation of infrared samples, Anal. Chem., 29 (1957) 1564-1564

[21] J.R. Thorpe, D.M.R. Harvey, J. Optimization and investigation of the use of 2,2-dimethoxypropane as a dehydration agent for plant tissues in transmission electron microscopy, J. Ultrastruc. Res., 68 (1979) 186-194

[22] M.D. Maser, J.J. Trimble, Rapid chemical dehydration of biologic samples for scanning electron microscopy using 2,2-dimethoxypropane, J. Histochem. Cytochem., 25 (1977) 247-251

[23] L.L. Muller, T.J. Jacks, Rapid chemical dehydration of samples for electron microscopic examinations, J. Histochem. Cytochem., 23 (1975) 107-110

[24] K. Conway, J.A. Kiernan, Chemical dehydration of specimens with 2,2-dimethoxypropane (DMP) for paraffin processing of animal tissues: practical and economic advantages over dehydration in ethanol, Biotechnic Histochem., 74 (1999) 20-26

[25] A. De Ruiter, P. Van Banning, J.J. Willemse, Rapid histological results in aquaculture research by using the time-saving embedding procedure with 2,2-dimethoxypropane, Aquaculture, 25 (1981) 293-297

[26] Public Health England, Ethylene glycol: health effects, incident management and toxicology, 1 July 2014. Part of Chemical hazards compendium.

[27] T.W. Green, P. G. M. Wuts, Protective Groups in Organic Synthesis, Wiley-Interscience, New York, 1999, 207-215, 716-719

Chapter 4 - A headspace gas chromatography based methodology for the analysis of aromatic substituted quaternary ammonium salts

Niels van Boxtel, Kris Wolfs, Marta Guillén Palacín, Ann Van Schepdael, Erwin Adams

Pharmaceutical Analysis, Department of Pharmaceutical and Pharmacological Sciences

KU Leuven, Leuven, Belgium

Submitted to J. Chromatogr. A

Abstract

The analysis of quaternary ammonium salts (QAS) using GC is often performed by ‘’in injector’’ pyrolysis to create volatile degradation products for quantification purposes. Besides the risk of severe system contamination, the application of this approach on aqueous samples is problematic. In this work, the sample is treated in a vial with 2,2-dimethoxypropane (DMP) under acidic catalysis. In addition to the removal of water and sample enrichment, the QAS are decomposed. As HS transfers only volatile compounds to the GC system, contamination is avoided. It was found that depending on the presence of benzyl, phenyl or methyl groups on the quaternary nitrogen; benzyl chloride, N,N-dimethylaniline or chloromethane are formed respectively in the sealed vial. All these can be used as an analytical target. A calibration curve for benzyl chloride could be derived from the pure compound. Chloromethane was generated from pure benzyldimethyldecylammonium chloride (BEDIDE), a pure QAS with benzyl and methyl groups, to construct a secondary calibration curve using a back analysis approach. It has been proven that by quantifying the formed analytical targets, the mass balance for the QAS under investigation was close to 100%. The presented procedure allows the quantification of any aromatic substituted QAS without the need for a matching reference, which is a major advantage over existing CE and HPLC methods. The proposed methodology was validated for mouth sprays containing benzethonium chloride (BZTCl) or benzoxonium chloride (BZOCl) and for denatonium benzoate (DB) in ethylene glycol (EG) based cooling liquids. Results showed that the approach provided excellent linearity ($R^2 \geq 0.999$) and limits of detection around 0.01 µg/vial for benzyl chloride. It was found that the reaction product of DMP and glycerol which was also present in the mouthspray and some cooling liquids, caused chromatographic interference with benzyl chloride. Treating those samples in the vial with N,O-bis(trimethylsilyl)trifluoroacetamide (BSTFA) after the enrichment step removes the interference and leaves a possible pathway for the simultaneous determination of glycerol in those samples.

Keywords

Headspace, quaternary ammonium salts, gas chromatography

4.1. Introduction

Quaternary ammonium salts (QAS) are synthesised by reaction of tertiary amines with halogenated compounds and are mostly used as disinfectants, surfactants, corrosion inhibitors or pest controllers. The analysis of QAS is usually performed using liquid chromatography (LC) [1-9], capillary electrophoresis (CE) [10-12] or gas chromatography (GC) [13, 14]. Although LC is often combined with mass spectrometry (MS), LC-MS based methods often suffer from matrix effects that cause ion suppression in the ion source. This can be (partly) counteracted by using labelled standards which are however not always easily available and can be very expensive. It is also known that CE does not offer the best repeatability/reproducibility and is more problematic towards method transfer. GC methods are based on pyrolysis GC in which a sample is introduced into a heated injector. This has the disadvantage that when not all the resulting pyrolysis products are volatile, parts of the GC system can become contaminated by the gradual build-up of residues that cannot be evaporated. The determination of QAS in aqueous samples poses an even larger challenge. Evaporation of large amounts of water in an injection liner is problematic due to the large resulting gas volume after evaporation leading to flooding of the injection liner. Moreover, the introduction of large amounts of water on a GC column leads to column damage unless special water resistant columns are used. Static headspace (sHS)-GC on the other hand allows clean sample introduction as only volatile sample constituents are introduced in the GC system. However, the use of sHS-GC in combination with aqueous samples is limited as the used incubation temperature should be kept below the boiling point of water. This limits the sensitivity for analytes with a high boiling point and large affinity for the aqueous matrix. Recently, a method was published in which an acetone acetal was used for the complete removal of water prior to the analysis of a selection of typical high boiling polar residual solvents [15]. Acetone acetals such as 2,2-dimethoxypropane (DMP) react with water to form acetone and methanol under acidic catalysis. The fact that the resulting products are much more volatile than the analytes (which have a high boiling point), enables sample enrichment by simple evaporation using either a vacuum oven or a stream of nitrogen.

This work covers the use of full evaporation (FET)-HS-GC for the analysis of benzyl substituted QAS in aqueous samples after removal of water with DMP. First, a screening of typical QAS was performed to determine the resulting products and to evaluate the quantitative relationship of this approach. Finally, the method was applied to the analysis of denatonium benzoate (DB) in cooling liquids that contain both water and ethylene glycol (EG). The same approach was used to analyse benzethonium chloride (BZTCl) and benzoxonium chloride (BZOCl) in mouth sprays.

4.2. Experimental

4.2.1. Reagents

DMP (98+%), o-xylene (99%), N,O-bis(trimethylsilyl)trifluoroacetamide (95%) (BSTFA), sodium dodecyl sulphate (99.0%) (SDS) and N,N-dimethylaniline (99%) were purchased from Acros Organics (Geel, Belgium). Hydrochloric acid (37.5%) (HCl) was bought from VWR International S.A.S. (Fontenay-sous-Bois, France). DB (98%), BZTCl (99.0%), benzyldimethyldecylammonium chloride (BEDIDE) (97.0%), benzyl chloride (99%), sodium phosphate monobasic and trimethylphenyl ammonium chloride (TMPACl) (98%) were from Sigma Aldrich (New Jersey, USA). Toluene (99.8%) was purchased from Alfa Aesar GmbH & Co KG (Karlsruhe, Germany). Water was purified using a milliQ-system (Darmstadt, Germany). Phosphoric acid (85%) was obtained from Chemlab NV (Zedelgem, Belgium). Cooling liquids denatured with DB and consisting out of about 50 % v/v of EG and 50 % v/v of water were purchased in a local shop while mouth sprays containing BZTCl and BZOCl respectively were obtained from a local pharmacy (See Table 4.1 for their composition).

Table 4.1: Composition of the analysed mouth sprays.

BZTCl mouth spray	**BZOCl spray**
435 ppm BZTCl	~0.2% BZOCl
Chlorhexidine digluconate Maltitol Ethanol Menthol Castor oil Water	Sorbitol Ethanol Glycerol Peppermint oil Menthol Hydrochloric acid Water

4.2.2. Chromatographic systems

4.2.2.1. GC analyses

HS-GC analyses with flame ionization detection (FID) were carried out with an Agilent 6890 series GC equipped with a Perkin Elmer Turbomatrix 40 HS autosampler (balanced pressure system) (Waltham, MA, USA). GC-MS identifications and single ion monitoring (SIM) on *m/z* 91 and *m/z* 126 were performed with a Perkin Elmer Autosystem XL equipped with a Turbomatrix 40 HS autosampler and Perkin Elmer Turbomass mass spectrometer (parameters are given in Table 4.2). HS vials and PTFE/Sil caps were purchased from Perkin Elmer as well. All separations were carried out on an AT-1 column (30 m x 0.53 mm, d_f = 5.00 µm) from Grace Alltech (Deerfield, IL, USA). The used oven program for separations is given in Table 4.3.

Table 4.2: HS parameters used.

Parameter	HS parameters
Equilibration temperature	170 °C
Equilibration time	60 min
Needle temperature	180 °C
Transfer line temperature	190 °C
Pressurization time	1.0 min
Injection time	0.04 min
Needle withdrawal time	0.4 min
Injection port temperature	200 °C
Carrier gas pressure	130 kPa
Split ratio	1:5
Detector temperature FID	250 °C

Table 4.3: GC oven program used.

t (min)	T (°C)
0	40
6.25 (8 °C/min)	90
16 (15 °C/min)	240
24.25	240
40	40

4.2.2.2. LC analyses

LC-UV analyses for the determination of DB in cooling liquids were performed using an ion pair method reported in literature [16]. A system, consisting of a Spectra system pump P1000 XR from Thermo Fisher Scientific (Waltham, MA, USA), an autosampler from Spark Holland (Emmen, the Netherlands) and a L-2400 UV detector from Hitachi Elite LaChrom (San Jose, CA, USA) was utilized. The column used was a Waters (Milford, MA, USA) Symmetry C_{18} (100 Å, 5 µm, 150 * 3.9 mm I.D.) The LC-system was monitored by Chromeleon software (Dionex, Sunnyvale, CA, USA). See Table 4.4 for the method parameters.

Table 4.4: LC-UV method for the analysis of DB.

Parameter	Setting
Injection volume	20 µL
Mobile phase	buffer solution pH3 with SDS (10 mM) - acetonitrile (50:50, % v/v)
Column	Symmetry C_{18}, 100 Å, 5 µm, 150 x 3.9 mm I.D.
Flow	1.2 mL/min., isocratic
Column temperature	35 °C
Detection wavelength	210 nm

4.2.3. Preparation of solutions and samples

4.2.3.1. GC analyses

4.2.3.1.1. Screening samples of different QAS

An overview of the QAS included in this study is given in Table 4.5. Solutions of pure QAS available as their chloride salt (BZTCl, BEDIDE and TMPACl) and DB having benzoate as counter ion with concentrations of 15 mg/mL were prepared in methanol. For BZTCl, BEDIDE and TMPACl, 100 µL of each solution was transferred to a HS vial. As DB is not a chloride salt, the reaction did not proceed and so the procedure was adapted. 100 µL of methanolic DB solution and 10 µL of HCl were introduced in a HS vial. After evaporation to dryness using a vacuum oven, vials were sealed with a PTFE/Sil cap and analysed using the described HS-GC method to identify the major volatile decomposition (or pyrolysis) products.

BZOCl was not available as pure salt. Therefore, 10 µL of mouth spray containing BZOCl was treated with 1 mL of DMP (to which 10 µL of HCl was added) for water scavenging. This procedure was carried out directly in the HS vial which was dried under vacuum afterwards. Next, the vial was sealed with a PTFE/Sil cap.

4.2.3.1.2. Internal standard solution

200 mg of toluene was dissolved in 10 mL of o-xylene and diluted 10 times by transferring 5.0 mL of the solution to a volumetric flask of 50 mL. o-Xylene was used to bring the solution up to volume.

4.2.3.1.3. Calibration solutions for the determination of benzyl chloride

200 mg of benzyl chloride was dissolved in 10 mL of o-xylene and diluted 10 times by transferring 5.0 mL to a volumetric flask of 50 mL and bringing to volume with o-xylene. A 6-point calibration series was prepared in the range from 100 – 600 mg/L. Before bringing to volume with o-xylene, each time 4.0 mL of internal standard solution was added. Calibration was performed by analysing 10 µL of each solution.

4.2.3.1.4. Calibration solutions for the determination of chloromethane

A solution of BEDIDE in methanol was prepared by dissolving 20 mg in 25 mL of methanol. A 6-point calibration curve in the range from 1 – 10 mg/L was prepared using appropriate dilutions in methanol. 200 µL of each calibration solution was transferred into a HS vial and methanol was removed by vacuum evaporation. Then, 10 µL of o-xylene was added to the vial which was sealed with a PTFE/Sil-cap.

4.2.3.1.5. Sample preparation for the HS analysis of DB in cooling liquids (50% EG)

Samples were diluted 20-times with water from which an aliquot of 1.0 mL was transferred to a HS vial. After adding 10.0 mL of DMP and 50 µL of HCl, the mixture was left for 5 minutes to react. After the water scavenging process, samples were placed in a vacuum oven at 30 °C for 2 hours to evaporate all solvents and HCl. After the drying step, another 1.0 mL of DMP and 10 µL of HCl were added to react with residues of EG. Once again, samples were evaporated before adding 10 µL of o-xylene to the sample vial. Finally, vials were sealed with a PTFE/Sil-cap and analysed with the described HS method. In case of FID detection, 100 µL of BSTFA was transferred into the sample vial for silanisation and evaporated to dryness before addition of 10 µL o-xylene and closure of the vial.

4.2.3.1.6. Sample preparation for the HS analysis of BZTCl in a mouth spray

A mouth spray containing BZTCl was diluted 100 times in water. 1.0 mL of the resulting solution was brought into a HS vial and 10.0 mL of DMP and 50 µL of HCl were added. After reacting for 5 minutes, samples were evaporated to dryness in a vacuum oven at 30 °C. Before sealing the vials with a PTFE/Sil cap, 10 µL of o-xylene was added.

4.2.3.1.7. Sample preparation for the HS analysis of BZOCl in a mouth spray

A mouth spray containing BZOCl was diluted 250 times in water. 1.0 mL of the resulting solution was brought into a HS vial and 10.0 mL of DMP and 50 µL of HCl were added. After reacting for 5 minutes, samples were evaporated to dryness in a vacuum oven at 30 °C. Before sealing the vials with a PTFE/Sil cap, 10 µL of o-xylene was added.

4.2.3.2. LC analyses

4.2.3.2.1. Preparation of the mobile phase

A 0.1 M buffer solution of NaH_2PO_4 and phosphoric acid was prepared by adjusting the pH to 3.0. Next, 100 mL of the buffer was diluted 10 times in a volumetric flask of 1000 mL. Before bringing to volume, 2.88 g of SDS was added. Finally, 500 mL of the resulting buffer solution was mixed with 500 mL of acetonitrile.

4.2.3.2.2. SDS solution

560 mg of SDS was dissolved in water using a volumetric flask of 100 mL.

4.2.3.2.3. DB standard solution

40 mg of DB was weighed and dissolved in 50.0 mL of water using a volumetric flask. This solution was diluted 10 times by transferring 10.0 mL to a volumetric flask of 100 mL. Finally, 5.0 mL of this solution was transferred to a 50 mL volumetric flask; 35 mL of ethanol was added and brought up to volume with water. Finally the resulting reference solution was diluted twice with SDS solution.

4.2.3.2.4. Sample preparation for the HPLC analysis of DB in cooling liquids (50% EG)

5.0 mL of sample was transferred into a volumetric flask of 10 mL and brought up to volume using the SDS solution.

4.2.4. Procedures

4.2.4.1. Study of degradation compounds

For all compounds under investigation, vials were prepared as described in 4.2.3.1.1. and analysed using the parameters listed in Table 4.2 with an equilibration time of 60 min. The data were collected using MS in full scan mode for identification and FID in parallel.

The effect of the equilibration time on the decomposition yield was investigated as example for BZTCl and BEDIDE. The vials prepared as described in 4.2.3.1.1. were analysed using the parameters listed in Table 4.2, but with different equilibration times varying from 35 to 60 minutes. The resulting peak areas for benzyl chloride and chloromethane were measured.

4.2.4.2. Calibration for benzyl chloride

Three calibration curves were constructed. One was FID based, while the two others were SIM based (*m/z* 91 and *m/z* 126). Each six point calibration curve was constructed using the vials prepared in duplicate according to 4.2.3.1.3. The peak areas for benzyl chloride were corrected with the obtained peak areas for toluene which was used as internal standard.

4.2.4.3. Calibration for chloromethane

Decomposition of QAS like BEDIDE results in the formation of either benzyl chloride or chloromethane (see also Table 4.5). The benzyl chloride content of the vials prepared as described in 4.2.3.1.4. was determined using the analytical parameters from Table 4.2 with FID detection and the calibration curve obtained from 4.2.4.2. It was assumed that from the number of mmoles of BEDIDE and the number of mmoles of benzyl

chloride, the number of mmoles of chloromethane can be calculated. As the original amount of QAS with methyl groups like BEDIDE in the vials is known and the amount of formed benzyl chloride is measured, the formed amount of chloromethane in a vial can be calculated using formulae (1) and (2):

$$mmoles\ QAS\ left = \left(\frac{m_{QAS}}{M_{QAS}}\right) - \left(\frac{m_{BCl}}{M_{BCl}}\right) \qquad (1)$$

In which:

mmoles QAS left = mmoles of QAS that did not yield benzyl chloride

m_{QAS} = total mass in mg of QAS in HS vial

M_{QAS} = molecular mass of QAS

m_{BCl} = mass (mg) of released benzyl chloride

M_{BCl} = molecular mass of benzyl chloride

Using formula (1) the amount of QAS that can produce chloromethane is calculated enabling the determination of the amount of chloromethane in a vial. Since one mole of QAS (even with more than one methyl group) produces one mole of chloromethane:

$$m_{CM} = mmoles\ QAS\ left \times M_{CM} \qquad (2)$$

m_{CM} = mass (mg) of chloromethane

M_{CM} = molecular mass of chloromethane

From these calculations and the peak areas measured for chloromethane, a calibration curve was constructed.

4.2.4.4. Method validation

4.2.4.4.1. Linearity of the calibration curve

The generalized linearity depends on the combined response for benzyl chloride and chloromethane. For both compounds a six point calibration curve was created and assessed.

4.2.4.4.2. Repeatability

Repeatability was expressed as RSD% value using at least 4 measurements.

4.2.4.4.3. Recovery

Recovery in this procedure relies on the complete conversion of the analyte into the target compounds and their proper determination. Three solutions of DB in 50 % v/v EG with known concentrations (60, 80 and 100 ppm) were analysed. The GC results of the commercial samples were compared with those obtained with an LC method from literature [16]. For GC analysis, commercial samples were spiked with DB as a supplementary validation.

For the BZTCl mouth spray, three solutions of BZTCl with known concentrations in water (10, 15 and 20 ppm) were analysed. For the quantification of chloromethane, a baseline correction was performed. GC results obtained for the commercial mouth spray were compared with the label claim. For the BZOCl mouth spray, GC results were also compared with the labelled value.

4.2.4.5. Analysis of commercial samples

4.2.4.5.1. HS-GC analysis of cooling liquid samples

Two typical automotive cooling liquids were analysed with the validated protocol. Detection was performed using either MS operated in SIM mode to detect both toluene (*m/z* 91) and benzyl chloride (*m/z* 91 and *m/z* 126) or FID after BSTFA silanisation to avoid chromatographic interference.

4.2.4.5.2. HS-GC analysis of BZTCl in a mouth spray

HS-GC analysis of BZTCl was performed at 170 °C with an equilibration time of 60 min. Benzyl chloride and chloromethane amounts were measured using FID and the amount of BZTCl was calculated according to formulae (1) and (2).

4.2.4.5.3. HS-GC analysis of BZOCl in a mouth spray

HS-GC analysis of BZOCl was performed at 170 °C with an equilibration time of 60 min. Quantification of this QAS was done by calibration with benzyl chloride.

4.2.4.5.4. LC-UV analysis of DB in commercial cooling liquids

Cooling liquids were diluted ten times with water and analysed with the described protocol using DB for calibration.

4.3. Results & Discussion

4.3.1. Screening of various QAS

In literature, debenzylation of the quaternary nitrogen in benzyl substituted QAS is proposed as the favoured thermal decomposition pathway [17]. In the case of DB, this yields lidocaine and benzyl benzoate, both having boiling points over 300 °C making them unusable for a HS approach. Converting the DB into a chloride salt should produce benzyl chloride with a boiling point of 179 °C instead. The MS data obtained from the procedure described in 4.2.4.1. were compared with a NIST mass spectral library. The identified degradation products of the QAS studied (see Table 4.5) were benzyl chloride as major product (Figure 4.1), chloromethane, N,N-dimethylaniline and N,N-dimethyldecylamine (Figures 4.2 and 4.3). Looking at the structures of the QAS and formed decomposition products, a set of simple rules to predict the result can be proposed depending on the substitution of the quaternary nitrogen atom:

- if a benzyl group is present, benzyl chloride is formed.
- if a benzyl group and methyl groups are present, 1 molecule of benzyl chloride and 1 molecule of chloromethane are formed.
- if the aromatic substituent is a phenyl group then the corresponding aniline analogue is formed.

As a result, benzyl substituted QAS without methyl groups on the quaternary nitrogen like DB and BZOCl can be quantified using benzyl chloride only while for those bearing also a methyl group, quantification should be based on the combination of the produced amounts of all the chlorinated species being benzyl chloride and chloromethane. For phenyl and methyl substituted QAS like TMPACl, N,N-dimethylaniline can be used as calibrant. N,N-dimethyldecylamine which is found in case of BEDIDE, is the tertiary amine formed after removing the benzyl group. As BEDIDE is one of the components of benzalkonium chloride which contains several benzyldimethylalkanes (ranging from C_8 to C_{18}), it could be an option to assess a profile of QAS based on the formed N,N-dimethylalkylamines.

The results for DB (which was determined in partly aqueous solutions) prove that the use of DMP and HCl for water removal converts the benzoate salt into its chloride form and is not interfering with the decomposition process.

Table 4.5: Chemical structures of QAS included in this study.

Chemical name	Abbreviation	Chemical structure	Volatile degradation products for quantification	Other volatiles
Benzethonium chloride	BZTCl	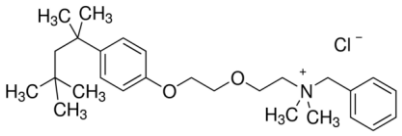	Benzyl chloride + Chloromethane	-
Denatonium benzoate	DB	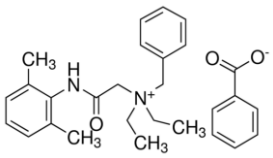	Benzyl chloride	-
Benzoxonium chloride	BZOCl	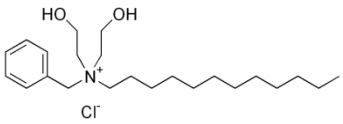	Benzyl chloride	-
Benzyldimethyldecylammonium chloride	BEDIDE	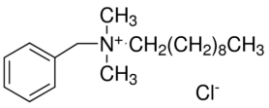	Benzyl chloride + Chloromethane	N,N-dimethyldecylamine
Trimethylphenylammonium chloride	TMPACl	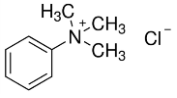	N,N-dimethylaniline	Chloromethane

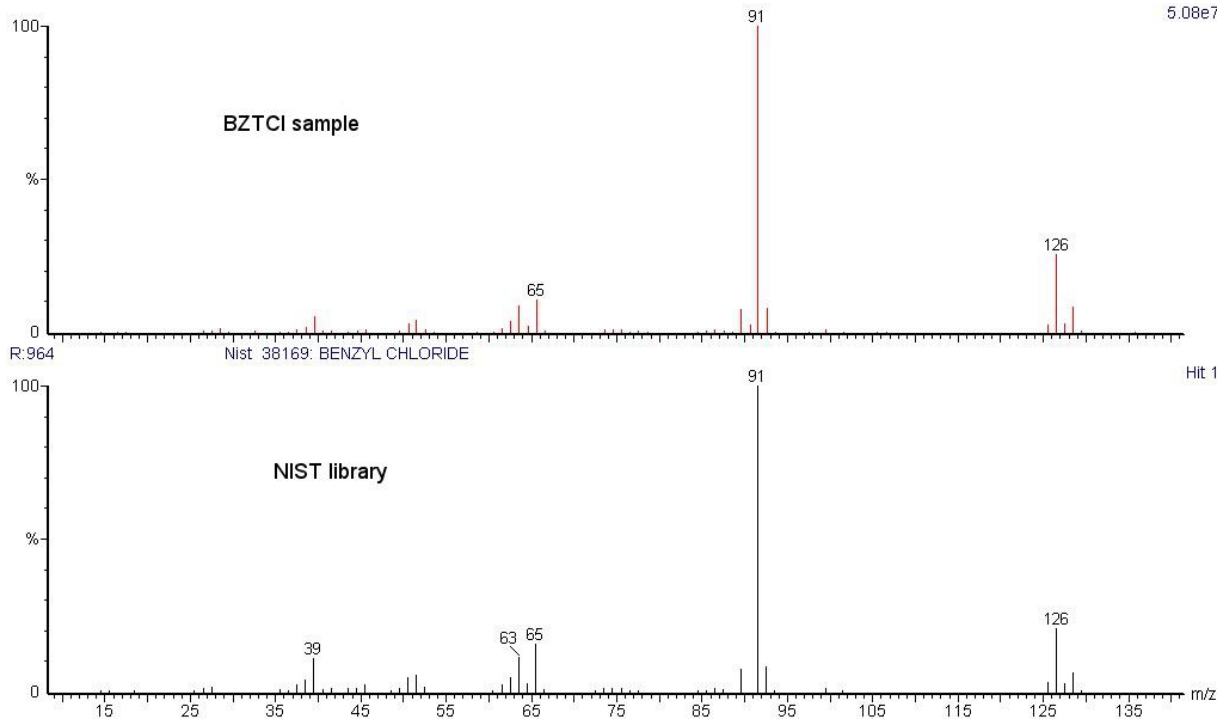

Figure 4.1: Mass spectral identification of benzyl chloride during screening of various QAS.

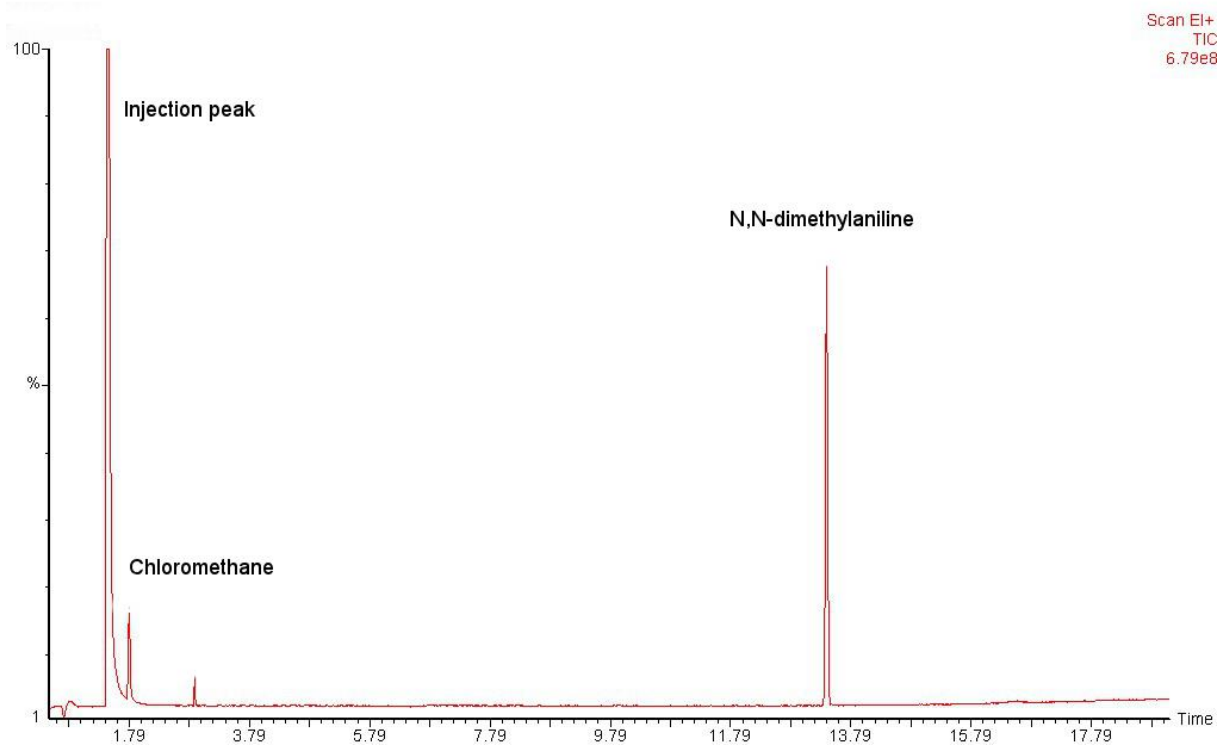

Figure 4.2: TIC chromatogram of the reaction products of TMPACl. Chromatogram was recorded using the instrumental parameters described in 4.2.2.

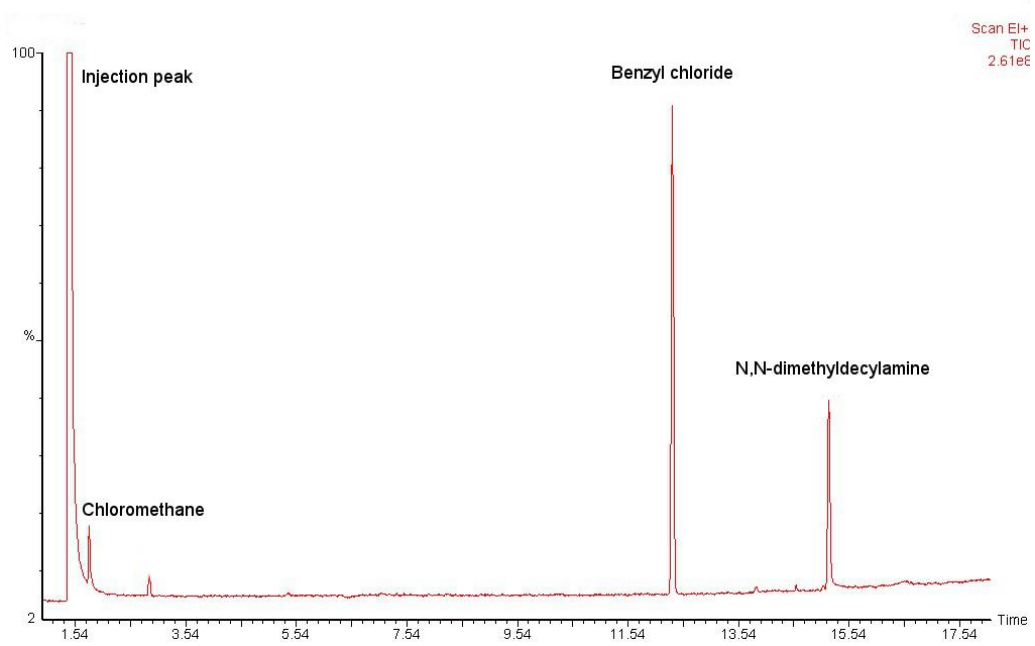

Figure 4.3: TIC chromatogram of the reaction products of BEDIDE. Chromatogram was recorded using the instrumental parameters described in 4.2.2.

4.3.2. Equilibration time

In HS analysis the equilibration time is an important factor and is chosen in such a way that a stable gas phase is formed without decomposition. In this case however, a stable gas phase with complete decomposition is the goal. From Figures 4.4 and 4.5 it can be concluded that the decomposition is complete after 60 min as both benzyl chloride and chloromethane peak areas are stable and repeatable.

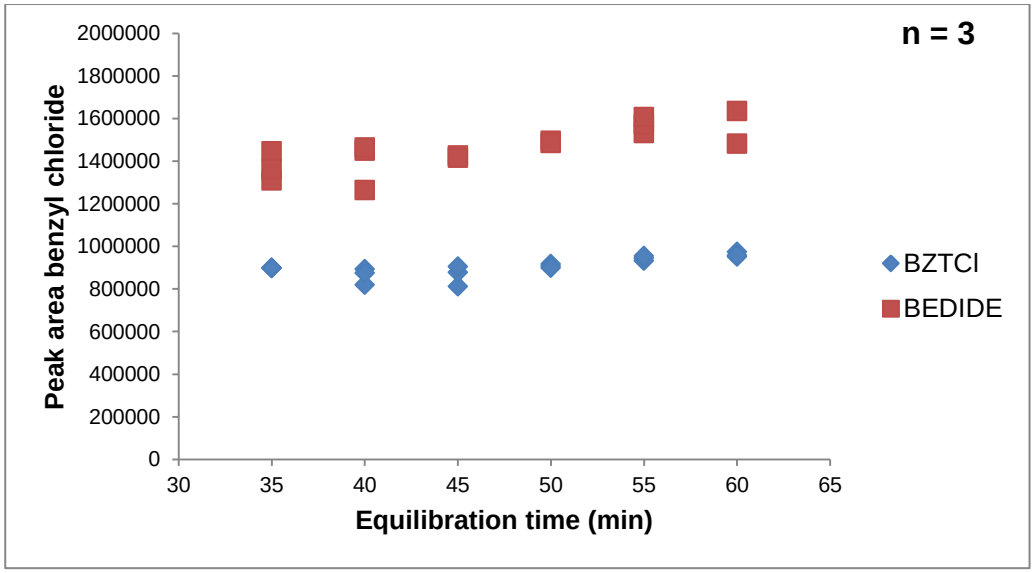

Figure 4.4: Obtained peak areas of benzyl chloride from BZTCl and BEDIDE vs. different equilibration times.

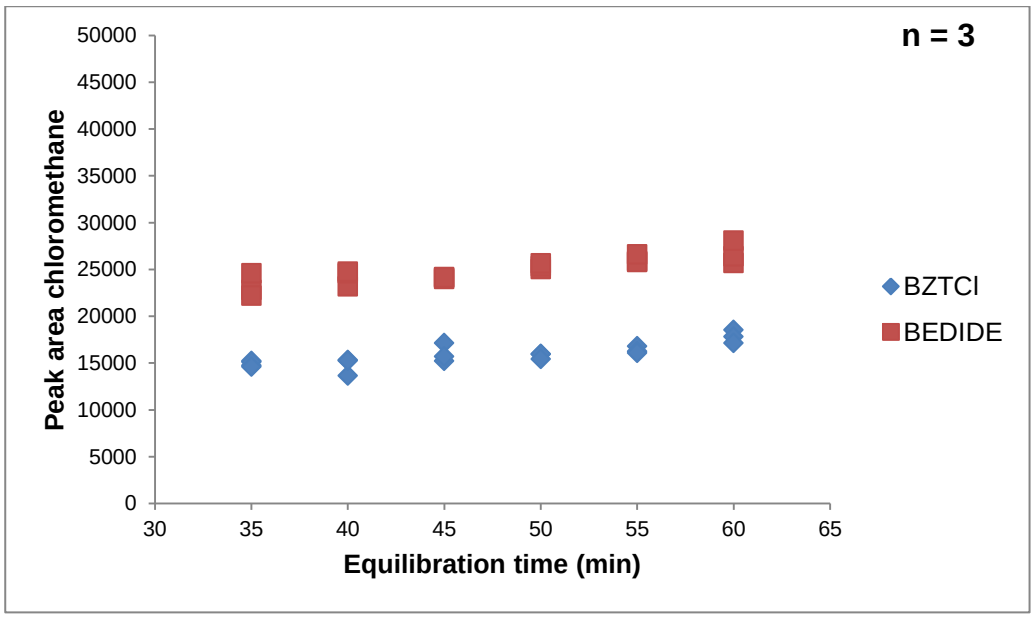

Figure 4.5: Obtained peak areas of chloromethane from BZTCl and BEDIDE vs. different equilibration times.

4.3.3. Method validation HS-GC method

4.3.3.1. Linearity of the calibration curve

A calibration curve of benzyl chloride was constructed in the range of 1-6 µg/vial by repetitive injections. The obtained R^2 value was higher than 0.999, indicating that a good linear relationship exists between analyte response and the amount of analyte. The use of an internal standard for calibration was necessary to correct for variations on the sample volume as the analysed sample volume was only 10 µL. o-Xylene was added to the sample vials before sealing to avoid possible viscosity effects in the gas phase, causing quantification errors [18].

The obtained calibration curve for chloromethane following the procedure described in 4.2.4.3. showed good linearity as well (R^2 = 0.999) after a lack of fit test (Table 4.6) and a check of the residuals. The obtained curve was used to calculate the mass balance for QAS producing both benzyl chloride and chloromethane.

Table 4.6: Lack of fit results for benzyl chloride and chloromethane.

	Benzyl chloride	Chloromethane
MS residuals	1638773	892
df residuals	10	11
MS pure error	2557917	688
df pure error	6	7
MS lack of fit	260058	1247
df lack of fit	4	4
F value	0.10	1.81
F critical	4.53	3.97

4.3.3.2. Recovery and repeatability

Results for the three DB recovery experiments are given in Table 4.7. Obtained recovery values were close to 100 % and RSD% values did not exceed 2.5%, demonstrating that the method is suitable for the analysis of DB in cooling liquids.

Table 4.7: Recovery and repeatability results for DB in EG/water samples.

	60 ppm DB		**80 ppm DB**		**100 ppm DB**	
	Recovery (%)	RSD (%) n = 6	Recovery (%)	RSD (%) n = 6	Recovery (%)	RSD (%) n = 6
	102.2	0.70	101.3	2.5	99.1	2.0

Recovery results for BZTCl are given in Table 4.8 and show that a mass balance of 100% can be obtained without needing a matching reference. The amounts of benzyl chloride and chloromethane were used to calculate the corresponding amount of BZTCl from which they both originated from. These results imply that any QAS producing both benzyl chloride and chloromethane can be quantified using another QAS with the same decomposition products.

Table 4.8: Recovery and repeatability results for BZTCl (as sum of benzyl chloride and chloromethane) in aqueous samples.

	10 ppm BZTCl		**15 ppm BZTCl**		**20 ppm BZTCl**	
	Recovery (%)	RSD (%) n = 4	Recovery (%)	RSD (%) n = 4	Recovery (%)	RSD (%) n = 4
	99.7	6.9	100.5	4.3	102.6	5.3

4.3.4. Analysis of DB in commercial cooling liquid samples

Two cooling liquid samples consisting mainly of water and EG (with some glycerol and anti-corrosive agents added) were analysed with the method described in 4.2.3.1.5. HCl was added as catalyst in the DMP reaction, but also to ensure complete conversion of DB into its chloride form. After evaporation of the solvents, another aliquot of 1.0 mL DMP was added to ensure the complete conversion of EG to 2,2-dimethyl-1,3-dioxolane [15]. Analysis of the samples resulted in very complex chromatograms (Figure 4.6). The benzyl chloride peak is situated around 12.3 min on the tail of a much bigger peak which was identified using the NIST library as 2,2-dimethyl-1,3-dioxolane-4-methanol. This compound is the reaction product of DMP and glycerol. The latter is often added to cooling liquids. Further evaluation of the MS-data revealed that another compound co-eluted with benzyl chloride.

The MS spectrum of the co-eluting compound with a molecular mass of 145 Da and its comparison with the NIST library is given in Figure 4.7. It is proposed to be 1-(2,2-dimethyl[1,3]dioxan-4-yl)ethanol.

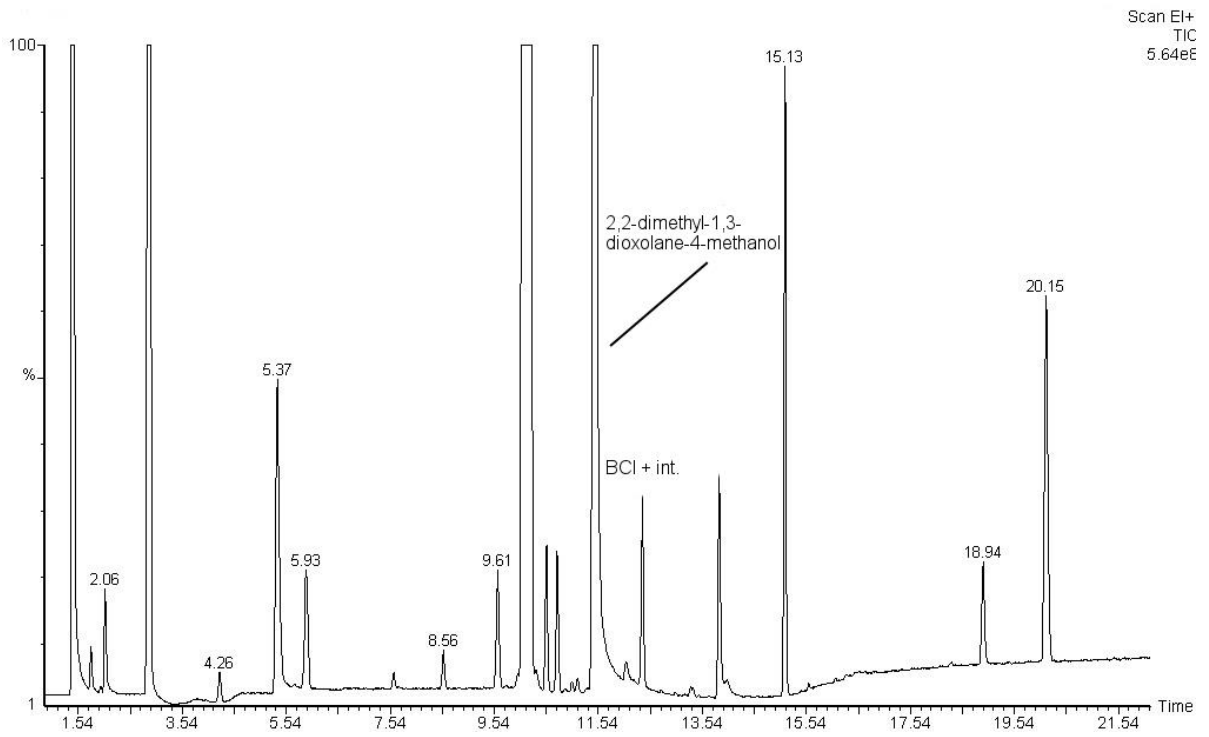

Figure 4.6: TIC chromatogram of a cooling liquid sample after analysis with the developed HS method. BCl = benzyl chloride, int. = interference. Chromatogram was recorded using the instrumental parameters described in 4.2.2.

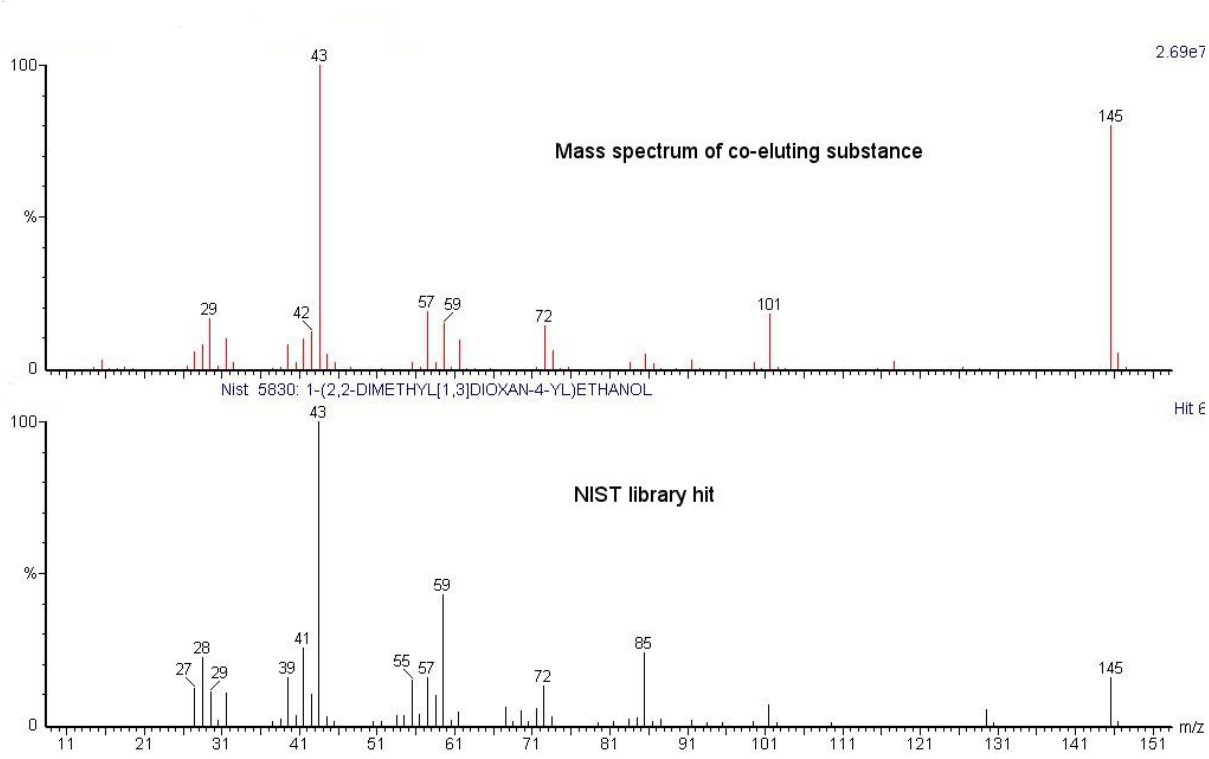

Figure 4.7: Mass spectra of the substance co-eluting with benzyl chloride in the chromatogram (indicated as interference) and its NIST library hit, (1-(2,2-dimethyl[1,3]dioxan-4-yl)ethanol).

The extracted ion chromatograms (EIC) of characteristic *m/z* values are shown in Figure 4.8. As the most abundant characteristic *m/z* values of benzyl chloride (*m/z* 91 and *m/z* 126) are not present in the mass spectrum of this interfering compound, it was decided to use MS operated in SIM mode using *m/z* 91 and *m/z* 126 for the quantification of DB in cooling liquids. As both compounds have an alcohol function, another approach is to apply BSTFA and so circumvent the interference and to enable FID detection. BSTFA will react with the alcohol function to form a trimethylsilyl derivative, thereby changing the properties of the interfering molecules. In Figure 4.9, a BSTFA treated sample is compared with an untreated sample. The peak interfering with benzyl chloride is completely removed and also 2,2-dimethyl-1,3-dioxolane-4-methanol is sufficiently removed so that a more reliable quantification of benzyl chloride can be performed.

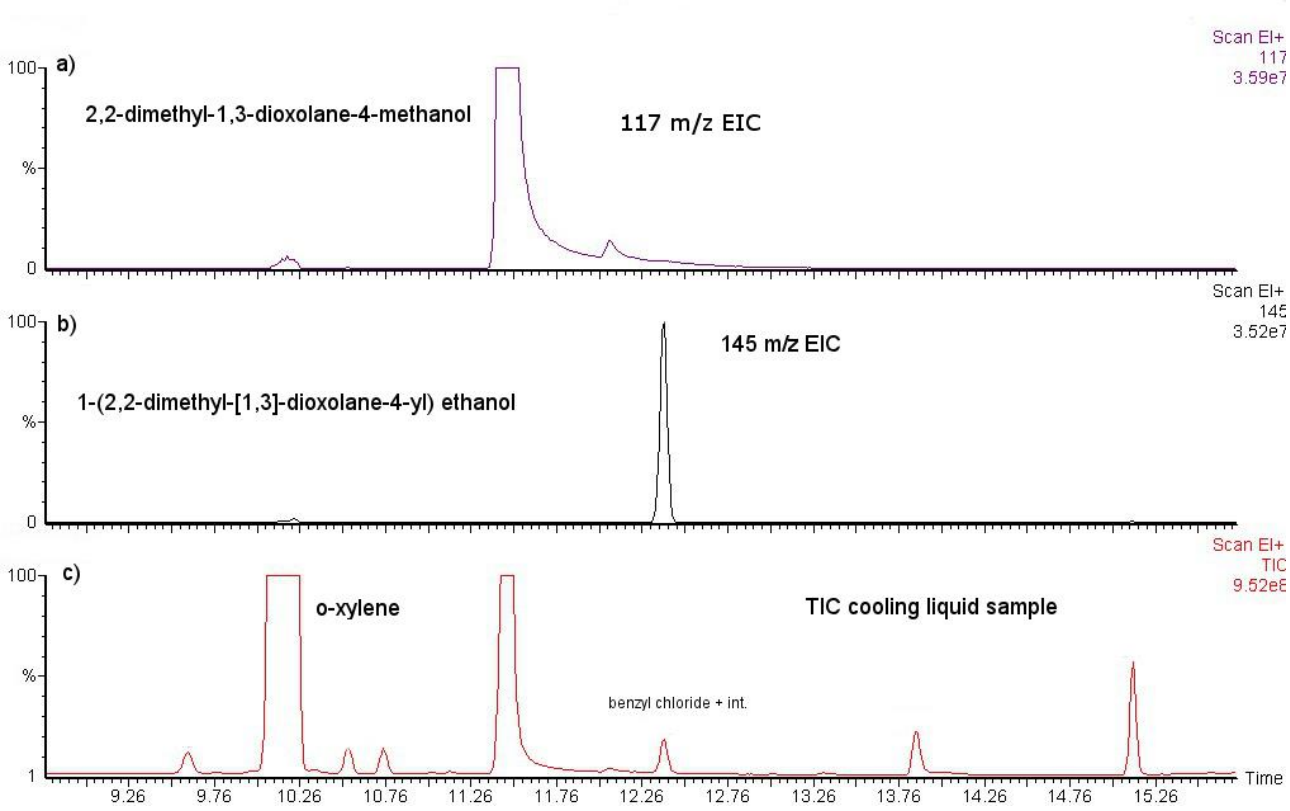

Figure 4.8: Chromatograms obtained by GC-MS illustrating the compounds interfering with the determination of benzyl chloride. Extracted ion chromatograms of most abundant *m/z* values of a) 2,2-dimethyl-1,3-dioxolane-4-methanol and b) 1-(2,2-dimethyl[1,3]dioxan-4-yl)ethanol processed from c) the TIC chromatogram. Chromatogram was recorded using the instrumental parameters described in 4.2.2.

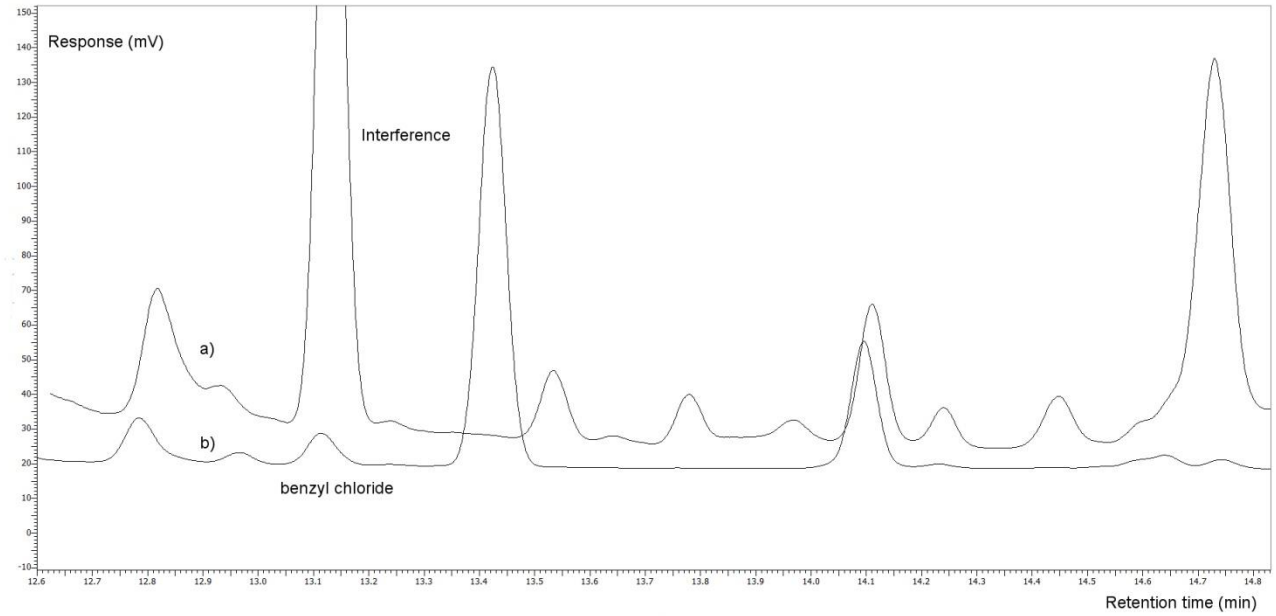

Figure 4.9: Comparison between a) a cooling liquid sample not treated with BSTFA and b) the same sample treated with BSTFA. Chromatogram was recorded using the instrumental parameters described in 4.2.2.

The analysis results of both cooling liquids with GC-MS and GC-FID after BSTFA treatment are given in Table 4.9. In case of the BSTFA treatment, samples were spiked with DB as well. The recovery of the spiked amount of DB was found to be 99.6% (RSD = 3.7%, n = 4) and 100.1% (RSD = 3.1%, n = 4) for sample 1 and 2, respectively. Both samples were also analysed using an LC-method and the obtained results for both samples are comparable indicating that the GC-FID method is suitable for the quantification of DB in cooling liquids. In comparison to GC-MS, GC-FID is in general far more robust as the ion source used for MS is prone to suffer from signal drift [19]. This signal drift can only be corrected by using expensive isotopes of the analytes of interest.

Table 4.9: Analysis results for DB in two commercial cooling liquid samples using GC-MS (*m/z* 91 and 126), GC-FID and LC-UV.

	SIM 91 (ppm)	**RSD% n=4**	**SIM 126 (ppm)**	**RSD% n=4**	**GC-FID* (ppm)**	**RSD% n=4**	**LC-UV (ppm)**	**RSD% n=3**
sample 1	40.5	3.7	37.9	6.9	40.7	2.0	35.6	0.1
sample 2	93.2	3.3	85.9	7.0	77.4	3.5	82.5	0.6

* After treatment with BSTFA

4.3.5. Analysis of BZTCl in a mouth spray

Analysis and quantification of the sample was performed by the procedure described in 4.2.4.5.2. The concentration of BZTCl in the mouth spray was found to be 438 ppm (RSD = 3.7%, n = 6). This analysis result corresponds to 100.7% of the labelled value.

4.3.6. Analysis of BZOCl in a mouth spray

As with the commercial cooling liquids, the same interfering peak was also seen here with GC-MS. Therefore, 100 µL of BSTFA was added to the sample vial after solvent evaporation to silanise the interfering compound with the alcohol function. Samples were evaporated to dryness again. The concentration of BZOCl was found to be 2010 ppm (RSD = 1.6%, n = 6), which is about the same as the label claim (0.2%) of the mouth spray. This is an indication that the method has an adequate recovery towards BZOCl.

4.4. Conclusions

From the obtained results it can be concluded that the use of HS-GC is an excellent tool to quantify several aromatic substituted QAS by calibration with the most abundant volatiles that are released after heating of a sample in a HS vial. In contrast to pyrolysis methods in which samples are introduced directly in a hot injection liner, this approach offers a clean way of sample introduction. After screening of several QAS, it was revealed that all benzyl substituted QAS released benzyl chloride as the major volatile product when chloride was the anion of the salt. Even when a particular QAS produces multiple volatiles, reliable quantification is still possible. It has been demonstrated for QAS that produce benzyl chloride and chloromethane, the mass balance is close to 100%. This means that it is possible to quantify all QAS that produce benzyl chloride and chloromethane without the need of having a matching reference standard. This is an important advantage towards LC or CE methodologies in which matching reference standards are necessary for quantification. In combination with an in-vial water scavenging procedure, a powerful GC method for the analysis of QAS in aqueous samples is established. The method was validated for the analysis of DB in cooling liquids during which adequate recovery values (99.1 - 102.2%) were obtained with RSD values not exceeding 2.5%. Obtained R^2 values were always equal to or larger than 0.999. Finally, the methodology was applied to commercial cooling liquid samples and the analysis of BZTCl and BZOCl in mouth sprays. For the cooling liquid samples and the BZOCl mouth spray, an interference that appeared to be an alcohol-like molecule, made accurate analysis impossible at first instance. Silanisation of the sample after DMP treatment removed this interference and enabled analysis of the samples. An advantage is also that all reactions can be performed in one HS vial.

4.5. References

[1] M.J. Ford, L.W. Tetler, J. White, D. Rimmer, Determination of alkyl benzyl and dialkyl dimethyl quaternary ammonium biocides in occupational hygiene and environmental media by liquid chromatography with electrospray ionisation mass spectrometry and tandem mass spectrometry, J. Chromatogr. A, 952 (2002) 165-172

[2] E.N.M. Ho, W.H. Kwok, A.S.Y. Wong, T.S.M. Wan, Detection of singly- and doubly-charged quaternary ammonium drugs in equine urine by liquid chromatography/tandem mass spectrometry, Anal. Chim. Acta, 710 (2012) 94-101

[3] K.C.H. Yiu, E.N.M. Ho, T.S.M. Wan, Detection of quaternary ammonium drugs in equine urine by liquid chromatography-mass spectrometry, Chromatographia, 59 (2004) 56-50

[4] X. Li, B.J. Brownwell, Analysis of quaternary ammonium compounds in estuarine sediments by LC-ToF-MS: Very high positive mass defects of alkylamine ions as powerful diagnostic tools for identification and structural elucidation, Anal. Chem., 81 (2009) 7926-7935

[5] I. Ferrer, E.T. Furlong, Accelerated solvent extraction followed by on-line solid-phase extraction coupled to ion trap LC/MS/MS for analysis of benzalkonium chlorides in sediment samples, Anal. Chem., 74 (2002) 1275-1280

[6] M.M. Ariffin, R.A. Anderson, LC/MS/MS analysis of quaternary ammonium drugs and herbicides in whole blood, J. Chromatogr. B, 842 (2006) 91-97

[7] R. Castro, E. Moyano, M.T. Galceran, Determination of quaternary ammonium pesticides by liquid chromatography-electrospray tandem mass spectrometry, J. Chromatogr. A, 914 (2001) 111-121

[8] R. Castro, E. Moyano, M.T. Galceran, On-line ion-pair solid-phase extraction-liquid chromatrography-mass spectrometry for the analysis of quaternary ammonium herbicides, J. Chromatogr. A, 869 (2000) 441-449

[9] P. Bassarab, D. Williams, J.R. Dean, E. Ludkin, J.J. Perry, Determination of quaternary ammonium compounds in seawater samples by solid-phase extraction and liquid chromatography-mass spectrometry, J. Chromatogr. A, 1318 (2011) 673-677

[10] O. Núñez, E. Moyano, M.T. Galceran, Solid-phase extraction and sample stacking-capillary electrophoresis for the determination of quaternary ammonium herbicides in drinking water, J. Chromatogr. A, 946 (2002) 275-282

[11] O. Núñez, E. Moyano, M.T. Galceran, Capillary electrophoresis-mass spectrometry for the analysis of quaternary ammonium herbicides, J. Chromatogr. A, 974 (2002) 243-255

[12] F.P.W. Tang, G.N.W. Leung, T.S.M. Wan, Analysis of quaternary ammonium drugs in horse urine by capillary electrophoresis – mass spectrometry, Electrophoresis, 22 (2001) 2201-2209

[13] W.J. Criddle, J. Thomas, Pyrolysis-gas chromatography of quaternary ammonium salts in aqueous solution, J. Anal. Appl. Pyrol., 2 (1980) 361-365

[14] W.J. Criddle, A. Christofides, Pyrolysis-gas chromatography of model ‘’all organic’’ quaternary ammonium compounds in aqueous solution, J. Anal. Appl. Pyrol., 4 (1982) 163-173

[15] N. van Boxtel, K. Wolfs, A. Van Schepdael, E. Adams, Application of acetone acetals as water scavengers and derivatization agents prior to the gas chromatogramphic analysis of polar residual solvents in aqueous samples, J. Chromatogr. A, 1425 (2015) 62-72

[16] A. Faulkner, P. DeMontigny, High-performance liquid chromatographic determination of denatonium benzoate in ethanol with 5% polyvinylpyrrolidone, J. Chromatogr. A, 715 (1995) 189-194

[17] [6] L.K. Ng, M. Hupé, J. Harnois, A. H. Lawrence, Direct injection gas chromatographic/mass spectrometric analysis for denatonium benzoate in specific denatured alcohol formulations, Anal. Chem., 70 (1998) 4389-4393

[18] D.M. Kialengila, K. Wolfs, J. Bugalama, A. Van Schepdael, E. Adams, Full evaporation headspace gas chromatography for sensitive determination of high boiling point volatile organic compounds in low boiling matrices, J. Chromatogr. A, 1315 (2013) 167-175

[19] W. D’Autry, K. Wolfs, S. Yarramraju, A. Van Schepdael, J. Hoogmartens, E. Adams, Chararacterization and improvement of signal drift associated with electron ionization quadrupole mass spectrometry, Anal. Chem., 82 (2010) 6480-6486

Chapter 5 - Development and characterization of an atmospheric micro cavity hollow cathode discharge based GC-detector

Niels van Boxtel, Kris Wolfs, Ward D'Autry, Ann Van Schepdael, Erwin Adams

Pharmaceutical Analysis, Department of Pharmaceutical and Pharmacological Sciences

KU Leuven, Leuven, Belgium

Anal. Chem, to be submitted

Abstract

Gas chromatography (GC) can be combined with many different types of both universal and selective detectors to cover a large range of volatile analytes. The majority of detectors relies on the ionization of the analyte to enable detection. Although they earned their praise in many different analytical fields, there is still plenty of room for improvement related to their ion source.

In this work, the application of a micro cavity hollow cathode discharge (µCHCD) plasma as ion source in combination with an ion capture electrode as a simple, versatile GC detector is investigated. The developed low power consuming µCHCD ion source can be operated at atmospheric pressure as predicted by theory using only one type of gas. It was found that the detector geometry (consisting of the hollow cathode, dielectric spacer, anode and capture electrode) was of great importance for the obtained signal. By making sure that the cathode-anode clearance angle is large enough, quantitative response with sensitivity in the lower picogram range was obtained for a variety of analytes. Depending on the chemical properties of the analyte, different ionization mechanisms may occur. For the non-halogenated analytes included in this work, these are most likely photo-ionization or ionization by collision with helium metastables. Halogenated analytes included in this study (carbon tetrachloride (CCl_4) and trichloroethylene (TCE)) seemed to follow an electron capture mechanism, generating negative ions in the electron rich µCHCD plasma. Actual detection of ionized analytes was performed by either a negatively biased or positively biased capture electrode to differentiate between positive and negative ions, respectively.

Keywords

Gas detection, microplasma, microhollow cathode discharge

5.1. Introduction

During the last decades, gas chromatography (GC) has been used as a versatile tool for the analysis of volatile constituents in various samples using different sampling techniques such as direct injection, headspace sampling and thermal desorption combined with many different detectors and identification techniques. The most widely used detectors are the flame ionization detector (FID), thermal conductivity detector (TCD) and electron capture detector (ECD). Less commonly used detectors include the atomic emission detector (AED), sulphur chemiluminesence detector (SCD) and the nitrogen phosphorus detector (NPD). Possible identification instruments include the mass spectrometer (MS) in combination with either electron ionization (EI) or chemical ionization (CI) and the ion mobility spectrometer (IMS). All the mentioned detectors and instruments have their own disadvantages. For instance, the FID provides poor sensitivity for compounds that contain carbon atoms that are partly or even fully oxidised and therefore only provides an adequate response for analytes with a sufficient number of carbon atoms that can be combusted in the used hydrogen diffusion flame. This flame has relatively poor ionization efficiency (only 1 ion per 10^6 carbon atoms) [1]. The FID is also less applicable to portable applications as it needs multiple gasses, although miniaturised versions exist [2]. The ECD is, in contrast to the FID, sensitive towards halogenated compounds, but it uses a radio-active material (^{63}Ni) as ionization source which gives rise to legislation issues. In cases where the use of radio-active material or explosive gasses such as hydrogen is not permitted, photoionization detectors (PID) are an option [3]. The used ionization source for the PID is typically a high energy ultraviolet (UV) lamp. In this type of detectors, positive molecular ions are formed and analytes are (as with the FID) detected with a capture electrode. In contrast to the FID, this detector is smaller and lighter, making it more suitable for portable applications. However, the PID is not extremely sensitive for chlorinated aliphatics and has no response at all for methane. These detectors do not give any structural information which often means that MS or IMS are needed for identification of unknown analytes. However, the filament used for EI in MS and the mass filter can only be operated under vacuum conditions and IMS utilises a radio-active material as well. So most limitations and drawbacks of these detection systems are related to the ion source.

Plasmas as ion source

More recent detectors rely on plasmas for the ionization of analytes [4]. A plasma [5,6] is a gas that is partially or fully ionised with a population of free electrons, ions and neutral gas species and is considered to be neutral as a whole. Plasmas are generally characterised by the density and the kinetic energy of the

particles. Based on this, plasmas can be divided into two main classes: non-thermal plasmas and thermal plasmas. In case of thermal plasmas, thermodynamic equilibrium is reached in which the kinetic energy of the neutral gas molecules, ions and electrons are similar. These plasmas reach very high gas temperatures and are often used for welding, cutting and melting applications. A thermal plasma in the form of an inductively coupled plasma (ICP) torch is being used for atomisation during elemental analysis. Using such hot plasma for ionization and detection purposes in combination with GC would result in a complete loss of structural information. On the other hand, non-thermal plasmas (that are often electrically driven) contain a high population of energetic electrons (several eV) and ions whilst the actual gas temperature remains relatively low (from room temperature to several hundreds of Kelvins) and are therefore more interesting to serve as ion source in a GC detector. Commercial detectors that use a non-thermal plasma such as the pulsed discharge detector (PDD) often work according to a similar principle in which interaction with high energetic photons emitted from the plasma (Hopfield emission) or long-lived species such as helium metastables govern ionization of analytes. Plasmas are usually generated by using two wires as cathode and anode which are in contact with the gas. The PDD is extensively reviewed by Forsyth and can be operated in three modes [7]: pulsed discharge helium photo ionization detection-mode (He-PDPID) [8-14], pulsed discharge emission detection-mode (PDED) [15] and pulsed discharge electron capture detection-mode (PDECD). As an exception on the plasma generation the dielectric barrier discharge (DBD) detector should be mentioned [16-22]. The electrodes in this detector are isolated from the gas and the plasma is generated using an alternating current (kHz range). All these detectors are using a separate compartment where helium is ionized. The produced photons and/or helium metastables are directed towards the column effluent in order to ionize the analytes after which they can be detected with biased capture electrodes. However, the sample availability is not optimal with this approach and these detectors were found to suffer from instability issues [23].

Glow discharges and the hollow cathode effect

Another type of non-thermal plasma, often used in spectroscopy [24,25], is the classic DC operated glow discharge (GD) (Figure 5.1). The zone of interest of a GD appears as a relatively uniform light emitting zone (called negative glow) near to the cathode and is formed at pressures up to 1 kPa. These phenomena were first described by Crookes in the late 1870's. In order to prevent a transition to a thermal plasma, current and pressure are limited. About twenty years later, Paschen related the breakdown voltage (V_B) of a gas to the anode-cathode distance (d) and the gas pressure (p). For two flat parallel electrodes (Figure 5.2) this relationship is described by Paschen's law [26] which is mostly presented as a gas specific curve where V_B is

a function of p*d showing a distinct minimum. Without precautions, passing the V_B criteria at pressures above 1 kPa will result in arching and thus the formation of a thermal plasma due to the magnitude of V_B and the number of gas molecules present. By choosing a set-up close to the Paschen minimum and limiting the current, arching can be avoided resulting in a stable GD. For helium, values from 1.5 to 4 Torr.cm are found as Paschen minimum for p*d (Figure 5.3) yielding electrode distances from 20 to 50 µm at atmospheric pressure. Apart from the difficulties involved in manipulating these small distances, every discontinuity or contamination of the surface would result in localised high field strengths initiating sparking.

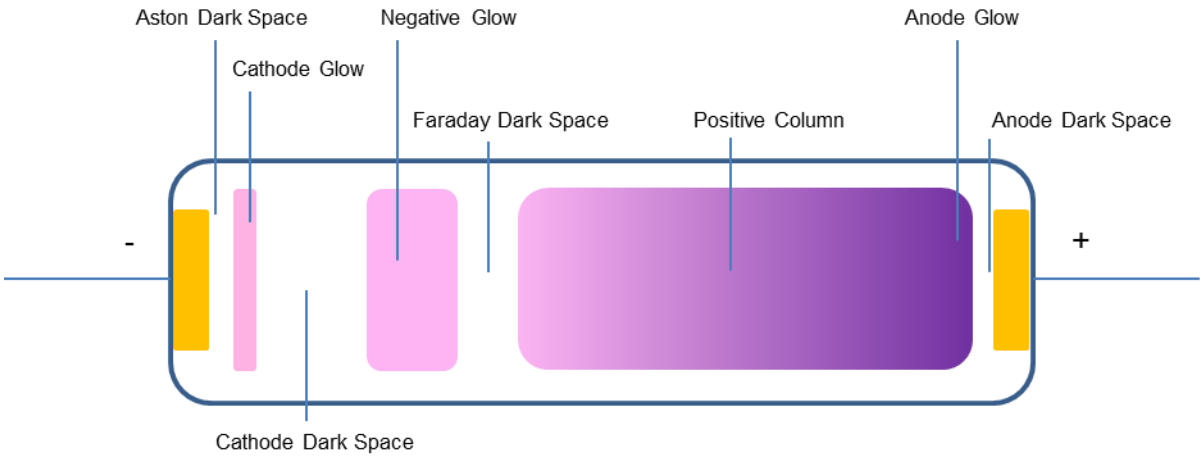

Figure 5.1: Schematic overview of a classic GD operated under vacuum with its characteristic zones.

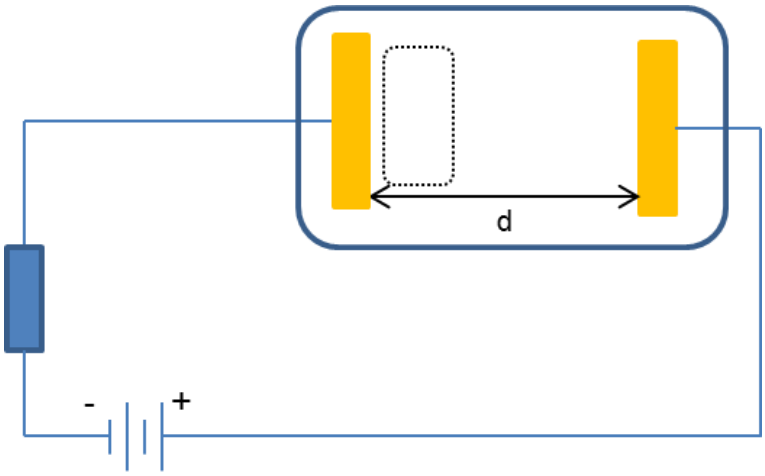

Figure 5.2: GD set-up having a flat parallel plate electrode geometry. The dashed line indicates the location of the negative glow and “d” the anode-cathode distance.

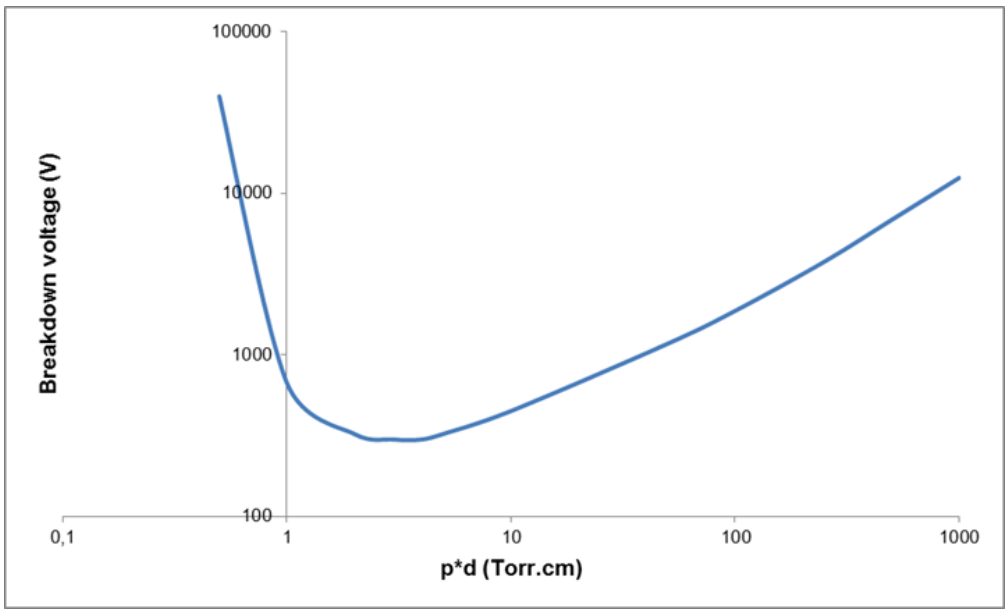

Figure 5.3: Paschen curve for helium and its Paschen minimum for flat parallel electrodes.

Early experiments [27,28] with GD and different cathode shapes revealed a special working regime when the cathode was split into two parallel plates located at a small distance (D) from each other (Figure 5.4). In this case, the plasma is formed at half the V_B [29] and located between the cathode plates. For this reason, the set-up was referred to as 'hollow cathode' and forms the origin of the well known hollow cathode lamp. At low current, the plasma in the hollow has a small positive resistance, but when the current increases the sustaining voltage starts to drop (negative differential resistance). In Figure 5.5, a comparison in U-I characteristics is schematically shown for both a conventional GD and a hollow cathode discharge in which the hollow cathode discharge possesses this negative differential resistance. This working regime is called hollow cathode mode. To avoid confusion, the term hollow cathode will be used here to refer to this working mode while the term micro cavity will be used to refer to the physical device. For low plasma currents, the electric field in the hollow is axial. When the plasma current is increased, this field changes from axial to radial and new electrons that are generated at the cathode surface are accelerated radially towards the cathode axis in the cathode fall. As a result, these 'pendulum electrons' [30] oscillate between the cathode plates giving rise to an increased ionization efficiency and a higher electron density. With the Paschen minimum of 4 Torr.cm in mind and the presence of the plasma (which can be regarded as a virtual electrode), one would expect the maximum distance between the cathode elements to be about 100 µm at atmospheric pressure. The White-Allis similarity law, which is based on the free pathway of the pendulum electrons, proposes 10 µm as maximum.

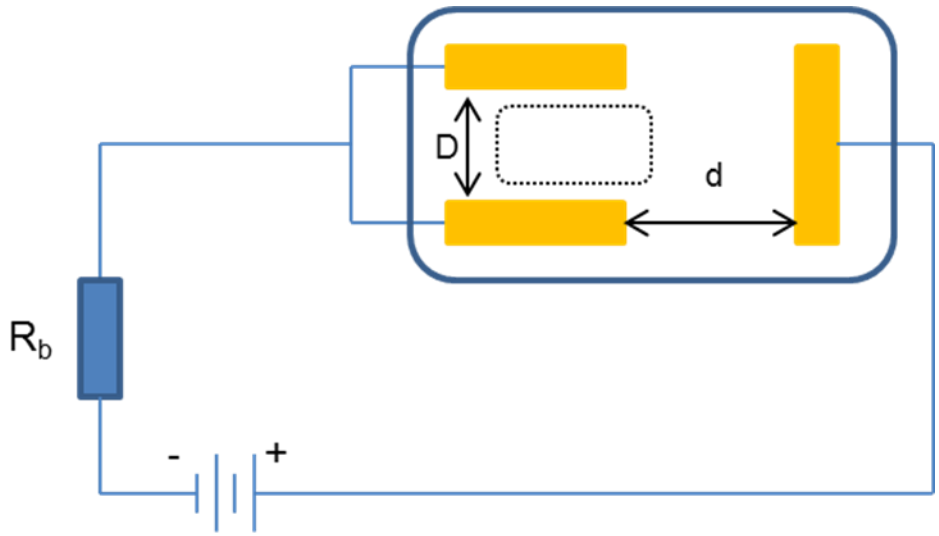

Figure 5.4: GD-setup with a cathode split into two separated plates with a distance D from each other. The dashed line indicates the location of the negative glow and “d” the anode-cathode distance R_b = ballast resistance.

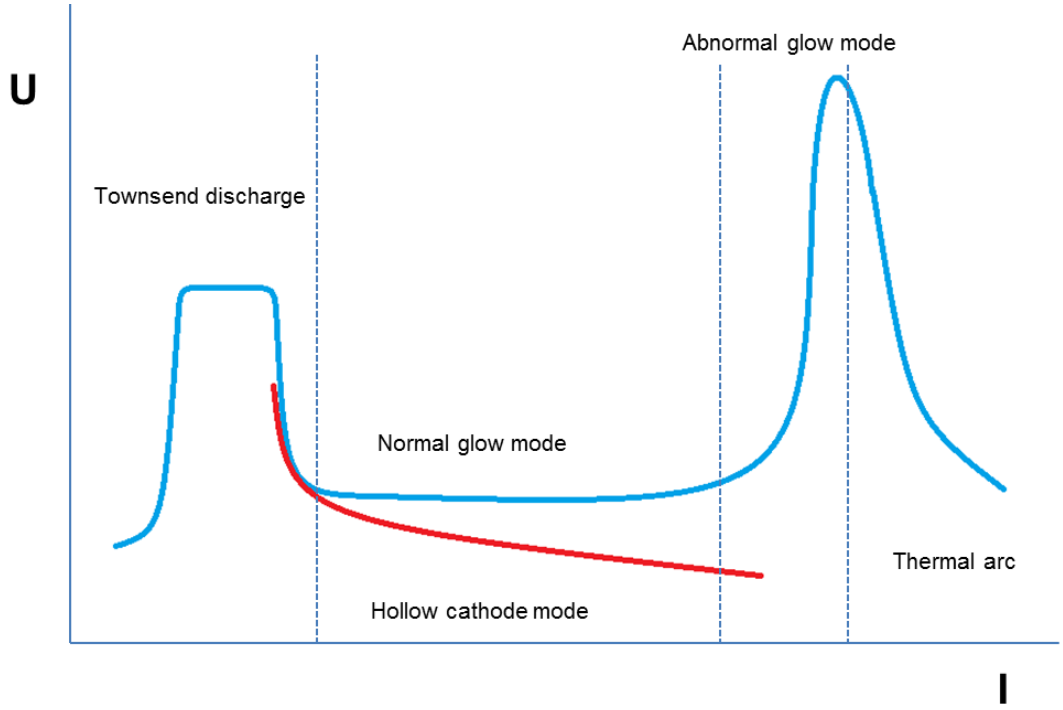

Figure 5.5: U-I diagram of a conventional GD and its various operating regimes vs. a hollow cathode discharge possessing a negative differential resistance.

More recently, hollow cathode plasmas gained new interests in plasma switches, ion thrusters, plasma surface treatment [31] and excimer sources. A lot of fundamental and practical work on hollow cathode discharges in micro cavities has been performed by Schoenbach et al. [32-35]. Different cylindrical geometries have been studied. The higher electron confinement in these structures compared to the cathode plate set-up allows the generation of a stable GD at atmospheric pressure up to diameters of 250 µm,

indicating that the hollow cathode discharge cannot be attributed completely to the pendulum effect [36]. Electron densities up to 10^{-15} cm^{-3} have been reported with gas temperatures ranging from room temperature up to 2000 K depending upon current and gas pressure. In order to create excited helium species (which are responsible for the typical appearance of a helium plasma), the electron population needs to contain a substantial amount of members with a energy of at least 24.6 eV which is the first ionization energy for helium. The high electron density, the increased ionization efficiency and the suitable electron temperature found in the µCHCD makes it an excellent candidate to replace the flame of an FID or the ^{63}Ni foil of an ECD. In this work the application of a µCHCD as ionization source for a versatile, low power GC detector will be investigated. In order to remain portable, no extra gas but the carrier gas should be employed.

5.2. Experimental

5.2.1. Reagents

1,1,2-Trichloroethylene (TCE) and methyl ethyl ketone (MEK) were both obtained from Merck (Darmstadt, Germany). Toluene was purchased from Alfa Aesar (Karlsruhe, Germany). Both carbon tetrachloride (CCl_4) and methyl t-butyl ether (MTBE) were obtained from Riedel-de Haën AG (Seelze, Germany). Ethanol was purchased from VWR International (Fontenay-sous-Bois, France) and methanol from Acros (Geel, Belgium). N,N-dimethylacetamide (DMA) was obtained from Sigma Aldrich (Diegem, Belgium). For chromatographic separations and plasma generation, helium 6.0 from Praxair (Schoten, Belgium) was used.

5.2.2. Chromatographic system and headspace (HS) sampler conditions

GC separations were carried out with a Perkin Elmer Autosystem XL GC equipped with a Perkin Elmer (Waltham, MA, USA) 40 XL HS auto sampler (balanced pressure system). HS-vials and PTFE/Sil-caps were purchased from Perkin Elmer as well. Separations were performed on an AT^{TM}-Aquawax column (30 m x 0.53 mm, d_f = 0.50 µm) from Grace (Lokeren, Belgium) using the oven program of Table 5.1. Injections for sensitivity comparison were performed on a similar system equipped with an FID and a Perkin Elmer Turbomass Gold MS system. For all experiments, HS-settings from Table 5.2 were used. 1 µL of sample was transferred to a headspace vial and injected using the Full Evaporation Technique (FET).

Table 5.1: Used GC-oven program.

t (min)	T (°C)
0	40
10	40
15.5	150
25.5	150

Table 5.2: Used HS-sampler parameters.

HS-parameters	Settings
Equilibration temperature	100 °C
Equilibration time	10 min
Needle temperature	105 °C
Transfer line temperature	110 °C
Pressurization time	1.0 min
Injection time	0.04 min
Needle withdrawal time	0.4 min
Injection port temperature	120 °C
Carrier gas	Helium

5.2.3. Preparation of solutions and sample vials

From the list of residual solvents published in ICH [37], five solvents with a low boiling point were selected based on retention characteristics and chemical structure: a partially and a completely chlorinated compound, a ketone, an alcohol and an aromatic compound. A stock mixture with equal volumes of toluene, CCl_4, MEK, TCE and ethanol resulting in a concentration of 20% v/v for each individual compound was prepared. Appropriate dilutions were made in MTBE. For analysis, 1 µL of test mixture was transferred to a HS vial which was sealed with a PTFE/Sil-cap.

5.2.4. µCHCD set-ups investigated

5.2.4.1. Co-axial µCHCD detector

A µCHCD detector using a co-axial electrode orientation (Figure 5.6) was constructed by using stainless steel capillaries in which the anode capillary was slid over the capillary that served as hollow cathode. A fused silica capillary with polyimide coating (320 µm I.D.) served as dielectric between the cathode and anode.

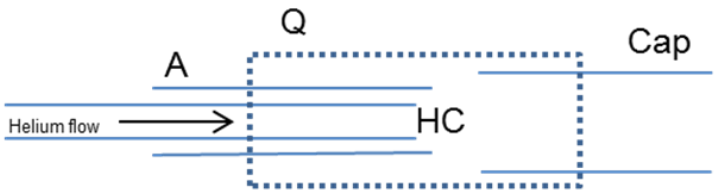

Figure 5.6: Co-axial µCHCD detector prototype (dielectric not shown): HC: hollow cathode (stainless steel tubing, I.D. 170 µm; O.D. 300 µm), A: anode (stainless steel tubing, I.D. 450 µm; O.D. 750 µm, Q: quartz glass tube (I.D. 1.55 mm, O.D. 3.50 mm), Cap: capture electrode (stainless steel tubing, I.D. 1.00 mm; O.D. 1.53 mm),

This initial set-up was never coupled to a GC system, but He and sample were supplied with the set-up described in Figure 5.7. This injection system made use of a three-way solenoid valve, a mass flow controller, a headspace vial and a bypass branch. The three-way switch allows selection between pure He and He loaded with sample (DMA). In order to avoid the µCHCD detector to become saturated with DMA vapour, the vial was immersed in an ice bath (0 °C). Injections were performed by switching the solenoid valve for a certain time. The helium flow through the detector was maintained at 2 mL/min.

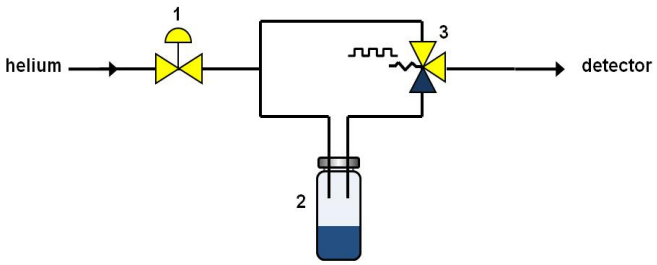

Figure 5.7: Used injection system to test the initial µCHCD-detector set-up. 1 = mass flow controller, 2 = headspace vial with DMA, 3 = three-way solenoid valve [38].

5.2.4.2. Serial axial µCHCD detector - version 1

A serial axial µCHCD detector prototype was constructed according to Figure 5.8. The hollow cathode was made from a thin walled platinum capillary (160 µm I.D.) mounted in a stainless steel tube. This subassembly was fitted in the centre of a 1 mm thick copper disk (Figure 5.9). Mechanical fixation and electrical conductivity were ensured by applying a Pb/Sn/Ag solder between each co-axial transition. After soldering, the assembly was polished with aluminium oxide lapping film until a mirror finish was obtained. The anode consisted of a 1 mm thick copper disc with a centre hole and was aligned with the hollow cathode using a dielectric spacer. The 2 mm thick spacer was crafted from Macor (Corning Inc., New York, NY, USA). The detector was equipped with a quartz window through which the plasma could be observed.

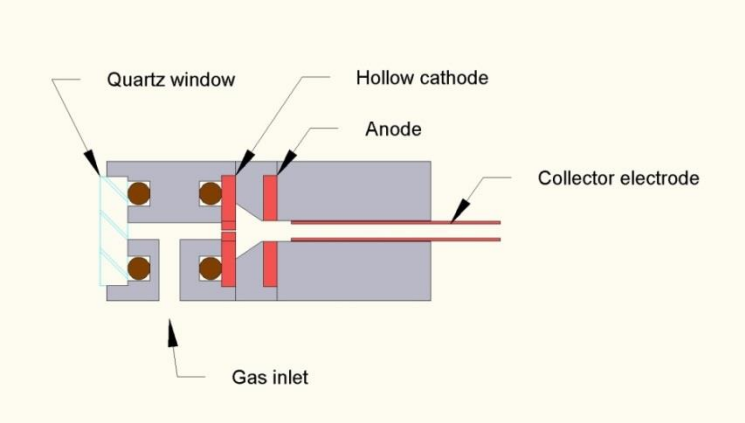

Figure 5.8: Schematic overview of the serial axial µCHCD detector - version 1.

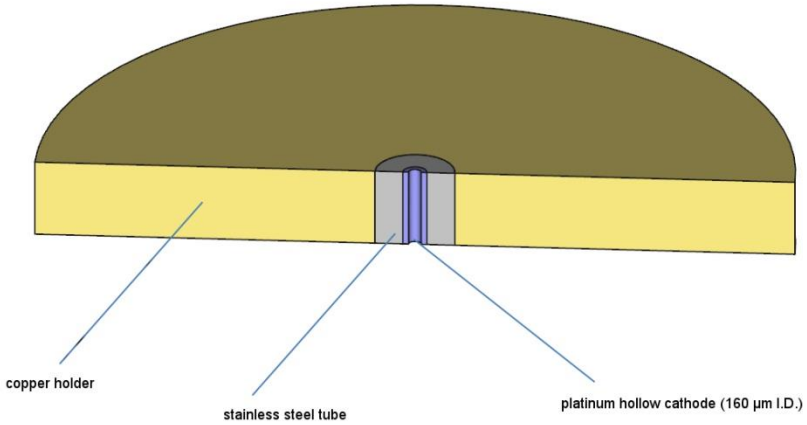

Figure 5.9: Cross section of the tubular hollow cathode used for serial axial µCHCD - version 1.

This prototype was coupled to a GC by inserting the column exit into the gas inlet of the detector. Different geometries (Figure 5.10) were used by varying (1) the shape and internal diameter of the dielectric spacer between the hollow cathode and anode and (2) the internal diameter of the anode.

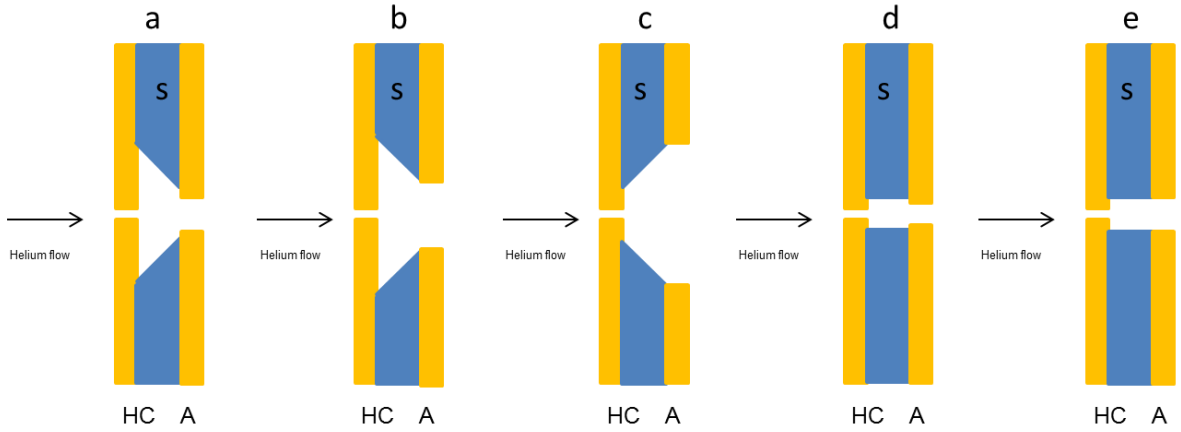

Figure 5.10: Tested geometries in µCHCD detector (s = dielectric spacer, HC = hollow cathode, A = anode).

5.2.4.3. Serial axial µCHCD detector - version 2

This µCHCD detector prototype (Figure 5.11) consisted of a brass detector housing with a Macor inner body that served as an electrode holder. The cathode assembly consisted of a copper disc in which the platinum/iridium hollow cathode was mounted (Figure 5.12) with Pb/Sn/Ag solder and which was polished as in section 5.2.4.2. This hollow cathode consisted of one piece (3 mm O.D., 0.5 mm thick) with a central orifice of 100 µm or 160 µm diameter (custom made by LADD Research, Wiliston, VT, USA). A ceramic high power aperture (9.5 mm O.D., 1 mm I.D., 0.254 mm thick) was used as dielectric for the separation of the hollow cathode and anode. A gold plated copper high power aperture (9.5 mm O.D., 1 mm I.D., 0.071 mm thick) served as anode after the backing paint was removed. Both apertures were purchased from Edmund Optics (Barrington, NJ, USA). The dimensions of the dielectric and the anode resulted in a wide anode clearance angle. A close up of this is given in Figure 5.11.

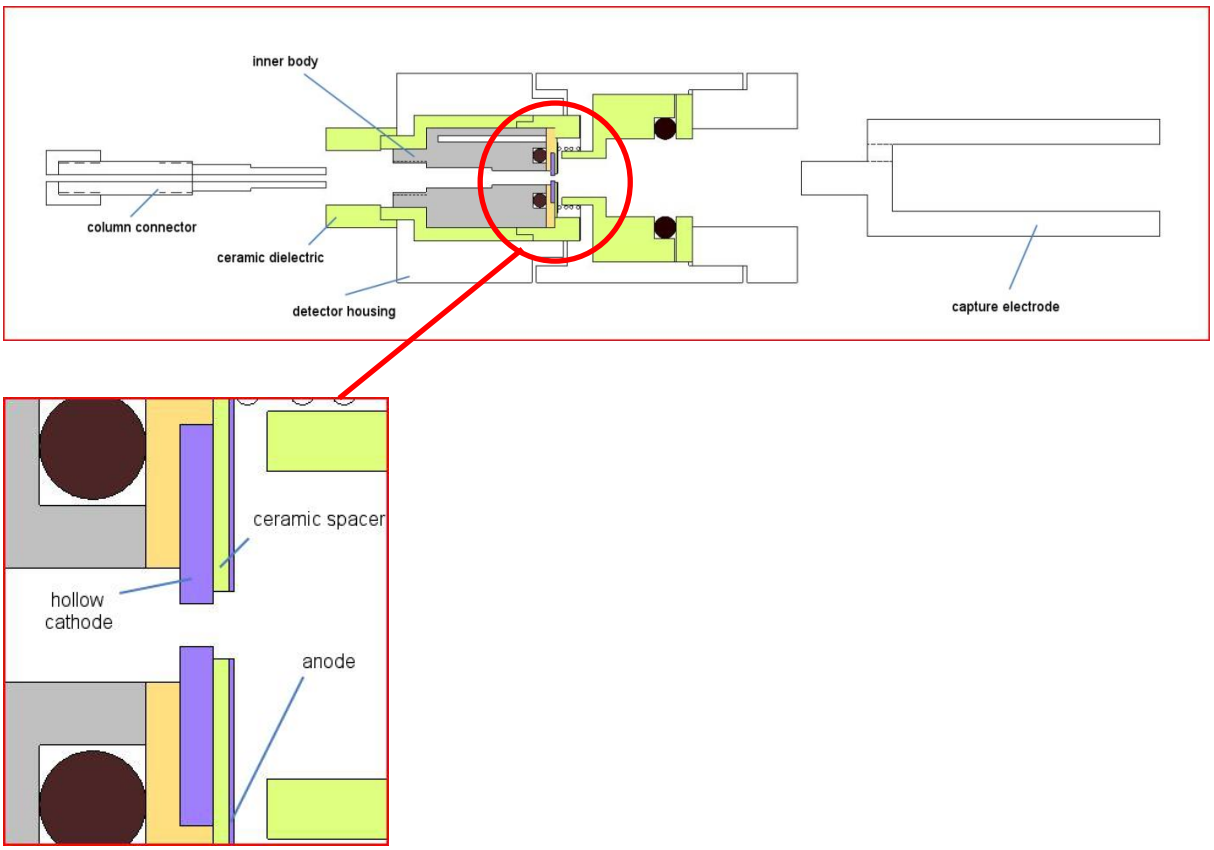

Figure 5.11: Schematic overview of serial axial µCHCD - version 2 with close-up of the hollow cathode (with wide anode clearance angle).

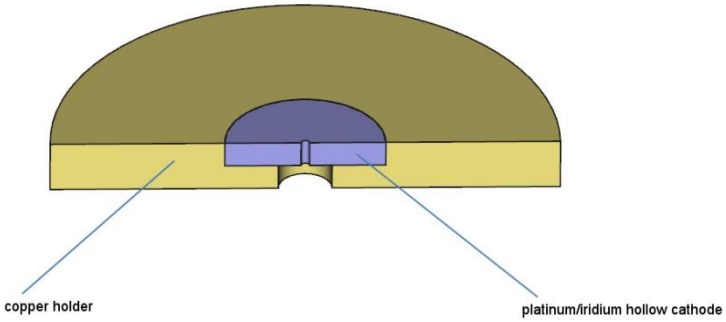

Figure 5.12: Cross section of the used hollow cathode assembly for serial axial µCHCD - version 2.

As with the first version of the serial axial µCHCD, this prototype was coupled to GC as well. The column exit was placed directly before the hollow cathode.

5.2.4.4. Electric scheme

Each constructed µCHCD detector set-up was tested by using the electric scheme of Figure 5.13. To ignite and sustain the plasma, a Spellman (New York, NJ, USA**)** CZE1000 high voltage supply (U_1) was used. The current through the plasma was limited by a set of high voltage resistors (R_b) with a total resistance of 110 MΩ. A Bio-Rad (Hercules, CA, USA) model 100 power supply (U_2) delivered the extraction tension. By reversing the connections of U_2, the capture electrode could be either negatively (as shown in Figure 5.13) or positively biased. Border conditions in the combination of extraction potential and extraction distance could create sudden discharges towards the capture electrode. The frequencies of these incidents increased with the deterioration of the microcavity surfaces. For this reason, an electron-valve based Pye (Cambridge, England) series 105 ionization amplifier was chosen to convert and subsequently amplify the current generated by captured ions instead of less robust modern semiconductor devices. A Chromperfect system from Justice Laboratory Software (Denville, NJ, USA) was used to perform AD-conversion and process the data. Special attention was taken regarding earth loops and electrical safety.

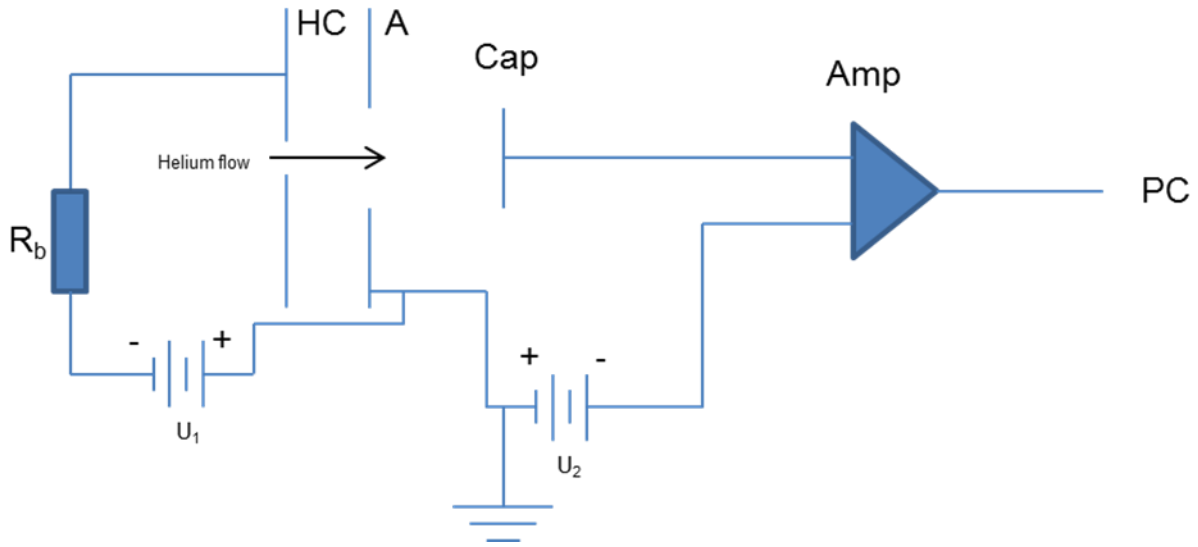

Figure 5.13: Used detection scheme to test various µCHCD-detector set-ups (dielectrics not shown). HC = hollow cathode, A = anode, Cap = capture electrode, Amp = ionization amplifier, DH = Detector housing, R_b = ballast resistance.

5.3. Results & Discussion

5.3.1. Initial testing with the co-axial µCHCD detector set-up

The co-axial µCHCD design is simple and derived from the hollow cathode lamp. A plasma current of 24 µA was the result when a voltage of 500 V was applied under the used helium flow. Pulsed injections of DMA vapour were performed in triplicate for 3 different times (2 s, 3 s and 4 s) resulting in a repeatable and concentration dependent signal (Figure 5.14). Although these results were very promising, some issues emerged during testing. The generated peaks are clearly tailing while a square-wave-like-response is expected from the used injection system. This is an indication that the flow pattern in the detector is far from ideal. More problematic was the short lifetime achieved with this set-up. After one hour, the system became unstable and started to spark. Visual inspection of the cavity revealed substantial erosion of all exposed electrode surfaces, cathode as well as anode. All three phenomena can be explained by taking into account the 'sudden expansion' of the gas flow at the cathode exit. As it is impossible for flow lines to follow the sudden change in dimension, a flow separation will occur, resulting in the creation of a vortex zone between the cathode and anode (Figure 5.15). This vortex may serve as a storage area explaining the tailing of the signal. For atmospheric pressure, the p*d-value for the used anode-cathode distance in this setup is 5.7 Torr.cm which is close to but still greater than the Paschen minimum. However, the pressure drop in the vortex zone could be large enough to initiate a 'secondary glow discharge' outside the hollow cathode, which could explain the noticed erosion pattern. Once erosion starts, sharp features will develop on the surfaces. Those are initiators for sparking due to the local high field strength. An extra complication may be expected from the surface properties of stainless steel. Under normal atmospheric conditions stainless steel is covered with a thin non-conductive oxide layer protecting it against corrosion. The plasma erosion will damage this layer locally and depending on the presence of oxygen, a new layer may be formed. As a consequence, the whole process will result in a non-uniform and non-defined surface condition.

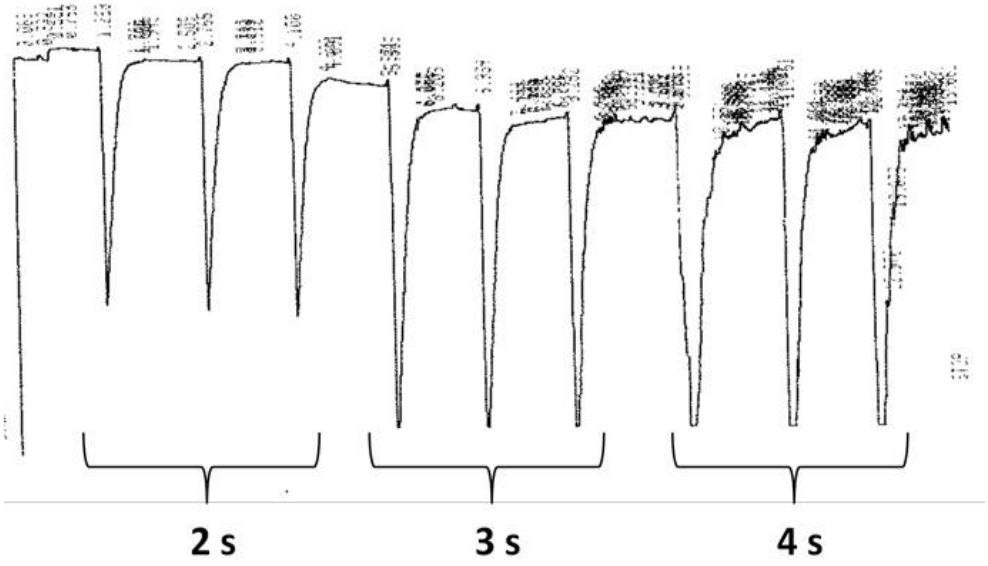

Figure 5.14: Generated responses from repetitive injections of DMA [38].

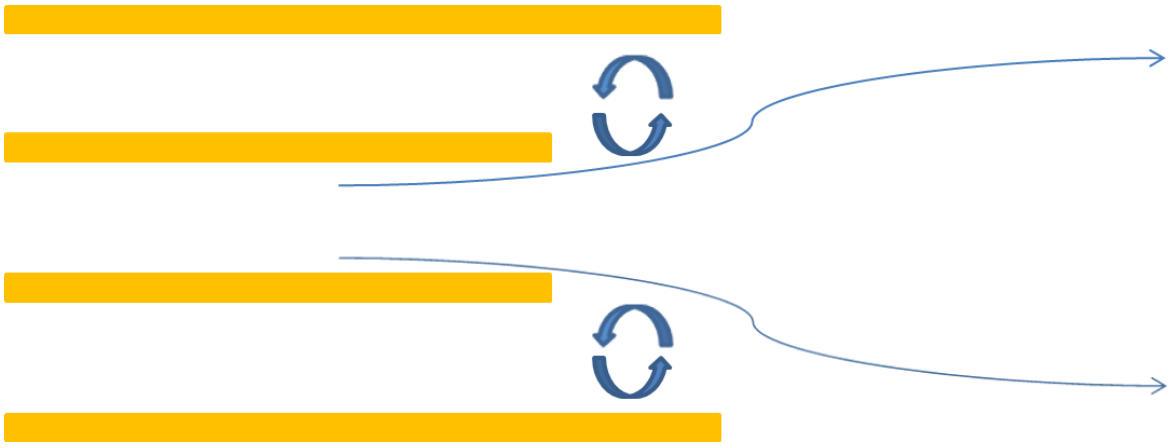

Figure 5.15: Schematic drawing of the hollow cathode and expansion of the gas flow creating a reduced pressure resulting in possible secondary glow discharges.

5.3.2. Serial axial µCHCD detector – version 1

From the experiments with the coaxial set-up three areas for improvement were identified.

The coaxial approach was abandoned in favour of a serial axial set-up using two parallel disc shaped electrodes with a central orifice. Several benefits are to be expected from this arrangement. This design places the anode outside the low pressure area, created by the sudden expansion, reducing the risk on a secondary glow discharge. The larger front area achieved by this arrangement translates in a more uniform electric field and it is easier to achieve a smooth surface. Both items reduce the chance on sparking.

Instead of using stainless steel as electrode material, platinum/iridium was used for its better resistance against plasma sputtering. Materials such as tungsten (W), molybdenum (Mo) or pure iridium (Ir) could be used as well, but are very hard to manipulate due to the characteristic hardness of these materials. The absence of an oxide layer results in a better conductivity and a more uniform surface chemistry.

A third area of optimization is the flow pattern. Nowadays, this kind of optimization is done with the aid of Computational Fluid Dynamics (CFD) software. In this case however it is extremely difficult to collect the data needed for the initiation and verification of such a process, without causing artefacts. Mainly the temperature and the exact location of the plasma are unknown and could change under the influence of a passing analyte. After establishing a flow pattern model, this should be used to study the ion trajectories, increasing the complexity of the process. For these reasons it was decided to use a more hands on approach and study the results generated with the geometries depicted in Figure 5.10. For each geometry, a set of chromatograms was recorded covering the whole range of parameter combinations. The capture distance was varied from 1 to 5 mm relative to the anode in steps of 1 mm. The plasma current ranged from 10 to 100 µA. For this range the µCHCD operates in hollow cathode mode as was indicated by the negative resistance behaviour. The effect of the bias voltage was examined from 50 to 300 V with both polarizations. The combination of sample size, sample concentration and split settings was calculated corresponding to 1 µg of each compound on column.

The general appearance, peak shape, signals and noise levels of the generated chromatograms were visually inspected and compared. Only the negative bias mode resulted in chromatograms. When the capture electrode was positively biased only noise was recorded. The influence of the plasma current (within one geometry) on the assessed parameters was negligible. As a consequence, a low current is preferred to reduce power consumption and heat load. The capturing distance has a small effect on the peak shape,

while signal strength is proportional to the field strength, i.e. the ratio of bias potential to distance. High field strength combined with short distances can create a destructive overload on the amplifier input.

Surprisingly the cavity shape turned out to be of major importance. Taking the general appearance of the chromatograms as selection criterion, the geometries can be divided into two groups. Geometries ‘’a’’, ‘’d’’ and ‘’e’’ (Figure 5.10) have a narrow anode bore in common. While a high baseline with negative peaks for all components (thus less positive ions reaching the capture electrode) are the main characteristics for this group (Figure 5.16), cell ‘’e’’ performed slightly better concerning noise and signal level which is probably attributed to the dielectric shielding of the anode. For geometries ‘’b’’ and ‘’c’’, a wide anode bore was used. The resulting chromatograms (Figure 5.17) show a lower baseline and less noise, while all components appear as positive peaks. Therefore it was decided to use geometries ‘’b’’ and ‘’c’’ as base for the next design.

The lifetime was improved dramatically too. After a few weeks, the µCHCD started to draw current without the generation of plasma. On inspection, a black gray deposit in the inner volume of the dielectric was noticed and the cathode had a mat appearance. Treating the spacer with hot hydrochloric acid and repolishing the cathode restored operation. After a few cycles it became clear that the solder between the capillaries was slowly etched away causing the deposit. At the end, the resulting cavity will cause sparking making the cathode useless. So, this issue was considered in the next design. It was however possible to complete this part of the work with only one cathode assembly.

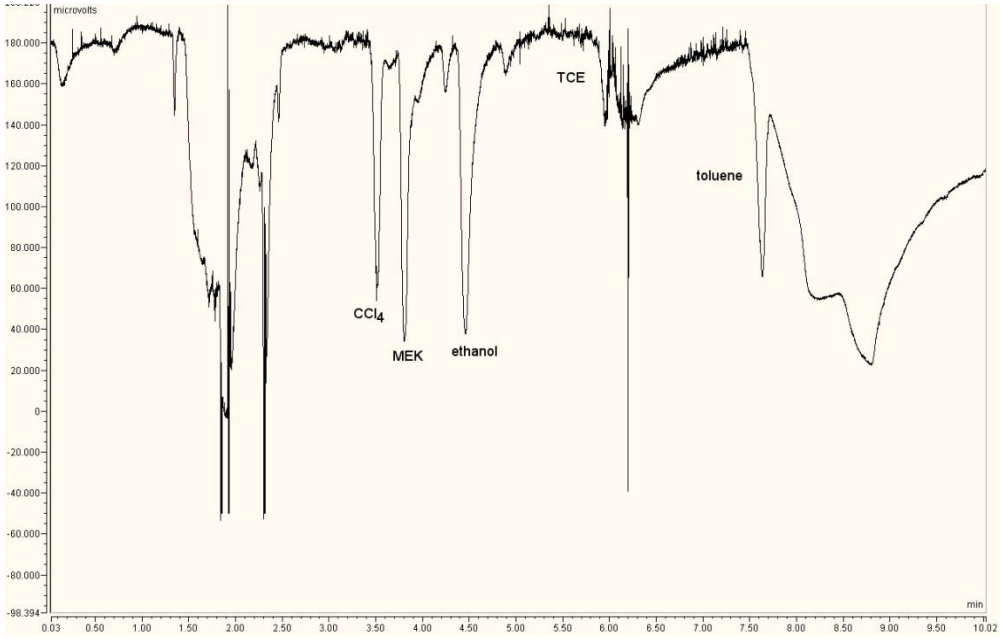

Figure 5.16: Chromatograms of the used analyte mixture (~1 µg each) obtained with the serial axial µCHCD detector – version 1 using the following parameters: plasma current of 30 µA, capture distance of 1 mm in combination with an extraction voltage of 100 V (1000 $V.cm^{-1}$), carrier gas flow of 3.5 $mL.min^{-1}$, geometry ‘’e’’.

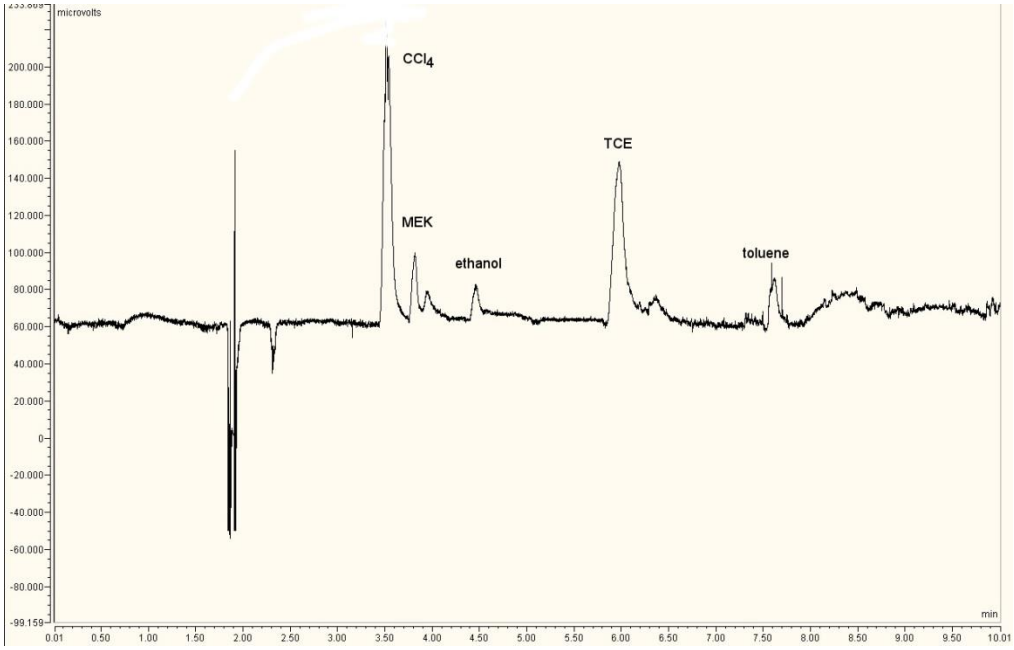

Figure 5.17: Chromatograms of the used analyte mixture (~1 µg each) obtained with the serial axial µCHCD detector – version 1 using the following parameters: plasma current of 30 µA, capture distance of 1 mm in combination with an extraction voltage of 100 V (1000 $V.cm^{-1}$), carrier gas flow of 3.5 $mL.min^{-1}$, geometry ‘’b’’.

5.3.3. Serial axial µCHCD detector – version 2

To avoid the solder sputtering noticed in the previous set-up, the hollow cathode subassembly was replaced by a hollow cathode disc. Due to production limitations, the thickness of this disc (and as a consequence also the length of the hollow cathode) was limited to 0.5 mm. The quartz window was dropped to avoid peak broadening caused by the relatively large dead volume of this side-branch. The results obtained with the first version suggested that a wide cathode-anode clearance angle would be the most promising approach towards a low background signal and an acceptable signal-to-noise ratio. To keep the anode dimensions small, a thin dielectric was chosen. This would make it also possible to place the capture electrode closer to the plasma where more analyte ions should still be alive, resulting in higher signal intensities. To check whether the device was operating in the hollow cathode mode, the plasma voltage was checked at different plasma currents. When the plasma voltage went down with increasing current (negative differential resistance) it was considered that operation of the µCHCD plasma occurred in the hollow cathode mode.

5.3.3.1. Influence of the hollow cathode diameter

First the influence of the internal diameter of the hollow cathode was investigated. Both sizes (100 µm and 160 µm) showed negative differential resistance in the measured range (10-100 µA). In order to use the same amplification as with the previous prototype, it was necessary to dilute the sample until a level of 100 pg on column was reached. The noise generated with the 160 µm cathode made measurements with a capture distance above 0.5 mm useless (Figure 5.18), while negative peaks are generated for the chlorinated solvents. However, the 100 µm cathode allowed to use distances up to 6 mm (limit of the construction) as further discussed in 5.3.3.2. For this reason the 100 µm cathode was used for the remainder of the experiments.

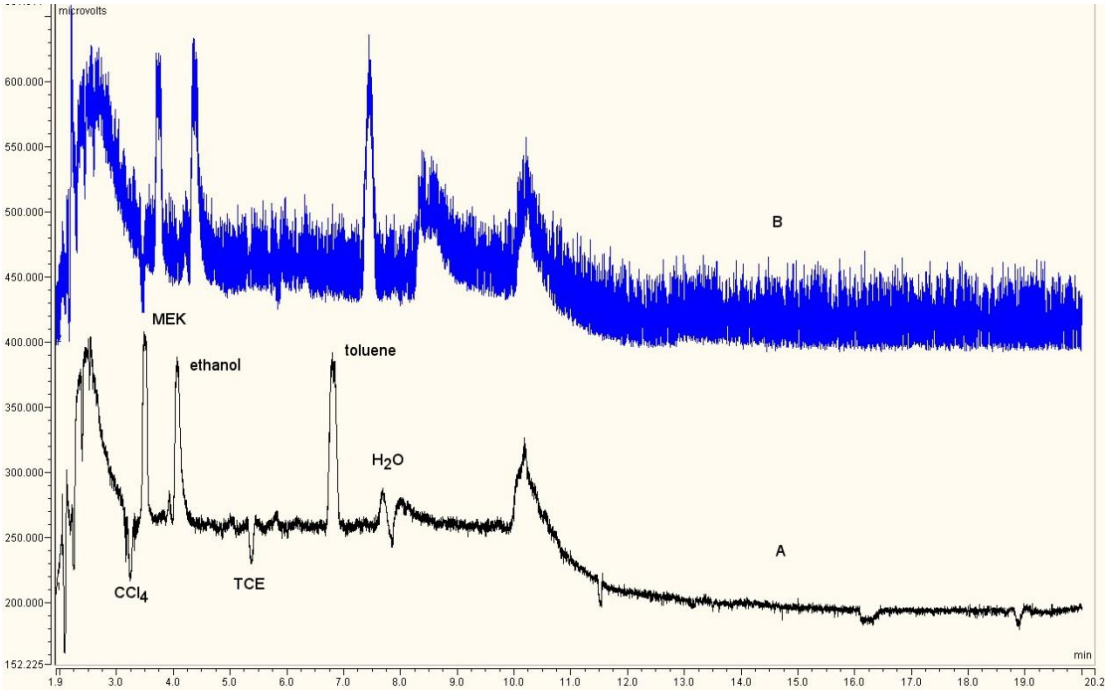

Figure 5.18: Comparison of chromatograms obtained with the 160 µm I.D. hollow cathode for a capture distance of 0.5 mm (A) vs.1 mm (B).

5.3.3.2. Operational parameters

5.3.3.2.1. Negatively biased capture electrode

Similar to the previous set-up, there was not much influence of the plasma current on the generated signals (Figure 5.19). 30 µA was chosen as standard operating current. The gas flow on the other hand has a strong influence on the signal (Figures 5.20 and 5.21). At higher speed, ions need less time to reach the capture electrode and less ions will be lost. Apart from the deviations at lower flows, higher flows result in larger signals. As 4 ml/min is the optimal working condition for a 530 µm GC column, this flow will be used in the remainder of this work. A smaller cathode diameter should have a similar effect, but 100 µm diameter at a thickness of 0.5 mm seems to be the limit for most manufacturers. For the same reason, longer cathode channels could not be used although this parameter may affect the dynamic range of the detector.

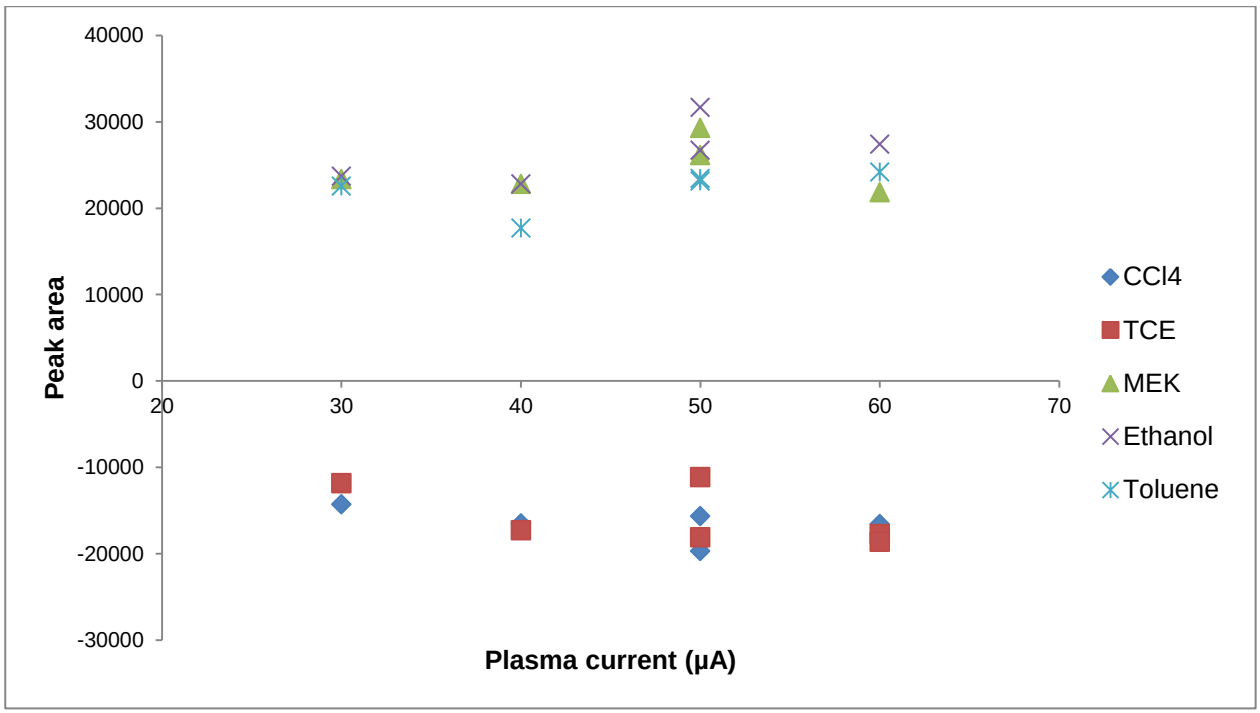

Figure 5.19: Influence of the plasma current on analyte response (100 µm hollow cathode, ~1 ng injected, capture electrode at 1 mm from anode, 500 $V.cm^{-1}$, carrier gas flow = 3.5 $mL.min^{-1}$).

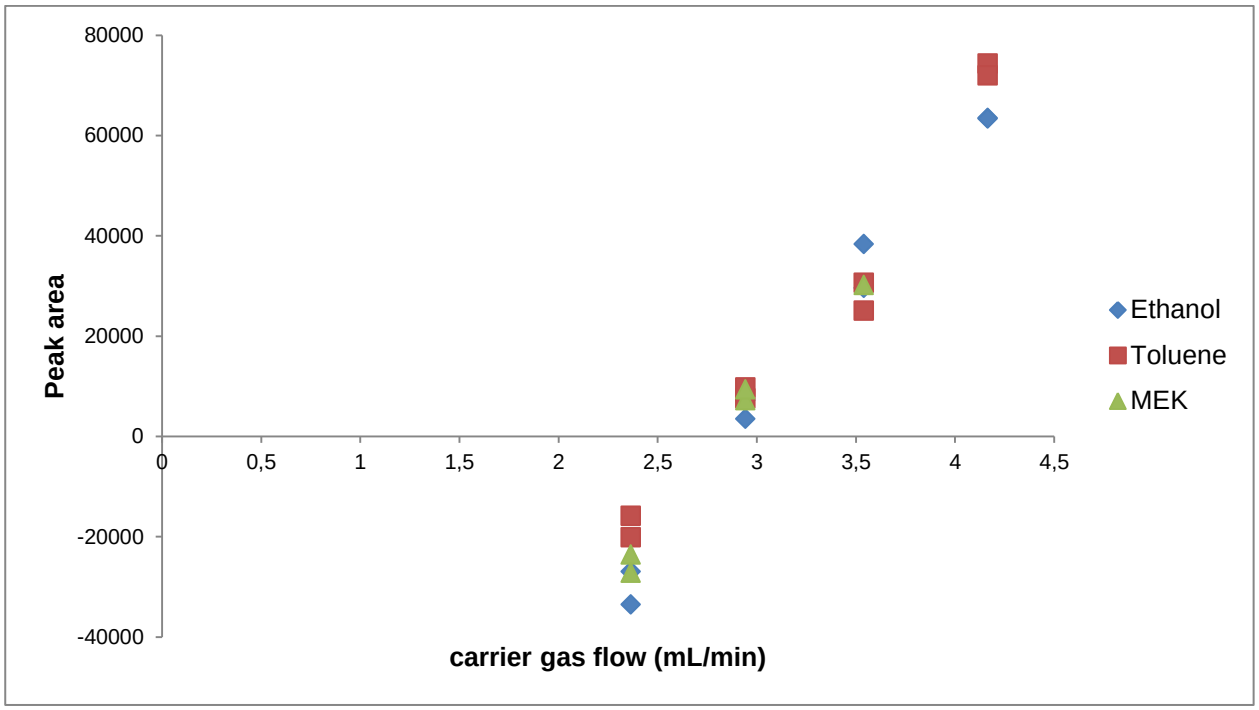

Figure 5.20: Peak area of toluene, ethanol and MEK vs. carrier gas flow. Peaks change from negative to positive polarity with increasing carrier gas flow. (100 µm hollow cathode, ~1 ng injected, 30 µA, capture electrode at 1 mm from anode, 500 $V.cm^{-1}$).

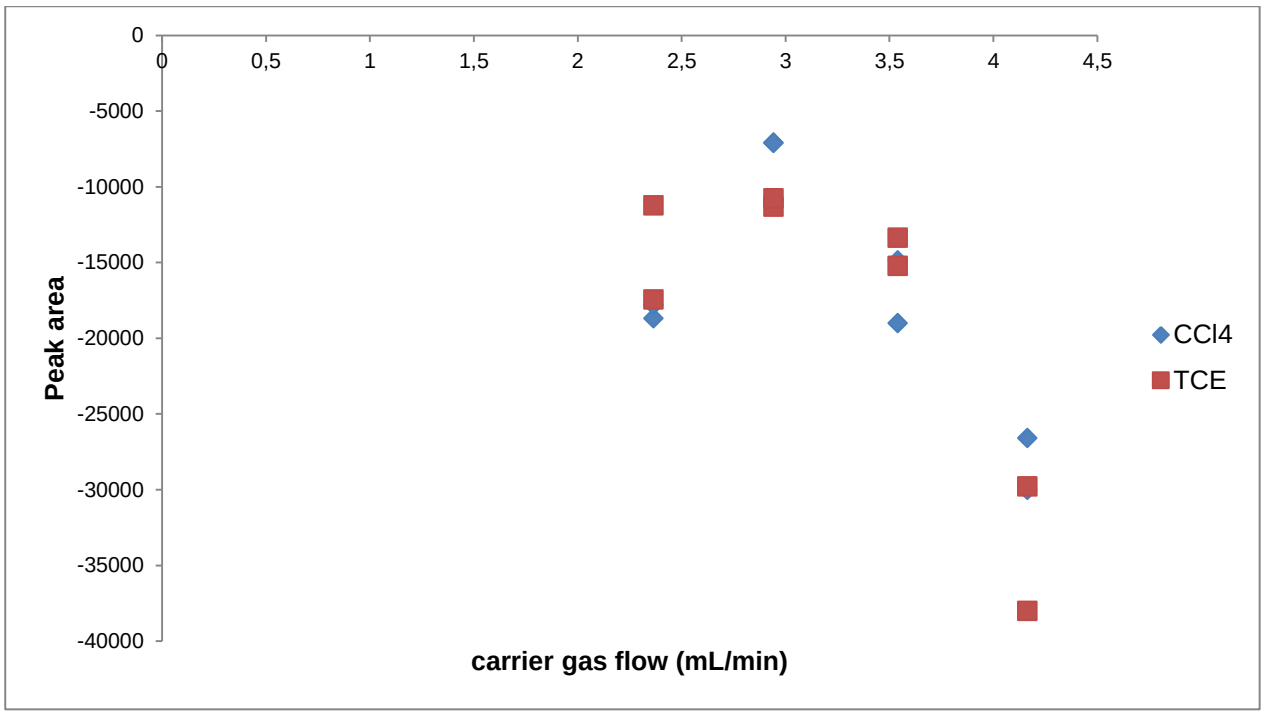

Figure 5.21: Negative peak areas of CCl_4 and TCE vs. carrier gas flow (100 µm hollow cathode, ~1 ng injected, 30 µA, capture electrode at 1 mm from anode, 500 $V.cm^{-1}$).

For capture distances from 2 to 6 mm the signal is slightly dropping at constant field strength (Figure 5.22). When going from a capture distance of 2 mm to 1 mm the signals of the compounds are becoming smaller. However, their behaviour is quite complex as illustrated in Figure 5.23. The analytes recorded as negative peaks are chlorinated ones showing a transition from a sharp negative peak (1 mm) via a hybrid form (2 mm) gradually to a broad positive hump (3 mm) with increasing capture distance. A similar behaviour is found if the capture point is fixed (for instance at 2 mm) and the concentration is gradually decreased. A schematic summary illustrating the influence of the capture distance and analyte concentration on the signal is shown in Figure 5.24. When the field strength is varied, the transition point remains at 2 mm, but the signals are proportional. The difference between chlorinated and non-chlorinated compounds can be explained by assuming a different ionization mechanism for both groups. In the plasma, He^+ ions, He metastables and photons are generated. A portion of the generated He^+ ions will reach the capture electrode and is responsible for the background signal. The non-chlorinated compounds are probably ionised after the plasma by photo ionization or chemical ionization, adding species to the positive ion population which is hitting the capture electrode. The chlorinated compounds on the other hand have a greater affinity towards electrons. So, the chance is high that an electron capture mechanism in the electron rich plasma is followed. When leaving the plasma, these negative ions will follow the gas flow towards the capture electrode, but they will be slowed down and beard off somewhat due to the anode-capture electrode field.

During their journey, they will be neutralised by He^+ ions resulting in a He^+ ion depletion which causes a dip in the background signal when the capture electrode is at close distance. As the trajectory of the chlorinated analyte compounds is disturbed, this will cause a deteriorated peak shape in the chromatogram. The longer the distance to the capture electrode, the higher the probability that the neutralised species (still following the gas flow) are ionised again by photons and He metastables to form positively charged ions which are attracted by the capture electrode and will contribute to the positive signal.

In 5.3.3.2.2 it will be demonstrated that negative ions are formed in the plasma and can be extracted before neutralisation by choosing the correct capture distance and polarisation.

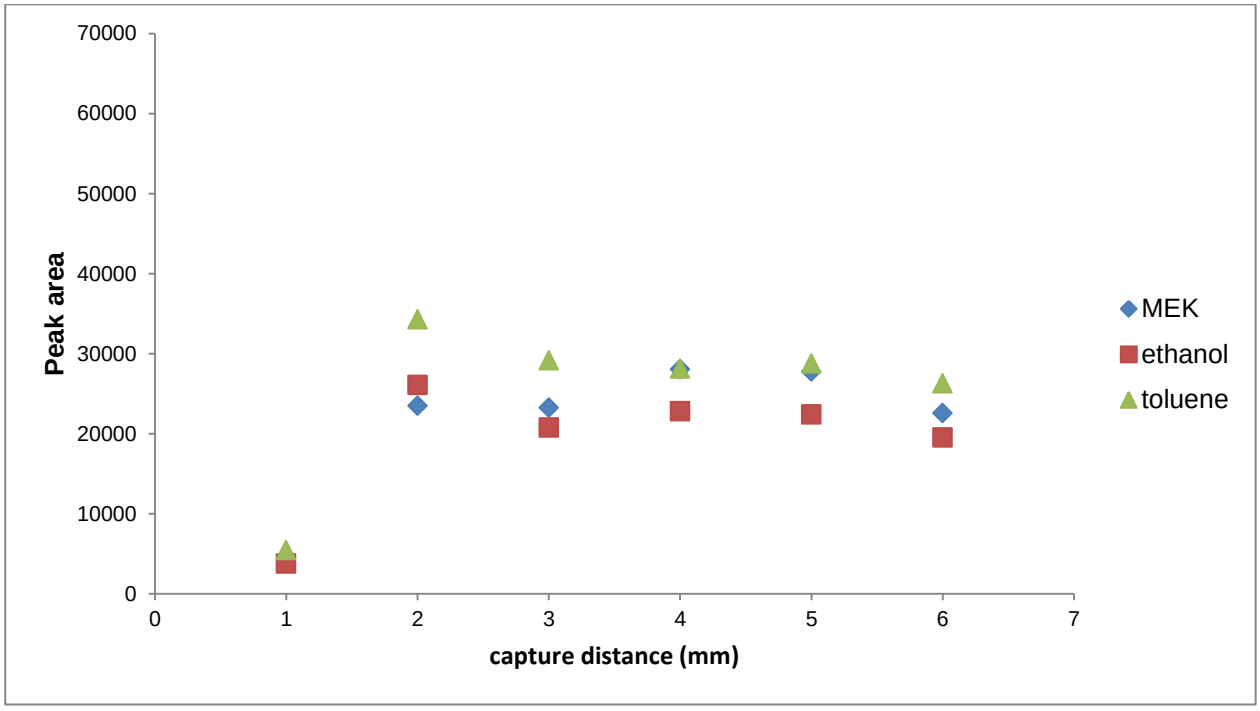

Figure 5.22: Influence of the capture distance on the signal obtained for non-chlorinated analytes

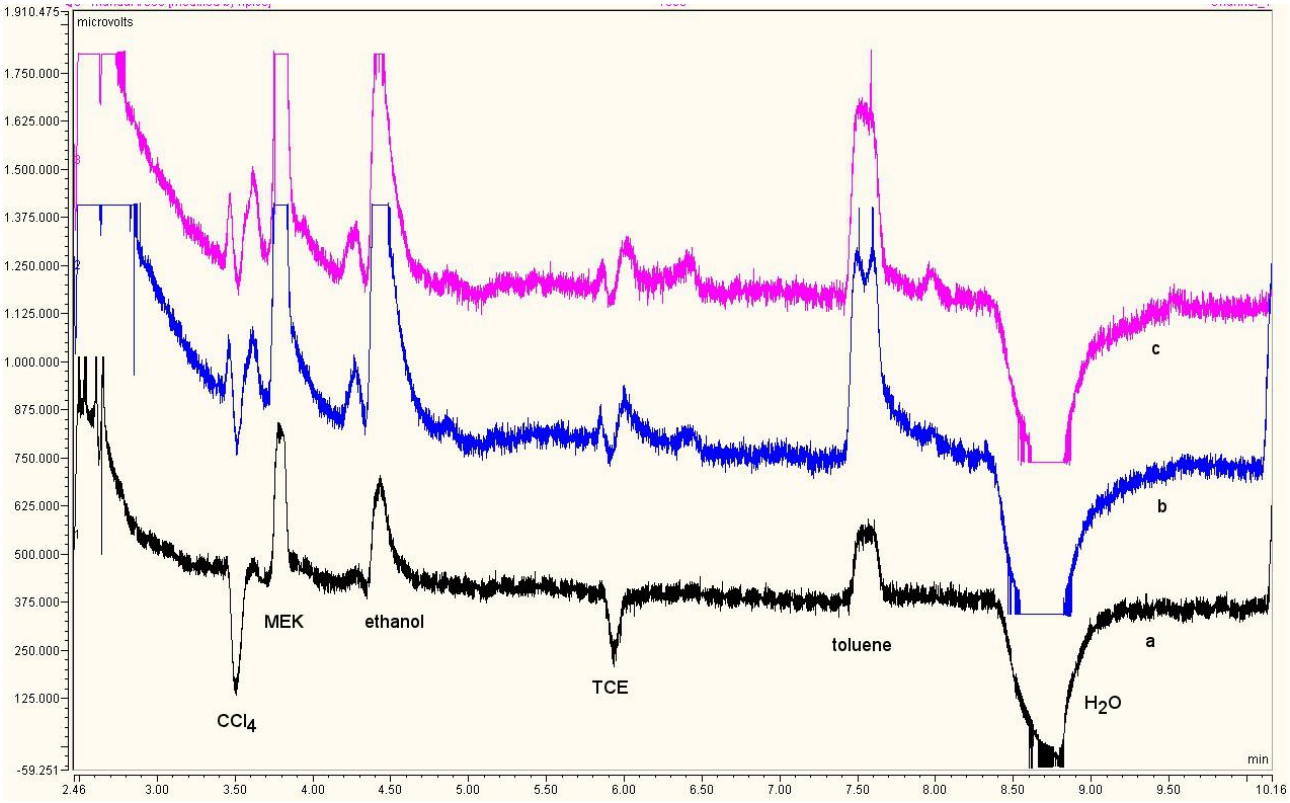

Figure 5.23: Chromatograms obtained with different capture distances (Trace a = 1 mm, trace b = 2 mm and c = 3 mm) using the 100 µm I.D. hollow cathode.

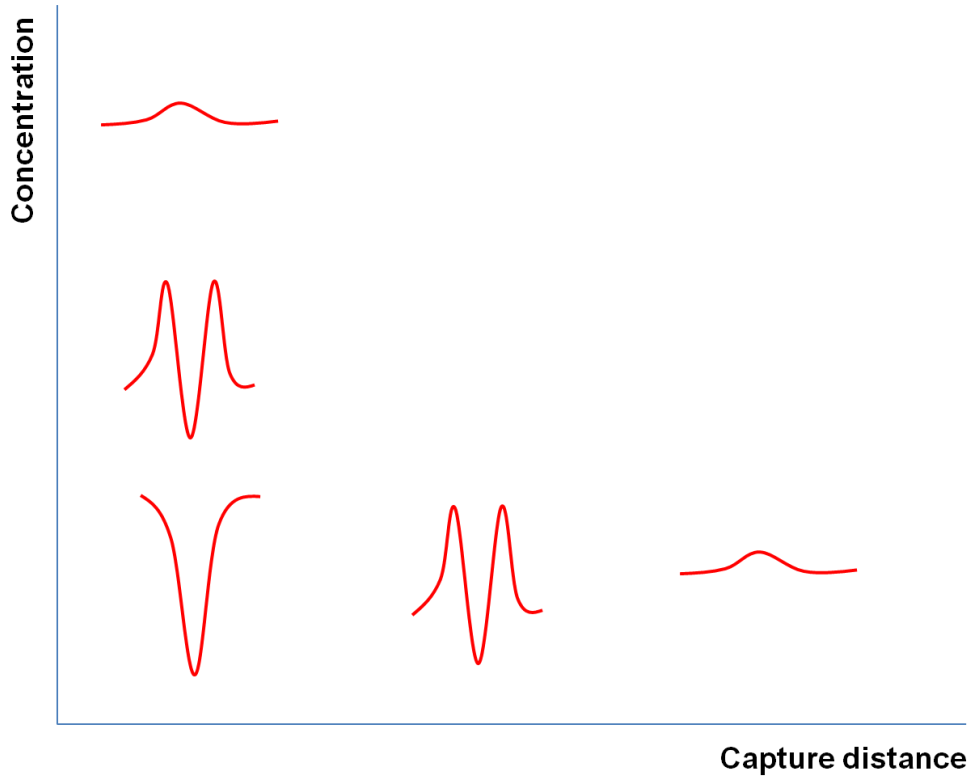

Figure 5.24: Schematic drawing demonstrating the effect of capture distance and analyte concentration on the signal obtained for chlorinated species.

5.3.3.2.2. Positively biased capture electrode

In order to retrieve negative ions, the capture electrode should be at a more positive potential than the anode which, in its turn, is already positive with respect to the plasma and the cathode. In the previous set-up, the small anode clearance angle created by the smaller anode orifice and larger dielectric, together with the large potential gradient between the plasma and the anode certainly created a barrier for negative species to reach the capture electrode. With the wide clearance angle used in version 2, the plasma-anode field is almost perpendicular to the hollow cathode axis and due to the thinner spacer, the effluent passes the anode at higher speeds. Both phenomena increase the possibility for negative charges to reach the positively biased capture electrode. However, bringing this concept into practice was not straightforward. The amplifier and AD-converter used are both asymmetric (-50mV to +1000mV combined range approximately) towards the polarity of the input signal. Most operational parameters with a positively biased capture electrode resulted in a negative background beyond the compensation capabilities of the equipment. The anode-capture electrode distance had to be at least 5 mm with a potential difference of maximum 100 V to get the baseline within range. The chromatograms recorded under these conditions are exhibiting sharp positive peaks for the chlorinated compounds (Figure 5.25) while the negative peaks are a representation of the non-chlorinated ones.

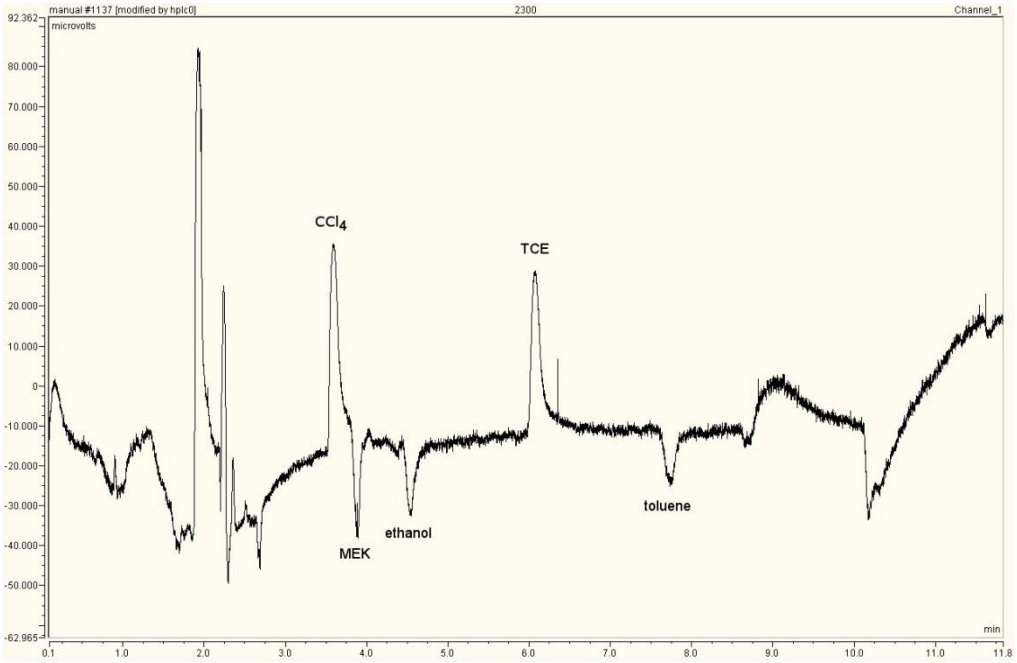

Figure 5.25: Obtained chromatogram using a positively biased capture electrode.

Due to the physical limitations of the µCHCD and the electronical limitations of the equipment, it was not possible to investigate the influence of the different parameters on the performance. As the positively biased capture electrode only captures negatively charged species, the presence of positive peaks under this mode can be regarded as a confirmation of the existence of negatively charged ions downstream of the plasma. The negative background is probably caused by a secondary GD between anode and capture electrode [39] where the capture electrode acts as final anode. Under these conditions electrons can reach the capture electrode. Negatively charged ions will contribute to the signal while positive ions will create electron depletion this time.

5.3.4. Comparison to other techniques

In order to compare with other techniques, the same test solutions in MTBE were injected under the same HS-GC conditions using an MS operated in full scan or FID. As with the µCHCD detector, 1 ng on the detector is easy to detect by both FID and MS. As expected, the FID is more sensitive for toluene due to the number of combustible carbon atoms that are present in its structure. CCl_4 generates a rather small peak due to poor ionization in the FID detector. Diluting the test mixture further to end up with ~100 pg on the detector, leaves all compounds undetected with MS and FID detector (Figure 5.27). These amounts are still detected well with the µCHCD detector prototype (Figure 5.28), clearly showing its potential as a simple and sensitive GC detector.

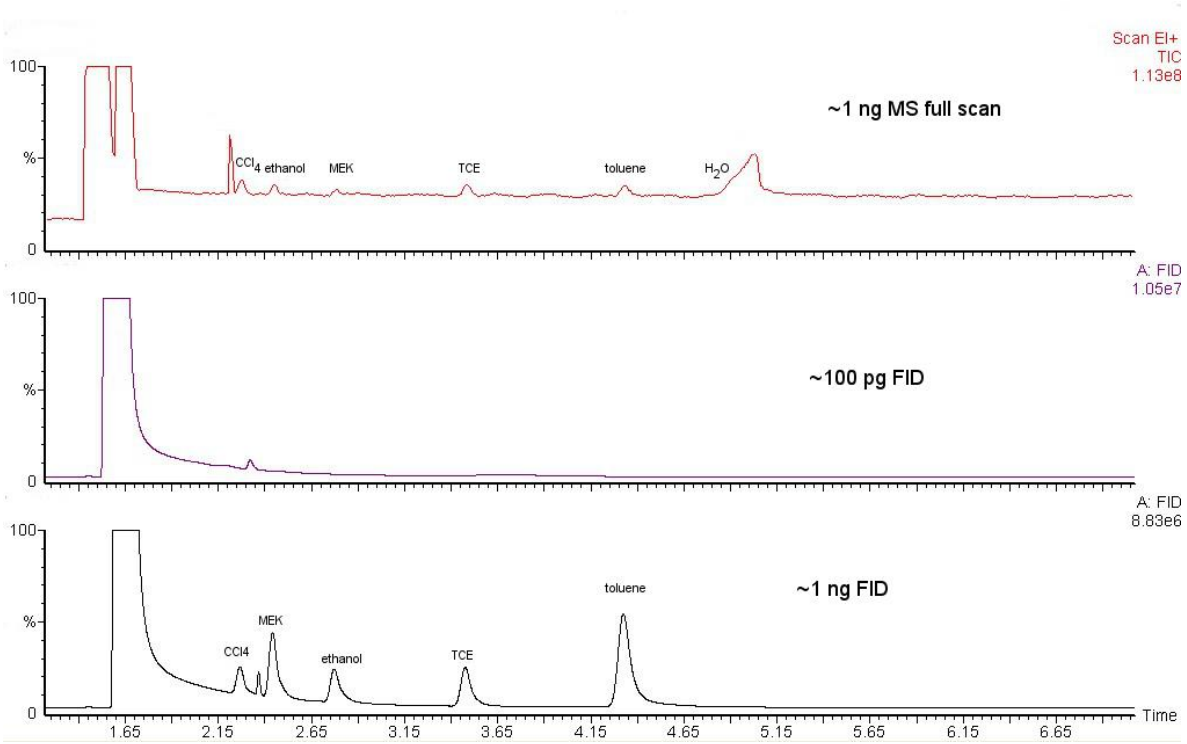

Figure 5.27: Obtained chromatograms with MS in full scan and FID detector.

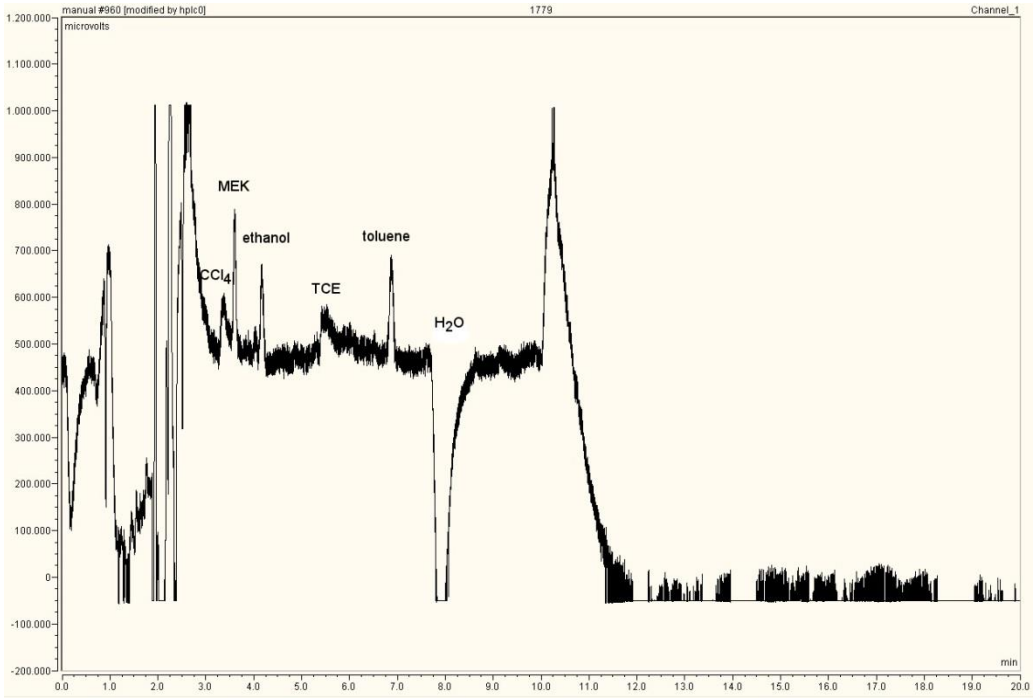

Figure 5.28: Chromatogram obtained with the serial axial µCHCD detector – version 2 with negatively biased capture electrode at 2 mm after introduction of ~100 pg of each analyte (30 µA, 4 mL/min^{-1}, 500 V.cm^{-1}).

5.4. Conclusions

It was demonstrated in this work that the use of a µCHCD plasma as ion source for a simple GC detector is a promising approach to replace many commercially available GC detectors. As predicted by the theory around µCHCDs it was possible to operate such detection system at atmospheric pressure and without radioactive material, which is a great advantage compared to an MS or ECD as GC detector. During development steps it became clear that the µCHCD ion source geometry is an important parameter for the detector to obtain a GC detector with quantitative behaviour and a reasonable lifetime. The initial design having a co-axial hollow cathode-anode geometry using stainless steel electrodes was found to have a limited lifetime caused by plasma sputtering. Changing the design from a co-axial set-up to a serial axial set-up with platinum electrodes increased the lifetime of the set-up significantly. It was revealed that the shape of the flow channel consisting out of the hollow cathode, dielectric spacer and anode of the µCHCD ion source was of great influence on resulting chromatograms. Using a wide hollow cathode-anode opening clearance angle lead to a quantitative detector towards a range of tested analytes included in this study such as CCl_4 and toluene. After reducing the dead volume of the µCHCD ion source, detection of volatile analytes in the 100 pg range was possible using either a positively or negatively biased capture electrode. The sensitivity of the µCHCD detector prototype was compared with FID and MS and was found to be more sensitive. So, the µCHCD detector prototype developed in this work is a very promising approach to replace the FID and other

detectors, as the μCHCD detector offers good detection capabilities towards halogenated species such as CCl_4 and TCE using only one type of gas with the advantage of operation at atmospheric pressure. Moreover, the μCHCD ion source can be used in small handheld portable detection devices as it has low power consumption.

5.5. References

[1] T. Holm, Aspects of the mechanism of the flame ionization detector, J. Chromatogr. A, 842 (1999) 221-227

[2] J. Wang, H. Wang, C. Duan, Y. Guan, Micro-flame ionization detector with a novel structure for portable gas chromatograph, Talanta, 82 (2010) 1022-1026

[3] Application note AP-226, Comparison of photoionization detectors (PID's) and flame ionization detectors (FIDs), RAE systems

[4] Q. Jin, W. Yang, A. Yu, X. Tian, F. Wang, Helium direct current discharge ionization detector for gas chromatography, J. Chromatogr. A, 761 (1997) 169-179

[5] A. Bogaerts, E. Neyts, R. Gijbels, J. van der Mullen, Gas discharge plasmas and their applications, Spectrochim. Acta B, 57 (2002) 609-658

[6] C. Tendero, C. Tixier, P. Tristant, J. Desmaison, P. Leprince, Atmospheric pressure plasmas: A review, Spectrochim. Acta B, 61 (2006) 2-30

[7] D.S. Forsyth, Pulsed discharge detector: theory and applications, J. Chromatogr. A, 1050 (2004) 63-68

[8] W.E. Wentworth, H. Cai, S. Stearns, Pulsed discharge helium ionization detector. Universal detector for inorganic and organic compounds at the low picogram level, J. Chromatogr. A, 688 (1994) 135-152

[9] S. Mendoca, W.E. Wentworth, E.C.M. Chen, S.D. Stearns, Relative responses of various classes of compounds using a pulsed discharge helium photoionization detector: Experimental determination and theoretical calculations, J. Chromatogr. A, 749 (1996) 131-148

[10] M.T. Roberge, J.W. Finley, H.C. Lukaski, A.J. Borgerding, Evaluation of the pulsed discharged helium ionization detector for the analysis of hydrogen and methane in breath, J. Chromatogr. A, 1027 (2004) 19-23

[11] J.G. Dojahn, W.E. Wentworth, S.N. Deming, S.D. Stearns, Determination of percent composition of a mixture analysed by gas chromatography. Comparison of a helium pulsed-discharge photoionization detector with a flame ionization detector, J. Chromatogr. A, 917 (2001) 187-204

[12] H. Cai, S.D. Stearns, Pulsed discharge helium ionization detector with multiple combined bias/collecting electrodes for gas chromatography, J. Chromatogr. A, 1284 (2013) 163-173

[13] S.H. Kim, S.M. Nam, K.O. Koh, Y.W. Choi, Analysis of natural gas using single capillary column and a pulsed discharge helium ionization detector, Bull. Korean. Chem. Soc., 20 (1999) 843-845

[14] M.C. Hunter, K.D. Bartle, P.W. Seakins, A.C. Lewis, Direct measurement of atmospheric formaldehyde using gas chromatography-pulsed discharge ionisation detection, Anal. Commun., 36 (1999) 101-104

[15] W.E. Wentworth, K. Sun, D. Zhang, J. Madabushi, S.D. Stearns, Pulsed discharge emission detector: an element-selective detector for gas chromatography, J. Chromatogr. A, 872 (2000) 119-140

[16] R. Gras, J. Luong, M. Hawryluk, M. Monagle, Analysis of part-per-billion level of arsine and phosphine in light hydrocarbons by capillary flow technology and dielectric barrier discharge detector, J. Chromatogr. A, 1217 (2010) 348-352

[17] R. Gras, J. Luong, M. Monagle, B. Winniford, Gas chromatographic applications with the dielectric barrier discharge detector, J. Chromatogr. Sci., 44 (2006) 101-107

[18] K. Kunze, M. Miclea, J. Franzke, K. Niemax, The dielectric barrier discharge as a detector for gas chromatography, Spectrochim. Acta B, 58 (2003) 1435-1443

[19] F.A. Franchina, M. Maimone, D. Sciarrone, G. Purcaro, P.Q. Tranchida, L. Mondello, Evaluation of a novel helium ionization detector within the context of (low-)flow modulation comprehensive two-dimensional gas chromatography, J. Chromatogr. A, 1402 (2015) 102-109

[20] L.A. Frink, C.A. Weatherly, D.W. Armstrong, Water determination in active pharmaceutical ingredients using ionic liquid headspace gas chromatography and two different detection protocols, J. Pharm. Biomed. Anal., 94 (2014) 111-117

[21] F. Pena-Pereira, L. Marcinkowski, A. Kloskowski, J. Namiesnik, Silica-based ionogels: Nanoconfined ionic liquid-rich fibers for headspace solid-phase microextraction coupled with gas chromatography-barrier discharge ionization detection, Anal. Chem., 86 (2014) 11640-11648

[22] C.A. Weatherly, R.M. Woods, D.W. Armstrong, Rapid analysis of ethanol and water in commercial products using ionic liquid capillary gas chromatography with thermal conductivity detection and/or barrier discharge ionization detection, J. Agric. Food. Chem., 62 (2014) 1832-1838

[23] R.T. Talasek, M.P. Schoenke, Comparison of universal chromatographic detectors for trace gas analysis, J. Chromatogr. A, 667 (1994) 205-211

[24] A. Bogaerts, R. Gijbels, Fundamental aspects and applications of glow discharge spectrometric techniques, Spectrochim. Acta B, 53 (1998) 1-42

[25] F. Leis, E.B.M. Steers, Boosted glow discharges for atomic spectroscopy-analytical and fundamental properties, Spectrochim. Acta B: Atomic Spectroscopy, 49 (1994) 289-325

[26] F. Paschen, Ueber die zum Funkenübergang in Luft, Wasserstoff und Kohlensäure bei verschiedenen Drucken erforderliche Potentialdifferenz, Ann. Phys., 273 (1889) 69-75

[27] F. Paschen, Bohrs Heliumlinien, Ann. Phys., 50 (1916) 901-940

[28] P. Gill, C.E. Webb, Electron energy distributions in the negative glow and their relevance to hollow cathode lasers, J. Phys. D; Appl. Phys., 10 (1977) 299-311

[29] H. Eichhorn, K.H. Schoenbach, T. Tessnow, Paschen's law for a hollow cathode discharge, Appl. Phys. Lett., 63 (1993) 2482-2483

[30] G. Stockhausen, M. Kock, Proof and analysis of the pendulum motion of beam electrons in a hollow cathode discharge, J. Phys. D: Appl. Phys., 34 (2001) 1683-1689

[31] R.M. Sankaran, K.P. Giapis, High-pressure micro-discharges in etching and deposition applications, J. Phys. D: Appl. Phys., 36 (2003) 2914-2921

[32] K.H. Schoenbach, A. El-Habachi, W. Shi, M. Ciocca, High-pressure hollow cathode discharges, Plasma Scources Sci. Technol., 6 (1997) 468-477

[33] K.H. Schoenbach, R. Verhappen, T. Tessnow, F.E. Peterkin, Microhollow cathode discharges, Appl. Phys. Lett., 68 (1996) 13-15

[34] K.H. Schoenbach, M. Moselhy, W. Shi, R. Bentley, Microhollow cathode discharges, J. Vac. Sci. Technol. A, 21 (2003) 1260-1265

[35] K.H. Becker, K.H. Schoenbach, J.G. Eden, Microplasmas and applications, J. Phys. D: Appl. Phys., 39 (2006) 55-70

[36] K.H. Becker, K.H. Schoenbach, In Low Temperature Plasmas. Fundamentals, Technologies and Techniques, 2nd ed.; R. Hippler, H. Kersten, M. Schmidt, K.H. Schoenbach, Eds.; Wiley-VCH Verlag GmbH & Co: Weinheim, 2008; Vol. 2, pp 463-493

[37] Q3C(R4) Impurities: Guidelines for Residual Solvents, International Conference on Harmonisation of Technical Requirements for Registration of Pharmaceuticals for Human Use: Geneva, 2009

[38] W. D'Autry, Optimization and development of sampling and detection techniques coupled to gas chromatography in pharmaceutical analysis, Doctoral thesis, Leuven 2010

[39] R.H. Stark, K.H. Schoenbach, Direct current high-pressure glow discharges, J. Appl. Phys., 85 (1999) 2075-2080

Chapter 6 - General discussion

Since its introduction, gas chromatography (GC) has been the tool of choice for the analysis of volatile constituents in various samples from many different fields such as forensics, food, petrochemical and pharmaceutical industries. GC is also often applied in environmental analysis of various organic contaminants in water, soil, air, etc. In pharmaceutical analysis, GC is used in quality control to evaluate the identity, purity and content of active pharmaceutical ingredients (APIs) and excipients. As mentioned above, the analytes should be volatile as such or after derivatization. Another important area of application is the identification and quantification of residual solvents. Guidelines about this are established by the International Conference on Harmonization of Technical Requirements for Registration of Pharmaceuticals for Human Use (ICH) and are adopted by compendia such as the European Pharmacopoeia.

The most common sampling method in combination with GC is direct injection in which an aliquot of sample is introduced and evaporated in a hot injector liner. After evaporation, the sample is transferred to the analytical column where it is separated into individual constituents followed by detection. This approach can lead to robustness issues for the analysis of residual solvents as many of the APIs are non-volatile molecules that cannot be evaporated in the injection liner. The repetitive introduction of such samples can lead to clogging and contamination of the injection system and can possibly lead to the existence of active sites and damage of the GC column. Another problem is related to the analysis of aqueous samples which frequently occur in the aforementioned fields. The introduction of large amounts of water into a GC with direct injection can lead to flooding of the injection liner due to the large expansion volume of water. This flooding can lead to backlash into the gas lines leading to irreproducible results. Moreover, most GC columns are not compatible with the introduction of large amounts of water leading to damage of the column.

To avoid laborious extraction procedures for such samples, GC analysis is often performed in combination with static headspace (sHS) sampling. For detection, the flame ionization detector (FID) is most popular. This hyphenation of techniques has proven to be a powerful tool for residual solvent analysis in pharmaceutical products and aqueous samples. However, several shortcomings on both sample introduction and detection still exist.

First, a typical issue that can be mentioned is the possible occurrence of matrix effects causing recovery problems. A matrix effect is any interaction in the sample phase that can influence the established equilibrium in a HS vial and will result in deviating behaviour towards a non-matrix matched calibration standard. Normally, recovery problems caused by matrix effects are circumvented by matching the calibration matrix with that of the sample.

Another possible way is the use of the standard addition method (SAM) or multiple headspace extraction (MHE) in order to mathematically correct for a matrix effect. However, matching of calibration standards is not always possible, as the exact matrix composition is often not known or blank matrix is not available. Both SAM and MHE approaches are very laborious and SAM can only be performed when sufficient amounts of sample are available. Apart from these possible matrix effects, a second issue is the poor sensitivity towards high boiling analytes with a high affinity for the sample matrix when sHS sampling is applied. Increasing the HS temperature generally promotes the transfer of analytes towards the gas phase leading to a higher sensitivity. However, this can cause thermal degradation and has as limitation that the sample matrix can start to boil in the HS vial when a certain HS temperature is reached. Boiling of the sample in a HS vial leads to irreproducible injections caused by exceeding the maximum tolerable HS pressure. In case of a balanced pressure system used in this study, vials are pressurised before injection. When the HS pressure is too high as a result of a boiling sample, a preliminary injection takes place upon puncturing of the vial septum. The mentioned issues especially play a role for high boiling analytes in a relatively low boiling matrix. By using the full evaporation technique (FET) these issues can be addressed. By using FET, the complete amounts of volatile analytes of interest are brought to the vapour phase whereby no analyte in the condensed phase is left behind. As a consequence, no distribution of an analyte between the condensed and vapour phase is established. In this way, analyte response cannot be influenced by a matrix effect and even high boiling analytes can be completely evaporated to the vapour phase under the right analytical conditions. One of the novelties of this work is the extension of the applicability of FET as explained in the next sections.

In Chapter 2 the use of the full evaporation technique (FET) is proposed as a methodology for the analysis of a range of typical high boiling apolar analytes in a lower boiling apolar matrix (b.p. > 200 °C). Analytes included in the study were camphor (C), menthol (M), methyl salicylate (MeS) and ethyl salicylate (EtS) in various apolar matrices. It was demonstrated that matrix matching of calibration standards was not necessary by comparison of calibration series to which blank matrix was added. It was found that the slope and intercept were matching, meaning that possible matrix effects are circumvented by the use of FET for sample introduction. The methodology was validated for the quantitative analysis of these analytes in several topical pharmaceutical formulations showing excellent analytical performance. The method was compared to a conventional sHS method as well and was found to produce similar quantification results for a commercial sample. For the sHS approach, matrix matched calibration was necessary, making the method much more laborious. Even with the smaller sample amounts in the HS vial, FET was found to be more sensitive than the sHS method for the analytes included in the study.

The advantages of the FET approach are clear: possible matrix effects can be addressed and sensitivity issues for high boiling analytes with a high affinity for the matrix can be resolved. Furthermore, FET can be performed with standard HS equipment and avoids the use of the laborious matrix matching, SAM and MHE approaches. Apart from these advantages, there are still problems that could arise when the FET approach is used. For example, as with the conventional direct injection approach, care has to be taken that a certain maximum sample volume is not exceeded. In case that the solvent and/or analytes are not completely evaporated, sHS conditions will apply, and hence matrix effects could occur again. Also, HS pressure limits can exceed the maximum tolerable value and lead to irreproducible injections. Due to its small molecular mass compared to most solvents, water will give rise to a relatively large gas volume after evaporation, even when small sample volumes are used. For this reason, the FET approach for aqueous samples does not allow sample volumes larger than 10 µL to avoid the aforementioned problems. This limited sample volume restricts the sensitivity for analytes in aqueous samples. To deal with these shortcomings around GC analysis of aqueous samples, it is demonstrated in Chapter 3 that the use of acetone acetals such as 2,2-dimethoxypropane (DMP) as water scavenger can be an efficient approach for GC analysis of typical high boiling analytes with a large affinity for water. By using DMP, water is completely removed from the sample in which methanol and acetone are formed as reaction products under acidic catalysis. As both these products are rather volatile, removal of them by using vacuum or a stream of nitrogen is straightforward. This allows analyte enrichment increasing the sensitivity of FET analysis of aqueous samples. The DMP water scavenging approach was optimized and finally applied to the analysis of typical high boiling polar residual solvents such as dimethylsulfoxide (DMSO) in aqueous matrices. It was demonstrated that at least a gain in sensitivity of a factor 10 can be obtained as compared to FET with a sample volume of 10 µL. The sensitivity of the method could be improved further by introducing a higher sample volume (e.g. 5 mL instead of 1 mL) in the HS vial. The method was validated and provided good recovery results. An additional advantage of DMP water scavenging is that it enables the derivatization of analytes to make them amenable for GC-analysis. It was demonstrated that for the determination of ethylene glycol (EG) in water, EG is quantitatively converted to a more volatile dioxolane. Like DMSO, EG is a high boiling polar residual solvent and is notorious for adsorption to parts of the GC. By conversion to a less polar dioxolane with a significantly lower boiling point, analysis of EG can be performed by using the simple sHS approach. This approach was validated and applied to the determination of EG in contact lens fluids.

A bottleneck of the DMP water scavenging approach could be the fact that analytes have to be relatively high boiling in order to be able to retain them in the sample vial during the solvent removal step prior to FET analysis. In order to improve the sensitivity for more volatile analytes in aqueous samples, FET could be combined with for instance HS trap that uses an adsorbent for analyte collection leading to a significant improvement of the sensitivity and could be part of future research. Apart from using DMP as water scavenger, other chemical reactions could be used as well. An example is the use of tetraethyl orthosilicate which forms solely ethanol as solvent and silica particles under acid catalyzed reaction with water and could possibly be used for sHS applications as well. However, it has to be investigated whether these silica particles do not adsorp the analytes of interest in the HS vial.

Even more challenging is the GC analysis of analytes with a large affinity for water that are not volatile at all. Examples of such analytes are quaternary ammonium salts (QAS) which are normally analysed by pyrolysis-GC with a heated injector. This approach can leave non-volatile residues behind and contamination of the system will occur. As explained before, introduction of large amounts of aqueous QAS samples on a GC system should be avoided. As a consequence, QAS are usually analysed with capillary electrophoresis (CE) or liquid chromatography (LC) often combined with mass spectrometry (MS). It is well known that CE does not offer the best analysis repeatability and ion suppression can be a large issue with MS. As mentioned above, thermal degradation of analytes could occur with higher HS temperatures. This is however not always a disadvantage. Chapter 4 describes the analysis of various QAS using a novel in-vial HS reaction combined with DMP water scavenging as an alternative to pyrolysis-GC, CE and LC. Compared to pyrolysis-GC, this approach is a clean method of sample introduction leading to a robust method. After screening of various benzyl substituted QAS with a chloride counter ion, it was revealed that these types of QAS disintegrate during heating in the HS vial with the formation of benzyl chloride as most abundant volatile product. In case of QAS that solely form benzyl chloride, quantification can be performed by calibration with benzyl chloride. Some QAS included in the study, formed chloromethane as side-product and quantification of such QAS can be performed by using the mass balance of the chlorinated species. The methodology was applied to various QAS in aqueous samples including denatonium benzoate (DB). Using the approach on DB did not result in a volatile compound that can be used for quantification of this QAS. However, it was discovered that after treatment with DMP and hydrochloric acid as catalyst, benzyl chloride is formed during heating of the sample, enabling the quantitative GC determination of DB.

A validation was performed for the analysis of DB in cooling liquids containing a large amount of EG. As in chapter 3, EG was converted to the corresponding volatile dioxolane. This enabled enrichment of the samples and provided excellent recovery towards DB in cooling liquids. Another validation was performed for benzethonium chloride (BZTCl) in aqueous samples. BZTCl is a QAS that yields both benzyl chloride and chloromethane. Quantification was performed by using the aforementioned mass balance approach leading to good recoveries of BZTCl. Next to benzyl substituted QAS, other QAS might form other volatile analytical targets and could possibly be used for quantification purposes. This was however not tested in this work and could be included for future work.

Finally, within GC analysis many different detectors are used to universally or selectively detect various volatile analytes after separation. The most commonly used detector is the flame ionization detector (FID) due to its robustness and good sensitivity for carbon containing analytes. However, the hydrogen diffusion flame used in the FID is not able to efficiently ionise analytes when they contain too many electronegative atoms such as chlorine, bromine, sulphur, etc. For example, analytes such as polychlorobiphenyls (PCBs) contain many chlorine atoms, but do not contain a lot of carbon atoms that can be oxidised. As a consequence, for those compounds poor sensitivity will be obtained when FID is used for their detection. The electron capture detector (ECD) is often used as an alternative for these types of analytes. The ECD uses radioactive material for the production of electrons which gives rise to legislation issues. Although a mass spectrometer (MS) is a hyphenated technique, it is often used for quantification purposes and can be operated in modes such as single ion monitoring (SIM) and single reaction monitoring (SRM) to be selective for a particular analyte. However, the sensitivity of an MS varies over time and the only way to address this issue is the use of expensive isotopes. Most GC-MS implementations make use of electrons emitted by a hot filament to perform electron impact ionization. However, this mechanism does not provide the most efficient ionization of analytes. Only part of the produced electrons and part of the analyte molecules are involved in the generation of ions. Moreover, MS systems need an expensive vacuum system to operate. So, most of the disadvantages are related to the ion source of the aforementioned systems.

An alternative way to ionize analytes is the use of an electric plasma. Plasmas can be either in thermal equilibrium or non-thermal equilibrium. Plasmas in thermal equilibrium possess very high gas temperatures and are therefore used for typical applications that require heat such as welding and cutting. A typical thermal plasma used for chemical analysis is an inductively coupled plasma (ICP) capable of atomising molecules. The use of such plasmas has the disadvantage that all structural information about the analyte is lost. Non-thermal plasmas have significantly lower gas temperatures, but have a high electron temperature

(kinetic energy). This makes it possible to carry out certain chemical reactions or treatments under relatively mild conditions. Non-thermal plasmas are often used for surface treatment or coating applications. Recently, a detector that was based on a non-thermal plasma, the dielectric barrier discharge (DBD) detector was commercialised. In this system analytes are not directly fed into the plasma, but are merely ionised by photo-ionization and detected by a collector electrode as with the FID. The plasma thus acts as a UV lamp that emits ionizing photons and no interaction of the plasma with the analytes is established. A more interesting type of plasma is the micro cavity hollow cathode discharge (µCHCD) for its special feature being the hollow cathode mode. As the name implies, a cathode containing a hole is used. When the device is operated under such conditions that the product of the internal diameter of the hollow and the gas pressure is below a certain value, hollow cathode mode operation is governed. In this mode, electrons are trapped in the hollow and continuously accelerated from one side of the cathode wall to the opposite side. This is called the pendulum effect and results in a significant increase in ionization. A µCHCD can be operated at atmospheric pressure without the need for additional gasses.

Due to these advantages, a detector set-up was developed and constructed using a µCHCD as ion source and a collector electrode to detect ionized analytes. The results are reported in the last research chapter. It was found that the orientation of the electrodes and selection of plasma erosion resistant materials are a prerequisite for a detector with a long lifetime and low maintenance. When the electrodes are made from more sputter resistant materials such as platinum and placed in a serial axial orientation, a more robust detector is obtained. It was found that in a serial axial set-up, the clearance angle between the hollow cathode and anode exit was of large influence on the resulting chromatograms. By adapting a large cathode-anode clearance angle it was noticed that analyte peaks could generate peaks with either a negative or positive polarity. At this point, it is possible to detect various analytes including halogenated species at the lower pg range and the µCHCD detector was found to be more sensitive than an FID. The current prototype is however still a proof of concept and several aspects of the detector can be improved. Experiments with the different detector prototypes have been carried out using an electron-valve based ionization amplifier for robustness reasons. By using a more modern semiconductor amplification device, a signal with less noise could be obtained. Furthermore, heating of the detector would also be necessary for applications with analytes that have a higher boiling point to avoid condensation effects inside the detector. For possible future production, electrode materials other than platinum could be considered. Platinum is an expensive material and could be replaced by diamond which can nowadays be produced at lower cost. The advantage of

diamond is that it can be used as both a dielectric material and electrode. By doping with boron, diamond becomes conductive and could serve as electrode material in the µCHCD detector.

Next to further development of the above mentioned detector concept, the µCHCD ion source can be coupled to an ion mobility spectrometer (IMS) for collision induced identification possibilities. In IMS, gas phase separation of ions occurs in a drift tube against a flow of drift gas. The separation of ions is based on the fact that every ion has a different charge, shape or size that will give rise to a different drift time. Analytes can therefore be identified according to their drift time. Other advantages of IMS are apparent as, in contrast to mass spectrometry, no vacuum system is needed. Moreover, the use of the µCHCD as ion source would avoid legislation issues that are encountered with radioactive materials that are frequently used for ionization. Furthermore, such system would be suitable to use as portable system for the detection of warfare agents, illicit drugs, etc. on for example airports.

Summary

In this work, several aspects around headspace (HS) sampling and detection hyphenated with gas chromatography (GC) were covered. Regarding HS sampling, the results of three studies were reported around the problems encountered with the analysis of aqueous samples and/or high boiling analytes with a high affinity for the matrix in chapters 2 to 4 in this manuscript, whilst the final chapter covers the development and characterization of a novel GC detector.

In chapter 2, the use of the full evaporation technique (FET) for the analysis of high boiling analytes with a high affinity for apolar matrices was evaluated and compared with the conventional static HS (sHS) sampling approach. A FET method has been developed and validated for the analysis of typical high boiling analytes (bp. > 200 °C) including camphor, menthol, methyl salicylate and ethyl salicylate that are often used in various topical formulations. Data have shown that FET is an excellent approach to circumvent matrix effects that are often encountered with sHS methods. The method showed excellent recovery and repeatability during validation and was finally applied on commercial formulations such as Radosalil®, ThermoCream®, Vicks Vaporub® and Reflexspray®.

In chapter 3, acetone acetals were employed as water scavengers for the analysis of aqueous samples using HS-GC. After optimization of the scavenging reaction conditions, the approach was used for FET analysis of various typical high boiling polar residual solvents that are miscible with water. The procedure enabled sample enrichment which provided a significant gain in sensitivity of the FET analysis of these analytes and it was finally applied on a cefotaxime sample for the quantification of residual N-methylpyrrolidone (NMP). During experiments it was revealed that the same procedure can be used for the quantitative derivatization of ethylene glycol (EG) in aqueous samples. The formation of the significantly more volatile 2,2-dimethyl-1,3-dioxolane (2,2-DD) enabled determining EG using sHS sampling.

In chapter 4, a novel HS approach for the analysis of quaternary ammonium salts (QAS) in aqueous samples is presented in which the reported water scavenging method from chapter 3 is used for the removal of water and sample enrichment. Screening experiments revealed that QAS substituted with benzyl and methyl groups degrade to form benzyl chloride and chloromethane under the used experimental conditions. By using chloromethane and benzyl chloride for quantification of such QAS, matching calibration standards are not needed. This means that one kind can be used for the determination of other QAS that also yield chloromethane and benzyl chloride as reaction products. The methodology was used for the analysis of denatonium benzoate (DB) in EG based cooling liquids and the analysis of benzoxonium chloride (BZOCL) or benzethonium chloride (BZTCl) in mouth sprays.

Finally in chapter 5, work around the development and characterization of a novel GC detector is presented. The detector used a micro cavity hollow cathode discharge (µCHCD) plasma as ion source combined with an either positively or negatively biased capture electrode. Typical advantages of the used low power µCHCD are the increased ionization efficiency compared to the hydrogen flame used in the flame ionization detector (FID) and operation at atmospheric pressure without the need for additional gasses. During development of the µCHCD ion source it was found that the detector geometry was of great influence on the obtained signal. By adapting to a geometry with a wide anode clearance angle, a sensitive response in the pg range was obtained for various analytes including carbon tetrachloride (CCl_4) which is poorly detected with the FID. It was noticed that halogenated analytes were possibly subjected to a different ionization mechanism than the non-halogenated species. Halogenated ones most likely form negative ions in the electron rich plasma as these were most efficiently detected by a positively biased capture electrode.

Samenvatting

In dit werk werden verschillende aspecten behandeld omtrent headspace (HS) extractie en detectoren in combinatie met gaschromatografie (GC). In hoofdstuk 2 t/m 4 werden verschillende onderzoeksresultaten gerapporteerd rond de problematiek met HS extractie en/of GC. Hoofdstuk 5 behandelt de ontwikkeling en karakterisering van een nieuw type GC detector.

Hoofdstuk 2 beschrijft het gebruik van de zogenaamde 'full evaporation technique' (FET) voor de analyse van analieten met een hoog kookpunt en grote affiniteit voor apolaire matrices. De toepasbaarheid van de techniek werd getest op typische apolaire hoogkokende analieten (kookpunt > 200 °C) zoals kamfer, mentol, methylsalicylaat en ethylsalicylaat. Uit de onderzoeksresultaten is gebleken dat FET een goed alternatief is om typische matrixeffecten te omzeilen waar sHS extractie vaak mee te maken heeft. De uiteindelijk ontwikkelde methode werd gevalideerd en liet een goede accuraatheid en precisie zien voor de analieten in kwestie. De gevalideerde methode werd toegepast op de analyse van commerciële producten zoals Radosalil®, ThermoCream®, Vicks Vaporub® en Reflexspray®.

In hoofdstuk 3 werd het gebruik van een chemische reactie met acetonacetalen behandeld voor de complete verwijdering van water voor de analyse van waterige stalen met HS-GC. Na optimalisatie van de reactiecondities werd de methodiek voor de FET analyse van verschillende hoogkokende polaire residuele solventen in water toegepast. Dit type solventen zijn volledig mengbaar met water en vormen een probleem voor de veelgebruikte sHS techniek. Het gebruik van acetonacetalen maakt het mogelijk om de gevoeligheid voor FET significant te verhogen en voorkomt veel problemen rondom de GC analyse van waterige stalen (kolomdegradatie, overschrijding gascapaciteit liner, etc.). Uiteindelijk werd de gevalideerde methode toegepast op de analyse van residueel NMP in een cefotaximestaal. Gedurende het onderzoek werd er aangetoond dat wanneer 2,2-dimethoxypropaan (DMP) wordt gebruikt voor de verwijdering van water, ethyleenglycol (EG) kwantitatief omgezet kan worden naar 2,2-dimethyl-1,3-dioxolaan (2,2-DD) welk een veel minder hoogkokend en meer apolair product is. Door deze omzetting met DMP kon EG uiteindelijk bepaald worden door het toepassen van een eenvoudige sHS methode.

In hoofdstuk 4 werd een alternatieve aanpak gepresenteerd voor de analyse kan quaternaire ammoniumzouten (QAS) in waterige stalen in combinatie met het verwijderen van water zoals in hoofdstuk 3. Uit initiële experimenten is gebleken dat QAS die gesubstitueerd zijn met methyl- en benzylgroepen degraderen tijdens HS analyse onder de vorming van chloormethaan en benzylchloride. Door de kwantificering van chloormethaan en benzylchloride kan de totale hoeveelheid van een QAS indirect bepaald worden. Doordat verscheidene QAS van dit type op dezelfde manier reageren is een matchende

kalibratiestandaard niet nodig en kan elk ander QAS van dit type gebruikt worden. De ontwikkelde methode werd vervolgens toegepast op de analyse van denatoniumbenzoaat (DB) in koelvloeistoffen. Ook werden mondsprays geanalyseerd die benzoxoniumchloride (BZOCl) of benzethonium chloride (BZTCl) bevatten.

In hoofdstuk 5 werden onderzoeksresultaten beschreven rondom de ontwikkeling en karakterisering van een nieuw type GC detector dat gebruik maakt van een 'micro cavity hollow cathode discharge' (µCHCD) plasma als ionenbron. Deze detector maakt gebruik van een vangstelektrode die negatief of positief gepolariseerd is. Het gebruik van een (µCHCD) plasma brengt een aantal belangrijke voordelen met zich mee. De detector kan gebruikt worden onder atmosferische druk zonder dat additionele gassen nodig zijn. Ook heeft een dergelijk (µCHCD) plasma een verbeterde ionisatiegraad in verhouding tot de waterstofvlam die gebruikt wordt voor de FID. Gedurende de ontwikkeling is gebleken dat de geometrie van de detector een grote invloed heeft op het verkregen signaal. Door een grote kathode-anode openingshoek te kiezen werd er een gevoelige respons (pg-gebied) verkregen voor verschillende types analieten. In tegenstelling tot de FID was het ook mogelijk om gehalogeneerde verbindingen zoals tetrachloorkoolstof (CCl_4) te detecteren met goede gevoeligheid. Er werd opgemerkt dat de verschillende analieten waarschijnlijk op verschillende manieren geïoniseerd kunnen worden. Gehalogeneerde analieten konden goed worden gedetecteerd met een positief gepolariseerde vangstelektrode, wat erop duidt dat dit type verbindingen negatieve ionen zouden kunnen vormen door de vangst van elektronen in het plasma.